UNIVERSIDADE FEDERAL RURAL DE PERNAMBUCO

FÁBIO FARIAS AMORIM

IDENTIFICATION OF SEDIMENT SOURCES IN AGRICULTURAL CATCHMENT OF THE PERNAMBUCO STATE, BRAZIL

Recife

2020

Fábio Farias Amorim
Agronomist

Identification of sediment sources in agricultural catchment of the Pernambuco state, Brazil

A thesis submitted to the Post-Graduate Program in Soil Science, Federal Rural University of Pernambuco in collaboration with Rothamsted Research, North Wyke, United Kingdom, as part of the requirements for obtaining the title of Doctor in Soil Science.

Orientador: Prof. Dr. Yuri Jacques Agra Bezerra da Silva

Recife
2020

Dados Internacionais de Catalogação
na Publicação Universidade
Federal Rural de Pernambuco
Sistema Integrado de Bibliotecas
Gerada automaticamente, mediante os dados fornecidos
pelo(a) autor(a)

A524ii Amorim, Fábio Farias
Identification of sediment sources in agricultural catchment of the Pernambuco state, Brazil / Fábio Farias Amorim. - 2020.
110 f. : il.

Orientador: Yuri Jacques Agra Bezerra da Silva. Coorientador: Adrian L Collins .
Inclui referências e apêndice(s).

Tese (Doutorado) - Universidade Federal Rural de Pernambuco, Programa de Pós-Graduação em Ciência do Solo, Recife, 2020.

1. Sediment Fingerprint. 2. Modelagem Bayesiana. 3. Compostos orgânicos da matéria orgânica. 4. Espectroscopia. I. Silva, Yuri Jacques Agra Bezerra da, orient. II. Collins , Adrian L, coorient. III. Título

CDD 631.4

FÁBIO FARIAS AMORIM

Identification of Sediment Sources in Agricultural Catchment of the Pernambuco State, Brazil

Tese apresentada ao Programa de Pós-Graduação em Ciência do Solo, da Universidade Federal Rural de Pernambuco, como parte dos requisitos para obtenção do título de Doutor em Ciência do Solo.

Aprovada em 28 de fevereiro de 2020

_____

Orientador

Prof. Dr. Yuri Jacques Agra. Bezerra. da Silva / UFRPE

BANCA EXAMINADORA

_____

Profa. Dra. Caroline Miranda Biondi/ UFRPE

_____

Prof. Dr. Ygor Jacques Agra. Bezerra. da Silva / UFRPE

_____

Prof. Dr. Renato Paiva de Lima / UFRPE

_____

Prof. Dr. Ronny Sobreira Barbosa / UFRPE

Dedico

Aos meus pais Antônio e Iracema, pelos exemplos de vida, pela compreensão, carinho e amor a mim dedicados, e que sempre acreditaram, incentivaram e investiram na minha formação moral, intelectual e profissional.

AGRADECIMENTOS

A Deus, por me amparar nas horas mais difíceis da minha vida, em todas as conquistas nesses anos e por me lembrar de que sempre sou mais forte do que penso.

À Universidade Federal Rural de Pernambuco e ao Programa de Pós-Graduação em Ciência do solo pela oportunidade e pelos ensinamentos.

Ao Rothamsted Research e seus colaboradores pela oportunidade de desenvolver minha tese de doutorado e de conviver com pessoas de muitos países.

Ao Professor Yuri Jacques, pelo apoio, ensinamentos, compreensão e orientação.

Ao Dr. Adrian Collins pelo apoio, ensinamentos e orientação durante o doutorado sanduíche.

Aos amigos Renan e Igor, pelo companheirismo e inestimável colaboração nas fases de campo importantes para a consecução desta pesquisa.

Aos colegas do Programa de Pós-Graduação e amigos, pela atenção paciência e amizade.

Um super agradecimento à minha esposa Maria Reis, pelo amor, amizade, companheirismo, carinho e compreensão.

Enfim, a todos que de alguma forma contribuíram para a minha formação e para a realização deste estudo, meu MUITO OBRIGADO.

Identificação de fontes de sedimentos em bacia hidrográfica agrícola do estado de Pernambuco, Brasil

RESUMO

A má gestão da terra está entre os fatores que causam aumento nas taxas de erosão e transporte de sedimentos nas bacias hidrográficas. A técnica "fingerprint sediments" de identificação das fontes de sedimentos é cada vez mais usada para investigar as principais fontes de perdas elevadas de sedimentos. O objetivo desse estudo foi avaliar a capacidade de propriedades de cores, Espectroscopia no Infravermelho Próximo (NIR) e Espectroscopia no Infravermelho Médio (MIR) de distribuir fontes de sedimento de uso da terra (cana-de-açúcar (SC), estradas não pavimentadas (UR), terras cultivadas (CL) e bancos de canais (CB)) nas sub-bacias hidrográficas (1.338 km^2 e 1.453 km^2) e bacia hidrográfica (2.857 km^2) usando amostras de sedimentos em suspensão (SS) e de leito (BS). Os resultados para as propriedade de cores, NIR e MIR mostraram que as maiores fontes que contribuem para sedimentos na escala de captação são as CB que contribuem majoritariamente para a descarga de SS, seguidas pela fonte de SC com maior descarga de BS, para as propriedades do composto orgânico com espectroscopia NIR, componentes do solo com espectroscopia MIR e a combinação de cores, NIR e MIR (CNM). O uso dos espectros de compostos orgânicos do NIR como traçadores mostrou-se robusto e adequado para discriminação entre as fontes de sedimentos tanto nos sedimentos quanto no tamanho da escala da bacia, com erros (RMSE e MAE) abaixo de 8%. Concluímos que é urgente o uso de práticas de manejo, como a revitalização de áreas de preservação permanente que compreendem o conjunto de matas ciliares, encostas e cabeceiras de rios, juntamente com práticas conservacionistas que controlam a erosão e torrentes no perímetro agrícola da bacia hidrográfica para reduzir o impacto ambiental. impactos causados pela produção de sedimentos para os rios.

Palavras chaves: Isótopos estáveis. Espectroscopia. Constituintes do solo. Compostos orgânicos da matéria orgânica. Tamanho de partícula. Sedimento Fingerprint. Modelagem Bayesiana MixSIAR.

Identification of sediment sources in agricultural catchment of the Pernambuco state, Brazil

ABSTRACT

Poor land management is among the controlling factors causing an increase in erosion rates and sediment transport in river catchments. Sediment source fingerprinting is increasingly used to investigate key sources of elevated sediment loss. The objective of this study was to evaluate the ability of colour proprieties, Near Infrared Spectroscopy (NIR) and Mid Infrared Spectroscopy (MIR) to apportion land use sediment sources (sugarcane (SC), unpaved roads (UR), cropland (CL) and channel banks (CB)) at sub-catchments (1.338 km^2 and 1.453 km^2) and catchment (2.857 km^2) scales using both suspended (SS) and bed (BS) sediment samples. The results for the colour properties, NIR and MIR showed that the largest sources that contribute to sediments on the catchment-wide scale are the CB that contribute mostly to the discharge of SS, followed by the source of SC with the highest discharge of BS, for the properties organic compound with NIR spectroscopy, soil components with MIR spectroscopy and the combination of colours, NIR and MIR spectroscopy (CNM). Using the spectra of organic compounds from the NIR as tracers proved to be robust and suitable for discrimination between sediment sources in both sediments and basin scale size, with errors (RMSE and MAE) below 8%. We conclude that it is urgent to use management practices, such as the revitalization of areas of permanent preservation that comprise the set of riparian forests, slopes and headwaters of rivers, together with conservationist practices that control erosion and torrents in the agricultural perimeter of the hydrographic basin to reduce the environmental impact. impacts caused by the production of sediments for rivers.

Keywords: Stable isotopes. Spectroscopy. Soil constituents. Organic compounds of organic matter. Particle size. Fingerprint sediments. MixSIAR Bayesian modelling

SUMMARY

1 INTRODUCTION

The disordered occupation found in the catchment of the state of Pernambuco, Brazil, contributes to numerous occupation problems in urban and agricultural areas, promoting innumerable problems for the rivers that compose them. Currently contaminated by solid, liquid, organic and inorganic residues, in addition to having a high silting rate, they are the main sources of pollution, contamination, eradication and/or reduction of life in rivers. Furthermore, agricultural production chains have deforestation and inadequate soil management, the main factor in inducing erosion and silting processes, in addition to salinization and contamination by pesticides, herbicides and fertilizers.

Agricultural expansion to produce food and biofuel has been the largest exploration in the catchment of the Goiana River. Despite the production of “clean” fuel, the sugar cane production chain contributes to the degradation of the soil and watercourses. Expansion to large-scale fuel production produces large amounts of soil residues that are transported causing contamination by pesticides, fertilizers and silting. In addition, 50% of the straw is collected after harvesting, contributing to the reduction of soil cover and increased production of transported sediments. Other areas under banana cultivation and pastures contribute to runoff due to the steep slope and grazing of animals.

Studies seeking to optimize specific soil management techniques to reduce such impacts on the degradation process and costs and increase the methods' efficiency are essential. The method of identifying sources of sediments "fingerprint" assumes that the areas under cultivation have their own identity. Thus, the use of specific analytical methodologies, such as colours, near and medium infrared spectroscopy using different sizes particles of source soil and sediments (suspended and bed sediments) is helpful to improve the “fingerprint” method, reducing the uncertainties. These alternatives are faster, cheaper and reduce environmental impact by not using reagents.

In addition to the analytical methodologies, the improvement has been growing under the use of mathematical statistical models such as Monte-Carlo simulation with Bayesian methods in the MixSIAR model. It starts from the premise that these sophisticated models can not only identify and quantify the contributions of the individual source areas, but, also provide indications of uncertainties and variability caused by the types of tracers, particle size and study areas, allowing for more concrete decisions on the management of river catchments.

1.1 Hypotheses

Considering that pollution resulting from agricultural activities, due to inadequate soil management and the advance of deforestation, are the main factors of induction of erosive processes and silting, and that the discharge of contaminants adsorbed to sediments is affected by the hydrosedimentological regime of the catchment of the Goiana River, We presented the following hypotheses:

I. Water erosion, the process that causes the greatest degradation of the soil and the main agent for transporting contaminants to water courses, is enhanced by the lack of order in land use and management.

II. The use of colour properties and spectroscopic are useful to identify sediment sources in the basin.

III. The different scales and sediment types influence the final contribution of sources to sediments as well as the uncertainties in mathematical models.

IV. The fine sediments extracted from the bottom sediments can be used as a surrogate of the suspended sediment to identify the source of sediments.

1.2 General objective

To discriminate the sources of sediments transported in the catchment of the Goiana River, aiming to increase the understanding of the effects of different land uses on erosive processes and assisting the management of the region's water resources.

1.3 Specific objectives

To identify the main sources of erosion and sediment transport in the Goiana River basin;

To evaluate the efficiency of soil colour properties and soil components extracted from spectroscopic analyses as tracers of sediment sources;

To evaluate the potential effect of different scales (catchment and sub-catchments) and sediments on the uncertainties and variability of the results obtained in the final contributions of the sediment sources.

2 BIBLIOGRAPHIC REVIEW

2.1 The sediment identification process

The fingerprint method, shown in Figure 1 for a river system, is based on two assumptions. Firstly, the various sediment sources can be distinguished based on their physical, geochemical and biogenic properties. The use of various properties reduces the uncertainties as it is more representative of mixtures of source materials that comprise sediment samples (WALLING, 1999; COLLINS et al., 2001; COLLINS; WALLING, 2002; 2004). The second assumption is that the selected fingerprint properties can determine the relative importance of various areas that are sources of sediment when compared to suspended or bed sediments in the channels collected in rivers, lakes or estuaries (COLLINS; WALLING, 2002; 2004).

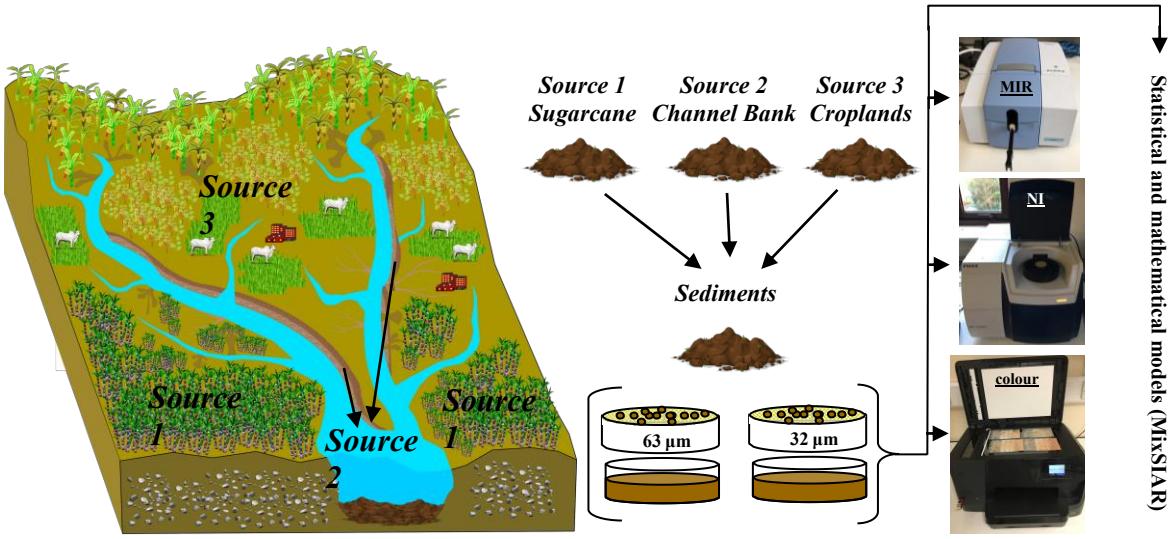

Figure 1. Necessary process for the fingerprint method in river systems, including sampling, selection of tracers and analyses, and selection of the mixed model to determine the contribution of sediment sources

Some studies have used the following tracers: rare earth elements (Ce, Eu, La, Lu, Dy, Sm, Tb, Yb), heavy metals (As, Ba, Co, Cr, Cs, Hf, Sc, Ta, Th, Zn Ag, Ba, Cd, Cu, Mn, Ni, Pb, Sb, Se, Tl, V), major elements (Fe, K, Na, Al, Ca, Mg, Ti, CaO, Na2O, K2O, Al2O3, Fe2O3 , P2O5, MgO, SiO2, TiO2, Mn2O4) (COLLINS; WALLING; LEEKS, 1997b; ZHANG; LEI; ZHAO, 2008; TIECHER et al., 2016), organic tracers, including total carbon, nitrogen and phosphorus (COLLINS et al., 2001; HANCOCK; REVILL, 2013), mineral magnetic properties, low and high frequency magnetic susceptibility (χbf, χaf), frequency dependent susceptibility (χdf), anisteretic remnant magnetization (ARM), isothermal remnant magnetization (MRI), remnant field magnetization (HIRM) and isothermal remnant magnetization saturated (MRIS) (WALLING; PEART, 1979; CAITCHEON, 1993; WALDEN; SLATTERY; BURT, 1997), mineralogical tracers, clay mineralogy, quartz cathodoluminecence (GÖTZE; PLÖTZE; HABERMANN, 2001; GINGELE; DE DECKKER, 2005; BENEDETTI et al., 2006), isotopic tracers and radionuclides such as $\delta^{15}N$, $\delta^{13}C$, $\delta^{87}Sr$, ^{204}Pb / ^{206}Pb, ^{137}Cs, ^{210}Pb and ^{7}Be (EVRARD et al., 2010; MUKUNDAN et al., 2010; WILKINSON et al., 2013), physical tracers such as colour, particle morphology and granulometric distribution (CARDONA et al., 2005; WELTJE, 2012).

Significant advances in the development of the fingerprinting sediment source identification method have been achieved using statistical methods to validate the tracers and contribution of the sediment sources. Statistical methods include Kruskal-Wallis (H) and Mann-Whitney (U) (COLLINS; WALLING; LEEKS, 1997b), and multivariate discriminant function (DE BOER; CROSBY, 1995; KELLEY; NATER, 2000). Several statistical improvements are being used to minimize aspects of uncertainty, including the use of a Bayesian (DOUGLAS et al., 2003) or Bayesian-Monte Carlo approach (FRANKS; ROWAN, 2000). Other advances include the incorporation of mixed model algorithms, which allows the quantitative estimate of relative contributions from different sources (YU; OLDFIELD, 1989; WALLING; WOODWARD; NICHOLAS, 1993). The development of these mixed models started from the premise of optimized linear regression incorporating iterative resolution with a series of least squares equations (COLLINS; WALLING; LEEKS, 1996; WALDEN; SLATTERY; BURT, 1997). The greater reliability of the estimates provided by the use of mixed models was further improved by the use of rigorous statistical procedures to test the properties' ability to properly discriminate the types of sources, including cluster analysis and multivariate discriminant function analysis (WALLING; WOODWARD, 1995; COLLINS; WALLING; LEEKS, 1997a, b).

Initial studies on the provenance of sediments have focused on direct measurements of potential sediment sources, using methods such as erosion pins (DAVIS; GREGORY, 1994), profilometers (SIRVENT et al., 1997) and surveys of erosion characteristics (VIRGO; MUNRO, 1978). The costs and time of these methods were quickly identified as a major limitation for carrying out investigations of sediment sources (PEART; WALLING, 1982). As a result, the use of markers has gained increasing popularity in determining the origin of suspended sediment sources in watersheds (KLAGES; HSIEH, 1975; WALLING, 2005).

In the 1970s, researchers used a series of properties (geochemical, mineralogical, mineral magnetic) to track sediments from different sources (WALLING, 2005). However, for a parameter to be useful in tracking the sediment source, the tracer must be measurable and conservative or it can vary in a predictable way along a transport channel (CAITCHEON, 1998; MOTHA et al., 2002; HADDADCHI et al., 2013). An example of a marker is Cesium-137, which binds onto soil particles (property provided) and is relatively constant during transport and can identify sources of surface and subsurface erosion (WALLBRINK; MURRAY, 1993).

Studies carried out in the late 1980s observed changes in the use of various tracers to discriminate between several potential areas and the development of quantitative methods to increase the accuracy of the determination of the source area. Quantitative methods included statistical tests such as Kruskal-Wallis to select properties, discriminant function analysis to determine the best fit of properties and mixed multivariate models to quantify the relative proportions of different source areas (WALLING, 2005).

Based on the first results applied in small and large hydrographic basins, researchers observed that the technique provides information to establish effective strategies to control the flow of sediments and contaminants, providing more comprehensive prediction and models about the distribution of sediments, depending on the use of soil in hydrographic basins, in addition to understanding the temporal and spatial patterns of sedimentation (COLLINS; WALLING; LEEKS, 1997b, COLLINS; WALLING, 2002; COLLINS; WALLING; LEEKS, 1998, COLLINS; WALLING , 2002).

In the watershed of the Kaleya River, Zambia province, Collins et al. (2001) evaluated the relative contribution of the origin of sediments in different sources according to soil use, using trace elements (As, Cd, Co, Cr, Cu, Fe, Mn, Sb, Sn, Sr), basic cations (Ca, K, Mg, Na), total carbon and nitrogen (TC and TN) and radionuclides (137Cs, 210Pb, 226Ra) as tracers. The results of using these parameters revealed that the contributions from individual sources, community culture (63.7%), channel banks / gullies (17.2%), shrub pasture (17.1%) and

commercial cultivation (2%), are consistent with the relative proportions of the study basin, represented by each land use, reflecting both the magnitude of local erosion rates and the rate of sediment distribution.

Evaluating erosive processes with rare earth elements (REEs) as tracers, Deasy and Quinton (2010) observed that less than 1% of the REE oxides applied in hill-scale cultivable soils were recovered. However, the recoveries of the markers were able to indicate the relative importance of different areas of sedimentary sources, which were found consistent between the events. Like Deasy and Quinton (2010), Polyakov et al. (2009) proved that the tracking of sediments using REEs is a useful tool to measure the redistribution of sediments in catchment. Alternative techniques for identifying sediment sources have been used in recent years to explore other tracing properties.

2.2 Tracer selection for source discrimination

In recent years, the search to improve the fingerprint method has enabled the use of different types of tracers, such as the bulk stable isotope (UPADHAYAY et al., 2018; COLLINS et al., 2019) and spectral properties (VIS, NIR, MIR) (TIECHER et al., 2016; EVRARD et al., 2019; UBER et al., 2019; COLLINS et al., 2014; COLLINS et al., 2013a; VISCARRA ROSSEL et al., 2006; CHANG et al., 2001). Although it is not possible to identify a universally applicable set of tracer properties, due to the dependence of the characteristics of the investigated source areas on a temporal and spatial scale, the most effective means of optimizing the discrimination of the sediment source is to identify several groups of tracers for use later in the establishment of a composite digital impression and that these tracers can be constant and preserve their properties from their source area and during transport in the drainage systems (WALLING; WOODWARD; NICHOLAS, 1993; COLLINS; WALLING; LEEKS, 1997a; COLLINS; WALLING, 2002 ; COLLINS et al., 2017).

2.2.1 Spectral fingerprinting for tracing sediment sources

Spectroscopy deals with the production, measurement and interpretation of spectra resulting from the study of light as a function of the wavelength that was emitted, reflected or scattered from matter, in a qualitative or quantitative way (PENNER, 2017; JESPERSEN, 2006; CLARK, 1999). The spectroscopic methods that investigate the UV, VIS, NIR and

MIR regions have been widely used to quickly analyse multiple parameters of sediment sources, using the sediment fingerprint method (ZHANG et al., 2017; COLLINS et al., 2013a, 2014; TIECHER et al., 2016, 2015; BROSINSKY et al., 2014a; BROSINSKY et al., 2014b MARTÍNEZ-CARRERAS et al., 2010). The ultraviolet UV (250-400 nm) and visible VIS (400-700 nm) regions have a significant contribution in the identification of sediment sources using colour properties. Differentiating characteristic for many soil classes, NIR correspond to overtones and combinations of fundamental bands above 700 - 2,500 nm or 14.000 – 4.000 cm^{-1}, while MIR regions correspond to more intense fundamental bands of molecular vibrations above 2,500 - 25,000 nm, typically expressed as 4.000 - 400 cm^{-1} (BURNS; CIURCZAK, 2007; DALAL; HENRY, 1986; JESPERSEN, 2006).

Several types of vibrations that cause absorptions in the infrared region. Probably the simplest way to visualize are bending and stretching, examples of which are illustrated below using a molecule of wate. If the vibration of these bonds result in the change of the molecule dipole moment then the molecule will absorb infrared energy at a frequency corresponding to the frequency of the bond's natural vibration (Figure 2) (WEYER; LO, 2006; JESPERSEN, 2006).

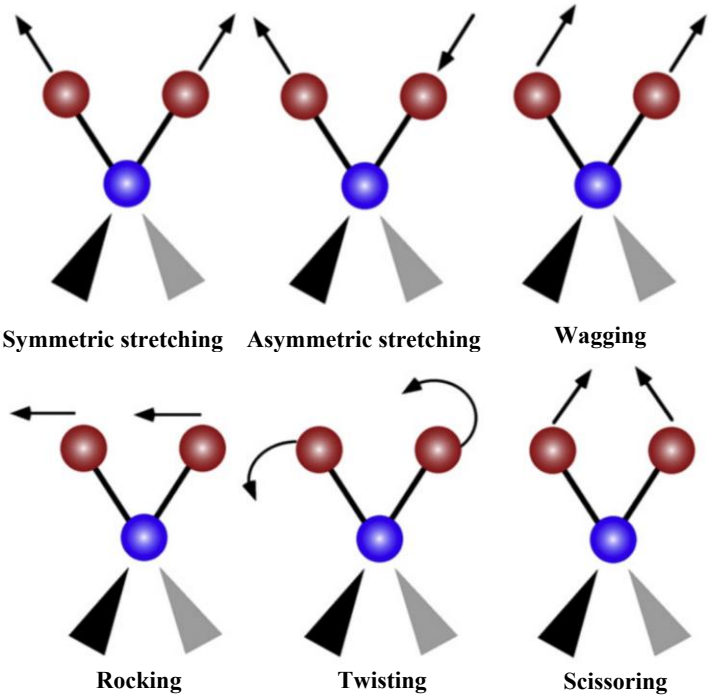

Figure 2. Examples of vibrational modes – Marcelli et al. 2012

Molecules vibrate when they absorb near infrared radiation, but the spectral features are fewer, broader, and more difficult to interpret than in the mid-infrared. Because of certain instrumental advantages, near infrared radiation is frequently used to measure sample

properties in difficult environments such as in the middle of a chemical reactor or of liquid owing through a pipe. Higher in energy than the near infrared are VIS light and UV radiation. When a molecule absorbs visible or ultraviolet light the electrons in the molecule transition from a lower electronic energy level to a higher one. Figure 3 shows that as you move from right to left across the electromagnetic spectrum there is an increase in energy, wavenumber, and frequency, but a decrease in wavelength, moving from left to right across there is a decrease in energy, frequency, and wavenumber and an increase in wavelength Figure 3. (IBÁÑEZ et al., 2019; HUTENGS et al., 2018; SCHWANNINGER; RODRIGUES; FACKLER, 2011; PARIKH et al., 2014; STENBERG et al., 2010; JESPERSEN, 2006).

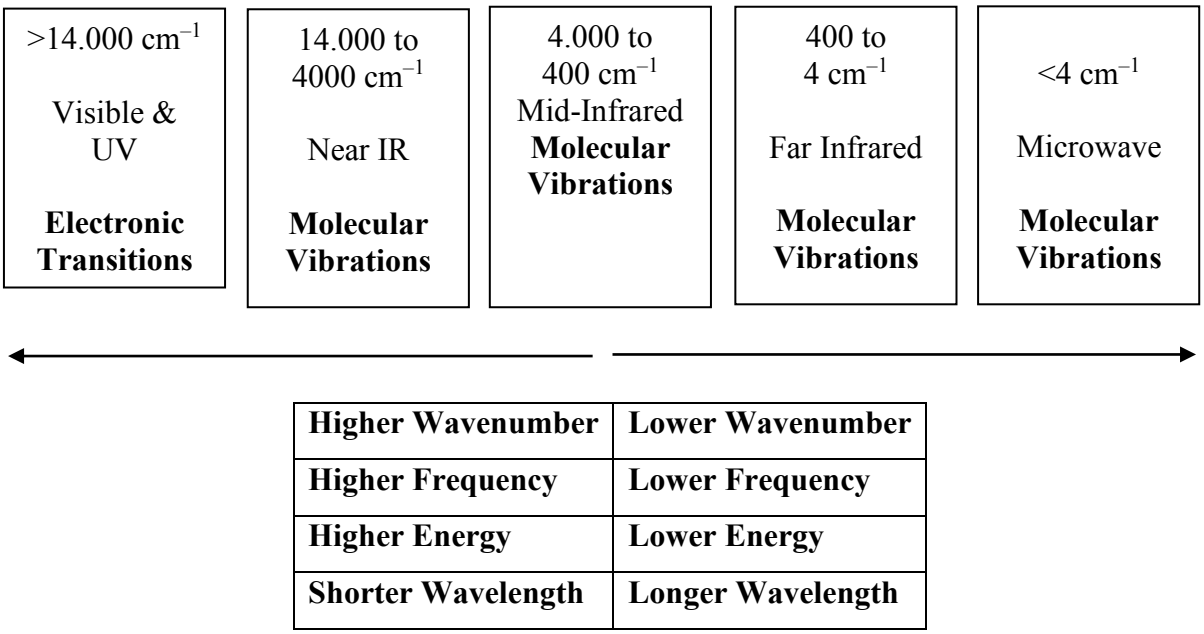

Figure 3. A diagram of part of the electromagnetic spectrum

Using DRIFT infrared spectroscopy to trace the sediment sources in a small watershed, Pouleonard et al. (2009) showed that the MIR approach has the potential to be used in order to apply cheap measurements with a relatively common infrared spectrometer, facilitating studies of suspended matter present during high flow events and spatial variations in the sediment mobilization and the effect changes in land use in sediment sources. Evrard et al. (2013) and Tiecher et al. (2016) showed that the Diffuse Reflectance Infrared Fourier Transform Spectroscopy (DRIFTS) is sensitive to the content of organic matter in the soil.

Moreover, Brosisnky et al. (2014a) showed that the properties of spectral and conventional fingerprints can potentially allow the discrimination of a greater number of types of sources.

Tiecher et al. (2016) showed that results from MIR spectroscopy is compared with those obtained using other sediment fingerprinting approaches, based on geochemistry and near - infrared and ultraviolet – visible spectroscopy. They observed an overestimation of channel banks' contribution and an underestimation of cropland and unpaved road contributions. Another approach was to combine geochemical tracers and colour parameters derived from the visible spectrum (VIS) in a single estimative of the contribution of the sediment source (TIECHER et al., 2015). Authors concluded that the use of colour parameters based on VIS and combined with geochemical tracers can be a quick and inexpensive way to improve discrimination of sediment sources.

REFERENCES

BENEDETTI, M.M.; RABER, M.J.; SMITH, M.S.; LEONARD, L.A. Mineralogical indicators of alluvial sediment sources in the Cape Fear River Basin, North Carolina. **Physical Geography**, Norwich, v. 27, n. 3, p. 258-281, 2006. https://doi.org/10.2747/0272-3646.27.3.258

BROSINSKY, A.; FOERSTER, S.; SEGL, K.; KAUFMANN, H. Spectral fingerprinting: sediment source discrimination and contribution modelling of artificial mixtures based on VNIR-SWIR spectral properties. **Journal of Soils and Sediments**, v. 14, n. 12, p. 949-1964, 2014a. https://doi.org/10.1007/s11368-014-0925-1

BROSINSKY, A.; FOERSTER, S.; SEGL, K.; LÓPEZ-TARAZÓN, J. A.; PIQUÉ, G.; BRONSTERT, A. Spectral fingerprinting: characterizing suspended sediment sources by the use of VNIR-SWIR spectral information. **Journal of Soils and Sediments,** v. 14, n. 12, p. 1965-1981, 2014b. https://doi.org/10.1007/s11368-014-0927-z

BURNS, D. A.; CIURCZAK, E. W. Handbook of Near-Infrared Analysis, eds: Marcel Dekker, Inc.: New York, 2007.

CAITCHEON, G.G. Sediment source tracing using environmental magnetism: a new approach with examples from Australia. **Hydrological Processes,** Chichester, v. 7, n. 4, p. 349-358, 1993. https://doi.org/10.1002/hyp.3360070402

CAITCHEON, G.G. The significance of various sediment magnetic mineral fractions for tracing sediment sources in Killimicat Creek. **Catena**, Amsterdam, v. 32, n. 2, p. 131-142, 1998. https://doi.org/10.1016/S0341-8162(97)00057-X

CARDONA, J.M.; MAS, J.G.; BELLÓN, A.S.; DOMÍNGUEZ-BELLA, S.; LÓPEZ, J.M. Surface textures of heavy-mineral grains: a new contribution to provenance studies. **Sedimentary Geology**, Amsterdam, v. 174, n. 3, p. 223-235, 2005. https://doi.org/10.1016/j.sedgeo.2004.12.006

CHANG, C. W.; LAIRD, D. A.; MAUSBACH, M. J.; HURBURGH, C. R. Near-infrared reflectance spectroscopy–principal components regression analyses of soil properties. **Soil Science Society of America Journal**, v. 65, n .2, p. 480-490, 2001. https://doi.org/10.2136/sssaj2001.652480x

CLARK, R. N. Chapter 1: spectroscopy of rocks and minerals and principles of spectroscopy. In: Rencz A (ed) Remote sensing for the earth sciences, vol. 3: manual of remote sensing. **John Wiley and Sons**, New York, pp 3–58, 1999.

COLLINS, A. L.; BURAK, E.; HARRIS, P.; PULLEY, S.; CARDENAS, L.; TANG, Q. Field scale temporal and spatial variability of δ13C, δ15N, TC and TN soil properties: Implications for sediment source tracing. **Geoderma**, v. 333, p. 108-122, 2019. https://doi.org/10.1016/j.geoderma.2018.07.019

COLLINS, A. L.; PULLEY, S.; FOSTER, I. D.; GELLIS, A.; PORTO, P.;HOROWITZ, A. J. Sediment source fingerprinting as an aid to catchment management: a review of the current state of knowledge and a methodological decision-tree for end-users. **Journal of Environmental Management**, v. 194, p. 86-108, 2017. https://doi.org/10.1016/j.jenvman.2016.09.075

COLLINS, A. L.;WILLIAMS, L. J.; ZHANG, Y. S.; MARIUS, M.; DUNGAIT, J. A. J.; SMALLMAN, D. J; DIXON, E. R.; STRINGFELLOW, A.; SEAR, D. A.; JONES, J. I.; NADEN, P. S.. Catchment source contributions to the sediment-bound organic matter degrading salmonid spawning gravels in a lowland river, southern England. **Science of the Total Environment**, v. 456, p. 181-195, 2013a. https://doi.org/10.1016/j.scitotenv.2013.03.093

COLLINS, A. L.; WILLIAMS, L. J.; ZHANG, Y. S.; MARIUS, M.; DUNGAIT, J. A. J; SMALLMAN, D. J; DIXON, E. R.;STRINGFELLOW, A; SEAR, D. A.; JONES, J. I.; NADEN, P. S. Sources of sediment-bound organic matter infiltrating spawning gravels during the incubation and emergence life stages of salmonids. **Agriculture, Ecosystems & Environment**, v. 196, p. 76-93, 2014. https://doi.org/10.1016/j.agee.2014.06.018

COLLINS, A.; WALLING, D. Selecting fingerprint properties for discriminating potential suspended sediment sources in river basins. **Journal of Hydrology**, Amsterdam, v. 261, n. 1, p. 218-244, 2002. 2008. https://doi.org/10.1016 / S0022-1694 (02) 00011-2

COLLINS, A.; WALLING, D.; LEEKS, G. Composite fingerprinting of the spatial source of fluvial suspended sediment: a case study of the Exe and Severn River basins, United Kingdom. **Géomorphologie: relief, processus, environement**, Paris, v. 2, n. 2, p. 41-53, 1996. https://doi.org/10.3406/morfo.1996.877

COLLINS, A.; WALLING, D.; LEEKS, G. Sediment sources in the Upper Severn catchment: a fingerprinting approach. **Hydrology and Earth System Sciences**, Göttingen, v. 1, n. 3, p. 509-521, 1997a. https://doi.org/10.5194 / hess-1-509-1997

COLLINS, A.; WALLING, D.; LEEKS, G. Source type ascription for fluvial suspended sediment based on a quantitative composite fingerprinting technique. **Catena**, Amsterdam, v. 29, n. 1, p. 1-27, 1997b. https://doi.org/10.1016/S0341-8162(96)00064-1

COLLINS, A.; WALLING, D.; LEEKS, G. Use of composite fingerprints to determine the provenance of the contemporary suspended sediment load transported by rivers. **Earth Surface Processes and Landforms**, Sussex, v. 23, n. 1, p. 31-52, 1998. https://doi.org/10.1002/(SICI)1096-9837(199801)23:1%3C31::AID-ESP816%3E3.0.CO;2-Z

COLLINS, A.; WALLING, D.; SICHINGABULA, H.; LEEKS, G. Suspended sediment source fingerprinting in a small tropical catchment and some management implications. **Applied Geography**, Oxford, v. 21, n. 4, p. 387-412, 2001. https://doi.org/10.1016 / S0143-6228 (01) 00013-3

COLLINS, A.L.; WALLING, D.E. Documenting catchment suspended sediment sources: problems, approaches and prospects. **Progress in Physical Geography**, London, v. 28, n. 2, p. 159-196, 2004. https://doi.org/10.1191%2F0309133304pp409ra

DALAL, R. C.; HENRY, R.J. Simultaneous determination of moisture, organic carbon, and total nitrogen by near-infrared reflectance spectrophotometry. **Soil Science Society of America Journal**, v. 50, p. 120-123, 1986. https://doi.org/10.2136/sssaj1986.03615995005000010023x

DAVIS, R.; GREGORY, K. A new distinct mechanism of river bank erosion in a forested catchment. **Journal of Hydrology**, Amsterdam, v. 157, n. 1-4, p. 1-11, 1994. https://doi.org/10.1016/0022-1694(94)90095-7

DE BOER, D.H.; CROSBY, G. Evaluating the potential of SEM/EDS analysis for fingerprinting suspended sediment derived from two contrasting topsoils. **Catena**, Amsterdam, v. 24, n. 4, p. 243-258, 1995. https://doi.org/10.1016/0341-8162(95)00029-4

DEASY, C.; QUINTON, J.N. Use of rare earth oxides as tracers to identify sediment source areas for agricultural hillslopes. **Solid Earth**, v. 1, n. 1, p. 111, 2010. https://doi.org/10.5194/se-1-111-2010

DOUGLAS, G.; FORD, P.; JONES, G.; PALMER, M. Identification of sources of sediment to Lake Samsonvale (North Pine Dam), southeast Queensland, Australia. **International Association of Hydrological Sciences, Publication**, Wallingford, v., n. 279, p. 33-42, 2003. http://hydrologie.org/redbooks/a279/iahs_279_0033.pdf

EVRARD, O.; DURAND, R.; FOUCHER, A.; TIECHER, T.; SELLIER, V.; ONDA, Y., LEFÈVRE, I.; CERDAN, O.; LACEBY, J. P. Using spectrocolourimetry to trace sediment source dynamics in coastal catchments draining the main Fukushima radioactive pollution plume (2011–2017). **Journal of Soils and Sediments**, v.19, p. 3290–3301, 2019. https://doi.org/10.1007/s11368-019-02302-w

EVRARD, O.; POULENARD, J.; NÉMERY, J.; AYRAULT, S.; GRATIOT, N.; DUVERT, C.; PRAT, C.; LEFÈVRE, I.; BONTÉ, P.; ESTEVES, M. Tracing sediment sources in a tropical highland catchment of central Mexico by using conventional and alternative fingerprinting methods. **Hydrological Processes**, v. 27, n. 6, p. 911-922, 2013. https://doi.org/10.1002/hyp.9421

EVRARD, O.; NÉMERY, J.; GRATIOT, N.; DUVERT, C.; AYRAULT, S.; LEFÈVRE, I.; POULENARD, J.; PRAT, C.; BONTÉ, P.; ESTEVES, M. Sediment dynamics during the rainy season in tropical highland catchments of central Mexico using fallout radionuclides. **Geomorphology**, Amsterdam, v. 124, n. 1, p. 42-54, 2010. https://doi.org/10.1016/j.geomorph.2010.08.007

FRANKS, S.; ROWAN, J. Multi-parameter fingerprinting of sediment sources: uncertainty estimation and tracer selection. **Computational Methods in Water Resources**, Southampton, v. 13, n. 1067-1074, 2000. https://doi.org/10.1016/S0341-8162(03)00085-7

GINGELE, F.; DE DECKKER, P. Clay mineral, geochemical and Sr–Nd isotopic fingerprinting of sediments in the Murray–Darling fluvial system, southeast Australia. **Australian Journal of Earth Sciences**, Victoria, v. 52, n. 6, p. 965-974, 2005. https://www.tandfonline.com/doi/ref/10.1080/08120090500302301?scroll=top

GÖTZE, J.; PLÖTZE, M.; HABERMANN, D. Origin, spectral characteristics and practical applications of the cathodoluminescence (CL) of quartz–a review. **Mineralogy and Petrology**, Wien, v. 71, n. 3, p. 225-250, 2001. https://doi.org/ 10.1007/s007100170040

HADDADCHI, A.; RYDER, D.S.; EVRARD, O.; OLLEY, J. Sediment fingerprinting in fluvial systems: review of tracers, sediment sources and mixing models. **International Journal of Sediment Research**, Beijing, v. 28, n. 4, p. 560-578, 2013. https://doi.org/ 10.1016/S1001-6279(14)60013-5

HANCOCK, G.J.; REVILL, A.T. Erosion source discrimination in a rural Australian catchment using compound-specific isotope analysis (CSIA). **Hydrological Processes**, v. 27, n. 6, p. 923-932, 2013. https://doi.org/10.1002/hyp.9466

HUTENGS, C.; LUDWIG, B.; JUNG, A.; EISELE, A.; VOHLAND, M. Comparison of portable and bench-top spectrometers for mid-infrared diffuse reflectance measurements of soils. **Sensors**, v. 18, n. 4, p. 993, 2018. https://doi.org/10.3390/s18040993

IBÁÑEZ, D.; PÉREZ-JUNQUERA, A;, GONZÁLEZ-GARCÍA, M. B.; HERNÁNDEZ-SANTOS, D.; FANJUL-BOLADO, P. . Resolution of mixed dyes by in situ near infrared (NIR) spectroelectrochemistry. **Physical Chemistry Chemical Physics**, v. 21, n. 12, p. 6314-6318, 2019. https://doi.org/10.1039/C9CP00484J

JESPERSEN, N. 2006. “General principles of spectroscopy and spectroscopic analysis”. In Wilson and Wilson's Comprehensine Analytical Chemistry, Barcelom, D., Ed. Vol 47. Modern Instrumental Analysis Edited by: Ahuja, S. and Jespersen, N. 111–137.

KELLEY, D.; NATER, E. Historical sediment flux from three watersheds into Lake Pepin, Minnesota, USA. **Journal of Environmental Quality**, Madison, v. 29, n. 2, p. 561-568, 2000. https://doi.org/10.2134/jeq2000.00472425002900040051x

KLAGES, M.; HSIEH, Y. Suspended solids carried by the Gallatin River of southwestern Montana: II. Using mineralogy for inferring sources. **Journal of Environmental Quality**, Madison, v. 4, n. 1, p. 68-73, 1975. https://doi.org/10.2134/jeq1975.00472425000400010016x

LACEBY, J. P.; OLLEY, J.; PIETSCH, T. J.; SHELDON, F.; BUNN, S. E. Identifying subsoil sediment sources with carbon and nitrogen stable isotope ratios. **Hydrological Processes**,v. 29, n. 8, p. 1956-1971, 2015. https://doi.org/10.1002/hyp.10311

MARTÍNEZ-CARRERAS, N.; KREIN, A.; UDELHOVEN, T.; GALLART, F.; IFFLY, J. F.; HOFFMANN, L.; PFISTER, L.; WALLING, D. E. A rapid spectral-reflectance-based fingerprinting approach for documenting suspended sediment sources during storm runoff events. **Journal of Soils and Sediments**, v. 10, n. 3, p.400-413, 2010. https://doi.org/10.1007/s11368-009-0162-1

MCCORKLE, E. P.; BERHE, A. A.; HUNSAKER, C. T.; JOHNSON, D. W.; MCFARLANE, K. J.; FOGEL, M. L.; HART, S. C. Tracing the source of soil organic matter eroded from temperate forest catchments using carbon and nitrogen isotopes. **Chemical Geology**, v. 445, p. 172-184, 2016. https://doi.org/10.1016/j.chemgeo.2016.04.025

MOTHA, J.A.; WALLBRINK, P.J.; HAIRSINE, P.B.; GRAYSON, R.B. Tracer properties of eroded sediment and source material. **Hydrological Processes**, Chichester, v. 16, n. 10, p. 1983-2000, 2002. https://doi.org/10.1016/j.chemgeo.2016.04.025

MUKUNDAN, R.; RADCLIFFE, D. E.; RITCHIE, J. C.; RISSE, L. M.; MCKINLEY, R. A. Sediment fingerprinting to determine the source of suspended sediment in a southern Piedmont stream. **Journal of Environmental Quality**, v. 39, n. 4, p. 1328-1337, 2010. https://doi.org/10.2134/jeq2009.0405

PARIKH, S. J.; GOYNE, K. W.; MARGENOT, A. J.; MUKOME, F. N.; CALDERÓN, F. J. Soil chemical insights provided through vibrational spectroscopy. **Advances in Agronomy.** v. 126, p. 1-148, 2014. https://doi.org/10.1016/B978-0-12-800132-5.00001-8

PEART, M.R.; WALLING, D.E. Particle size characteristics of fluvial suspended sediment. In: Recent developments in the explanation and prediction of erosion and sediment yield., 1982. Exeter, 1982. p.397-407.

PENNER M.H. Basic Principles of Spectroscopy. In: Nielsen S. (eds) Food Analysis. **Food Science Text Series**. Springer, Cham, 2017.

POLYAKOV, V.; KIMOTO, A.; NEARING, M.; NICHOLS, M. Tracing sediment movement on a semiarid watershed using rare earth elements. **Soil Science Society of America Journal**, v. 73, n. 5, p. 1559-1565, 2009. https://doi.org/10.2136/sssaj2008.0378

POULENARD, J.; PERRETTE, Y.; FANGET, B.; QUETIN, P.; TREVISAN, D.; DORIOZ, J. M. Infrared spectroscopy tracing of sediment sources in a small rural watershed (French Alps). **Science of the Total Environment**, v. 407, n.. 8, p. 2808-2819, 2009. https://doi.org/10.1016/j.scitotenv.2008.12.049

SCHWANNINGER, M.; RODRIGUES, J. C.; FACKLER, K. A review of band assignments in near infrared spectra of wood and wood components. **Journal of Near Infrared Spectroscopy**, v. 19, n. 5, p. 287-308, 2011. https://doi.org/10.1255/jnirs.955

SIRVENT, J.; DESIR, G.; GUTIERREZ, M.; SANCHO, C.; BENITO, G. Erosion rates in badland areas recorded by collectors, erosion pins and profilometer techniques (Ebro Basin, NE-Spain). **Geomorphology**, Amsterdam, v. 18, n. 2, p. 61-75, 1997. https://doi.org/10.1016/S0169-555X(96)00023-2

STENBERG, B.; ROSSEL, R. A. V.; MOUAZEN, A. M.; WETTERLIND, J. Visible and near infrared spectroscopy in soil science. **Advances in Agronomy**, v. 107, p. 163-215, 2010. https://doi.org/10.1016/S0065-2113(10)07005-7

TIECHER, T.; CANER, L.; MINELLA, J. P. G.; BENDER, M. A.; DOS SANTOS, D. R. Tracing sediment sources in a subtropical rural catchment of southern Brazil by using geochemical tracers and near-infrared spectroscopy. **Soil and Tillage Research,** v. 155, p. 478-491, 2016. https://doi.org/10.1016/j.still.2015.03.001

TIECHER, T.; CANER, L.; MINELLA, J.P.G.; DOS SANTOS, D.R. Combining visible-based-color parameters and geochemical tracers to improve sediment source discrimination and apportionment. **Science of the Total Environment**, Amsterdam, v. 527, n. 135-149, 2015. https://doi.org/10.1016/j.scitotenv.2015.04.103

UBER, M.; LEGOUT, C.; NORD, G.; CROUZET, C.; DEMORY, F.; POULENARD, J. Comparing alternative tracing measurements and mixing models to fingerprint suspended sediment sources in a mesoscale Mediterranean catchment. **Journal of Soils and Sediments**, v.19, n. 9, p. 3255-3273, 2019. https://doi.org/10.1007/s11368-019-02270-1

UPADHAYAY, H. R.; SMITH, H. G.; GRIEPENTROG, M.; BODÉ, S.; BAJRACHARYA, R. M.; BLAKE, W.; BOECKX, P. Community managed forests dominate the catchment sediment cascade in the mid-hills of Nepal: A compound-specific stable isotope analysis. **Science of the Total Environment**, v. 637, p. 306-317, 2018. https://doi.org/10.1016/j.scitotenv.2018.04.394

VIRGO, K.; MUNRO, R. Soil and erosion features of the Central Plateau region of Tigrai, Ethiopia. **Geoderma**, Amsterdam, v. 20, n. 2, p. 131-157, 1978. https://doi.org/10.1016/0016-7061(78)90040-X

VISCARRA ROSSEL, R.; WALVOORT, D. J. J.; MCBRATNEY, A. B.; JANIK, L. J.; SKJEMSTAD, J. O. Visible, near infrared, mid infrared or combined diffuse reflectance spectroscopy for simultaneous assessment of various soil properties. **Geoderma,** v.131, n. 1-2, p. 59-75, 2006. https://doi.org/10.1016/j.geoderma.2005.03.007

WALDEN, J.; SLATTERY, M.C.; BURT, T.P. Use of mineral magnetic measurements to fingerprint suspended sediment sources: approaches and techniques for data analysis. **Journal of Hydrology**, Amsterdam, v. 202, n. 1, p. 353-372, 1997. https://doi.org/10.1016/S0022-1694(97)00078-4

WALLBRINK, P.J.; MURRAY, A.S. Use of fallout radionuclides as indicators of erosion processes. **Hydrological Processes**, Chichester, v. 7, n. 3, p. 297-304, 1993. https://doi.org/10.1002/hyp.3360070307

WALLING, D. E.; WOODWARD, J. C.; NICHOLAS, A. P. A multi-parameter approach to fingerprinting suspended-sediment sources. **IAHS publication**, v. 215, p. 329-338, 1993.

WALLING, D.; PEART, M. Suspended sediment sources identified by magnetic measurements. **Nature**, v. 281, n. 110-113, 1979. https://doi.org/10.1038/281110a0

WALLING, D.; WOODWARD, J. Tracing sources of suspended sediment in river basins: a case study of the River Culm, Devon, UK. **Marine and Freshwater Research**, Collingwood, v. 46, n. 1, p. 327-336, 1995. https://doi.org/10.1071/MF9950327

WALLING, D.E. Linking land use, erosion and sediment yields in river basins. In: GARNIER, J. M., J-M, Ed. **Man and River Systems**, Springer. 1999. p.223-240. https://doi.org/10.1007/978-94-017-2163-9_2

WALLING, D.E. Tracing suspended sediment sources in catchments and river systems. **Science of the Total Environment**, Amsterdam, v. 344, n. 1, p. 159-184, 2005. https://doi.org/10.1016/j.scitotenv.2005.02.011

WELTJE, G.J. Quantitative models of sediment generation and provenance: state of the art and future developments. **Sedimentary Geology**, Amsterdam, v. 280, n. 4-20, 2012. https://doi.org/10.1016/j.sedgeo.2012.03.010

WEYER, L. G.; LO, S. C. Spectra–structure correlations in the near-infrared. **Handbook of vibrational spectroscopy**, p. 1-21, 2006. https://doi.org/10.1002/0470027320.s4102

WILKINSON, S.N.; HANCOCK, G.J.; BARTLEY, R.; HAWDON, A.A.; KEEN, R.J. Using sediment tracing to assess processes and spatial patterns of erosion in grazed rangelands, Burdekin River basin, Australia. **Agriculture, Ecosystems & Environment**, Amsterdam, v. 180, n. 90-102, 2013. https://doi.org/10.1016 / j.agee.2012.02.002

YU, L.; OLDFIELD, F. A multivariate mixing model for identifying sediment source from magnetic measurements. **Quaternary Research**, San Diego, v. 32, n. 2, p. 168-181, 1989. https://doi.org/10.1016/0033-5894(89)90073-2

ZHANG, Q.; LEI, T.; ZHAO, J. Estimation of the detachment rate in eroding rills in flume experiments using an REE tracing method**. Geoderma**, Amsterdam, v. 147, n. 1, p. 8-15, 2008. https://doi.org/10.1016/j.geoderma.2008.07.002

ZHANG, Y.; COLLINS, A. L.; MCMILLAN, S.; DIXON, E. R.; CANCER-BERROYA, E.; POIRET, C.; STRINGFELLOW, A. Fingerprinting source contributions to bed sediment-associated organic matter in the headwater subcatchments of the River Itchen SAC, Hampshire, UK. **River Research and Applications**, v. 33, n. 10, p. 1515-1526, 2017. https://doi.org/10.1002/rra.3172

3 SEDIMENT SOURCE APPORTIONMENT USING OPTICAL PROPERTY COMPOSITE SIGNATURES AT DIFFERENT SCALES IN A RURAL CATCHMENT, BRAZIL

Abstract

Identifying the key sources of fine-grained sediment is essential for protecting and improving soil and water quality. Accordingly, this contribution tested a combination of low-cost analytical procedures for assembling information on key sediment sources in an agricultural catchment in Brazil and in so doing, tested 24 components derived from a conventional printer scanner using various colourimetric models, 18 organic compounds derived from NIR spectra and 13 soil constituents derived from MIR spectra. In combining the application of these low-cost tracers, the study also aimed to investigate potential scale-dependency in sediment sources. Four main sediment sources were sampled: (i) sugarcane (SC); (ii) unpaved roads (UR); (iii) cropland (CL), and; (iv) channel banks (CB) and samples were collected from these at two different scales; sub-catchment (~1,453 km^2) and catchment-wide (~ 2,857 km^2). At both scales, CB was the most important sediment source followed by SC. At catchment-wide scale, CB accounted for 75.9 ± 6.7%, 56.4 ± 16.3%, 39.1 ± 20.7% and 68.3 ± 4.9% of sampled suspended sediment using composite signatures comprising NIR, MIR or colour tracers only, or a combination of all three types of low-cost tracers, respectively. For bed sediment samples, the corresponding respective source contributions were estimated to be 43.4 ± 4.7%, 32.8 ± 7.8%, 49.2 ± 18.6% and 32.0 ± 4.6%. Our results, regardless of optical property, target sediment type, or scale, suggest that CB represents the primary source of the sediment problem in the study catchment. Targeted remedial actions therefore especially need to deliver protection for eroding channel banks.

Keywords: Sediment fingerprinting. Catchment management. Near-infrared. Mid-infrared. Colour. Bayesian modelling.

3.1 Introduction

Quantifying key sources of fine-grained sediment is essential for targeting remedial actions for protecting the sustainability of soil and water resources. Information on source contributions is increasingly assembled using sediment source fingerprinting procedures (WALLING, 2013; OWENS et al., 2016; COLLINS et al., 2017; TANG et al., 2019). Conventionally, many fingerprinting studies have relied on sediment samples collected at the study catchment outlet only, drawing general management implications on that basis. More recently, however, investigators have been reminded that this type of sediment sampling strategy ignores the important role of connectivity and scale-dependency, resulting in a potential mismatch between sediment management recommendations and the evolution of the sources of the sediment problem across scales. Koiter et al. (2013), for example, investigated hydrogeomorphic connectivity and scale issues for sediment fingerprinting using a nested sampling approach in a catchment on the Canadian prairies. They estimated contributions ranging from 64% to 85% for topsoil sources in the upper reaches and 32% to 51% and 29% to 40% for streambank and shale bedrock sources in the lower reaches, respectively. Critically, these three sampled sources would have been estimated to have contributed equally if suspended sediment had been collected only at the overall outlet. It is therefore important to sample sediment at different scales to ensure that any potential switches in source dominance are captured and appropriate catchment management strategies are devised (KLAGES; HSIEH, 1975). This inevitably increases resource demands and it may therefore be necessary to rationalize sediment sampling by targeting important sub-catchments identified as having erosion and sediment problems, as well as the overall outlet.

Agricultural activities have been identified as a significant source of sediment and associated nutrients and contaminants with widespread soil degradation triggered by agricultural expansion to satisfy biofuel and food demand (ŽIVKOVIĆ; VELJKOVIĆ, 2018; CALICIOGLU et al., 2019; SHRESTHA; STAAB; DUFFIELD, 2019). In many areas of Brazil, land use changes have been driven by the production of biofuels, responsible for 42% of the country's renewable energy supply and with a prospect of more than a 40% increase in ethanol production over the next 10 years (OECD-FAO, 2018). Recent sediment sourcing studies in Brazil suggest that agriculture accounts for 48 % to 91 % of the sediment export (VALENTE et al., 2020; TIECHER et al., 2019; MINELLA et al., 2009; TIECHER et al., 2017a). In other countries, it has been estimated that agriculture contributes from 22 % to 56% of the sediment export from selected catchments (COLLINS et al., 2010; EVRARD et

al., 2019). In Brazil, land use change associated with the expansion of sugar cane crops for food and fuel supply is often associated with high soil loss rates (COUTO JÚNIOR et al., 2019), but Minella et al. (2018) observed a decrease in sediment yield from 400 t km^{-2} $year^{-1}$ to 50 t km^{-2} $year^{-1}$ after the adoption of soil conservation practices in an agricultural catchment, highlighting the utility of reliable sediment source apportionment data for guiding best management.

The fingerprinting approach has undergone numerous procedural changes over the past 40 years associated with the increasing use of multiple tracer properties (nutrients, contaminants, radionuclides, isotopes, elemental geochemistry) in composite signatures, statistical tests for confirming source discrimination, and un-mixing modelling with uncertainty analysis for source apportionment (WALLING; WOODWARD; NICHOLAS, 1993; COLLINS; WALLING; LEEKS, 1997a; WALLING et al., 2013; NOSRATI et al., 2014; TIECHER et al., 2015; LIU et al., 2017; COLLINS et al., 2017; ZHANG et al., 2017; NOSRATI and COLLINS, 2019; UBER et al., 2019). In tandem with the evolution of fingerprinting procedures, the use of non-destructive analysis of tracer properties including Portable X-ray fluorescence (XRF), colour scanning and the measurement of visible (VIS), near infrared (NIR) or medium infrared (MIR) spectra has increased (COLLINS et al., 2013, 2014; TIECHER et al., 2016, 2017b; ZHANG et al., 2017; ASTORGA et al., 2018; PULLEY et al., 2016, 2018; TURNER; TAYLOR, 2018). These studies have typically demonstrated the utility of the spectra generated by a specific low-cost procedure, rather than assessing the potential of the spectral information generated by a combination of low-cost laboratory methods. Accordingly, and to address this research gap, this contribution tested a combination of low-cost analytical procedures for assembling information on key sediment sources in an agricultural catchment in Brazil and in so doing, tested 24 components derived from a conventional printer scanner using various colourimetric models, 18 organic compounds derived from NIR spectra and 13 soil constituents derived from MIR spectra. In combining the application of these low-cost tracers, the study also aimed to investigate potential scale-dependency in sediment sources by comparing the results at a sub-catchment and catchment-wide scale.

3.2 Materials and methods

3.2.1 Study catchment description

The Goiana catchment drains an area of ~ 2,857 km^2 and is located in the northeast region of Brazil (203,808 - 292,248 mE and 9,183,026 - 9,126,146 mS). This catchment comprises the Capibaribe mirim sub-catchment, which constitutes ~54% (i.e. 1,453 km^2) of the total catchment area (Figure 1). The growing agricultural development along the Goiana watershed – a vital water resource for more than 26 municipalities and 465.500 inhabitants – poses an environmental threat due to the increase in sediment and contaminant transfer to the water resources. This watershed was chosen due to the high evidence of erosion processes, which is aggravated by sugarcane agricultural activities along the riverbanks. Both the total catchment area and sub-catchment are affected by domestic sewage and wastewater from industrial and agricultural production, mainly sugarcane farming and processing.

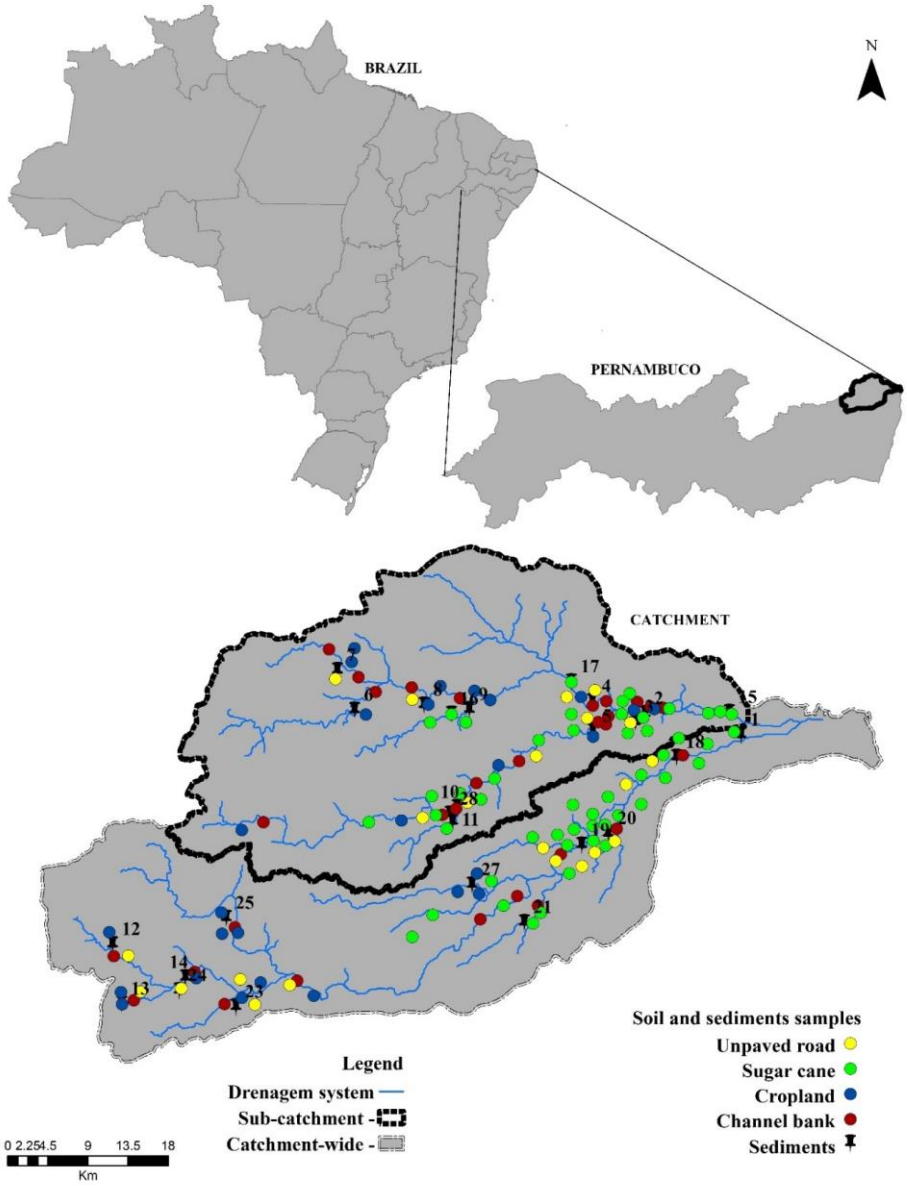

Figure 1. Map showing the locations of the sampling sites for sources and sediment in the Goiana study catchment

The climate of the study region is classified as "Ams" (Köppen classification scheme). The average annual rainfall ranges from 1000 to 2200 mm. The wettest period is March-July. A small portion (southwestern) of the study catchment crosses a semiarid region and exhibits average annual rainfall ranging from 1150 to 850 mm. The average annual air temperature is 24 °C. Relief is predominantly soft to moderately undulating (slopes of 3% to 12%), while in the western portion of the study catchment, there is a predominance of steeper slopes (> 20%) (Figure 2a).

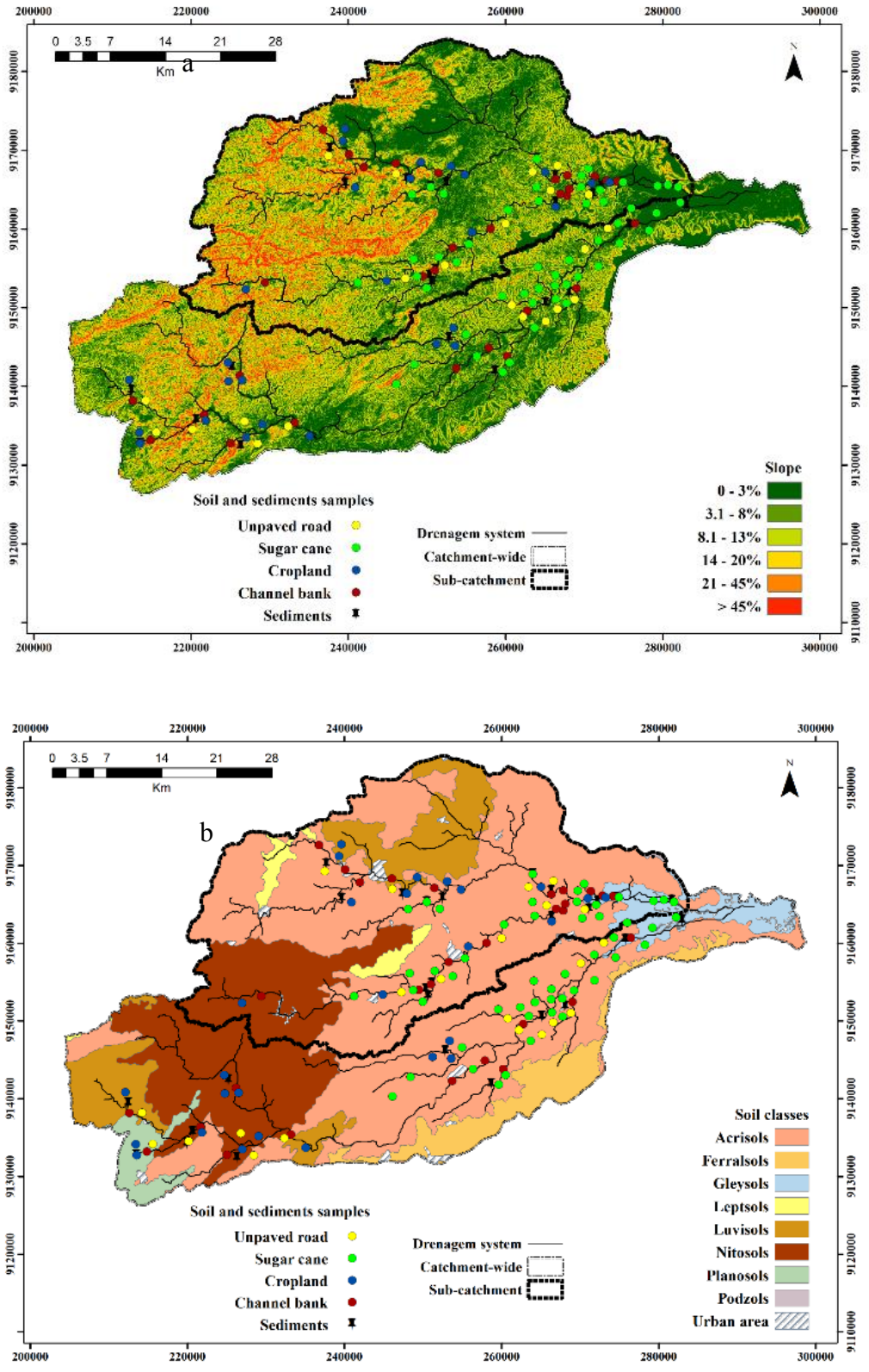

Figure 2. Slope (a) and soil (b) maps, showing the sampling sites for sources and sediment in the Goiana study catchment

Soils (Figure 2b) are mostly Acrisols (56.4%), Nitosols (19.7%), Luvisols (11%), Leptsols (3%) and Gleisols (2%) according to the World Reference Base for Soil Resources (WRB; IUSS Working Group WRB, 2006; 1:5000 scale). Field observations suggest that the Capibaribe mirim sub-catchment is particularly prone to erosion and sediment-related proboems, and so this study compared source apportionment estimates for this sub-catchment and for the entire study catchment to assess any potential change in the importance of individual sediment sources across these two scales.

3.2.2 Source material sampling

Sampling sites for potential sediment sources were identified by observing the sediment mobilization and transport processes within the study catchment. Four main sediment sources were identified on this basis: (i) sugarcane (SC); (ii) unpaved roads (UR); (iii) cropland (CL), and; (iv) channel banks (CB). Areas under pasture and other less expansive cultivation such as beans and banana were merged with CL. To generate representative source material sample sets, a composite sample was collected at each sampling location for each source category and each composite comprised 10 sub samples. Surface soil sampling locations were targeted at sites visibly connected to the river network and with evidence of erosion processes. At the catchment-wide scale (Figure 1), the numbers of composite samples retrieved per source category were as follows: SC (n = 53); UR (n = 22); CL (n = 26), and; CB (n = 30). Within sub-catchment 1 (Fig. 1), the corresponding source sample numbers were: SC (n = 27); UR (n = 9); CL (n = 14), and; CB (n = 18).

3.2.3 Suspended and bed sediments sampling

A total of 41 sediment samples were collected, comprising 13 suspended (SS) and 28 bed sediment (BS) samples. These two types of target sediment sample were retrieved to represent both high and low water discharge regimes. Both types of target sediment were collected at locations 1, 2, 3, 4, 7, 8, 9, 11, 19, 21, 22, 24 and 26 in Fig. 1. Only BS samples were collected at locations 5, 6, 10, 12, 13, 14, 15, 16, 17, 18, 20, 23, 25, 27 and 28 in Fig. 1. SS was sampled using time-integrated mass-flux samplers in duplicate at each location (TIMS; PHILLIPS; RUSSELL; WALLING, 2000). Composite BS samples were collected using steel shovels and stored in plastic containers, which were transported to the laboratory. Each composite sample was composed of ten replicate samples which were bulked into the composite.

3.2.4 Laboratory work and analyses

3.2.4.1 Size distribution

Sediment samples were oven-dried at 50 °C, and gently disaggregated using a pestle and mortar, and then sieved to <63 μm. The grain size distributions of the target sediment samples were analysed by laser granulometry, using 2 g of either SS or BS sample, after oxidation of the organic matter content with 100-150 mL of H_2O_2 5%, and heating on a hot plate to 60 °C. NaOH was used to provide chemical dispersion (MUGGLER; PAPE; BUURMAN, 1997).

3.2.4.2 Colourimmetry

For the analysis of colour tracers, samples were placed into clear polythene bags prior to being scanned using a HP Office pro 8710-colour scanner. All source material and target sediment samples were digitized. Scanned images were imported into GIMP 2 open source image editing software. The intensity of reflected measurements of source material or sediment sample colour was based on averaging regions of each spectrum corresponding to the blue (B: 450–520 nm), green (G: 520–600 nm) and red (R: 600–690 nm) colours that were extracted. The RGB model is an additive model, which uses combinations of different intensities of red, green and blue light to reproduce a broad array of secondary colours. Using RGB values, 24 colour parameters (i.e. Decorrelated RGB, CIE xyY, CIEXYZ, CIE Lab, CIE Luv, CIE LHC, Munsell HVC, Helmholtz chromaticity coordinates and Redness Index (RI)) were generated using the ColoSol software developed by Viscarra Rossel (2004) to perform both single tristimulus and multiple colour space transformations (Table 1).

Table 1. Tracers from different colour space models calculated using the ColoSol software

Colour space model	Colour tracer	Tracer abbreviation
RGB	Red	R
	Green	G
	Blue	B
Decorrelated RGB	Hue	H_{RGB}
	Light intensity	I_{RGB}
	Chromatic information	S_{RGB}
CIE xyY	Chromatic coordinate x	x
	Chromatic coordinate y	y
	Brightness	Y
CIE XYZ	Virtual component X	X
	Virtual component Z	Z
CIE Luv	Metric lightness function	L
	Chromatic coordinate opponent red–green scales	u*
	Chromatic coordinate opponent blue–yellow scales	v*
CIE Lab	Chromatic coordinate opponent red–green scales	a*
	Chromatic coordinate opponent blue–yellow scales	b*
CIE Lch	CIE chroma	c*
	CIE hue	h*
Munsell HVC	Hue	H
	Value	V
	Chroma	C
Helmholtz chromaticity	Dominant wavelength	λ_d (nm)
	Purity of excitation	P_e
Index	Redness Index	RI

The RGB system forms a cube comprising orthogonal R, G and B axes. A mixture of these three primary colours can produce every colour. Decorrelated RGB is a transformation of highly correlated RGB values into three statistically independent components. In the CIE

xyY system, Y represents luminance and x and y represent colour variations from blue to red and blue to green, respectively. In the case of the CIE Lab and CIE Luv models, L represents brightness or luminance, and a* and b* and u* and v* represent chromaticity coordinates as opponent red–green and blue–yellow scales. The CIE Lhc model represents a transformation of the CIE Lab spherical colour space into cylindrical coordinates, resulting in hue (h*) and chroma (c*) values. The Munsell HVC system is commonly used in soil science and describes the soil colour using hue (H), value (V) and chroma (C). Helmholtz chromaticity coordinates describe luminescence (L), dominant wavelength (λd), purity of excitation (Pe) and redness index (RI) for the estimation of haematite content in soil (VISCARRA ROSSEL et al., 2006).

3.2.4.3 Near Infrared Spectroscopy (NIRS)

NIR absorbance measurements were performed in reflectance mode, every 0.5 nm from 850 to 2500 nm (10000 – 4000 cm-1), using a NIRS DS2500 F spectrometer. All source material and target sediment samples were run five-fold with the average of these repeat runs used in subsequent statistical analysis and numerical un-mixing modelling. NIR data were finalised using scatter correction SNV + D, standard normal variate and detrending. The absorbance values of the peaks from NIR spectra were used to provide fingerprints of the spectral regions of organic properties (Table 2). Simple linear interpolation was performed with the spectra derived from the NIR results of Equation 1, thereby avoiding the need to develop predictive regression models for specific constituents of organic matter (COLLINS et al., 2013, 2014; ZHANG et al., 2017).

Table 2. Spectral regions of soil organic compost properties

ID	Property	Wave (nm)	ID	Property	Wave (nm)	ID	Property	Wave (nm)
Np1_1	Cellulose	2352	Np5_24	$CONH_2$	2030	Np10_47	ROH	2080
Np1_2	Cellulose	2336	Np5_25	$CONH_2$	1960	Np11_48	Starch	2461
Np1_3	Cellulose	1820	Np5_26	$CONH_2$	1520	Np11_49	Starch	2276
Np1_4	Cellulose	1780	Np5_27	$CONH_2$	1490	Np11_50	Starch	2252
Np1_5	Cellulose	1490	Np5_28	$CONH_2$	1483	Np11_51	Starch	2100
Np2_6	CH_2	2323	Np5_29	$CONH_2$	1460	Np11_52	Starch	1900
Np2_7	CH_2	2310	Np5_30	$CONH_2$	1430	Np11_53	Starch	1540
Np2_8	CH_2	1765	Np6_31	CONH.CONHR	2000	Np11_54	Starch	1528
Np2_9	CH_2	1725	Np6_32	CONH.CONHR	2110	Np12_55	$ArNH_2$	1492
Np2_10	CH_2	1415	Np7_33	CONHR	2160	Np12_56	$ArNH_2$	1020
Np2_11	CH_2	1395	Np7_34	CONHR	1490	Np13_57	AROH	1420
Np2_12	CH_2	1215	Np7_35	CONHR	1471	Np13_58	AROH	1000
Np2_13	CH_2	1053	Np8_36	HC=CH	1940	Np14_59	Aromatic	1685
Np3_14	CH_3	2280	Np8_37	HC=CH	2190	Np14_60	Aromatic	1446
Np3_15	CH_3	1705	Np8_38	HC=CH	2140	Np14_61	Aromatic	1417
Np3_16	CH_3	1695	Np8_39	HC=CH	1170	Np14_62	Aromatic	1143
Np3_17	CH_3	1360	Np8_40	HC=CH	2180	Np15_63	C=H	1533
Np3_18	CH_3	1195	Np8_41	HC=CH	1980	Np16_64	CH	1440
Np3_19	CH_3	1152	Np8_42	HC=CH	1510	Np16_65	CH	1225
Np3_20	CH_3	1015	Np8_43	HC=CH	1020	Np17_66	RNH_2	1530
Np4_21	CONH	1920	Np9_44	Protein	2380	Np17_67	RNH_2	1060
Np5_22	$CONH_2$	2150	Np9_45	Protein	1520	Np17_68	RNH_2	1030
Np5_23	$CONH_2$	2050	Np9_46	Protein	1410	Np18_69	Starch, Glucose	1580

For those peaks that have no measurements at the specified exact wavelengths, linear interpolation was undertaken to estimate the absorption ratio (Ynew) for a given wavelength (Xnew) based on measured absorption ratios at neighbouring wavelengths as below:

$$Ynew = \frac{y1 + (xnew - x1) * (y2 - y1)}{(x2 - x1)} \quad (1)$$

where x1 and x2 are the bounding wavelengths, which contain Xnew and have measured ratios. y1 and y2 are the corresponding absorption ratios at x1 and x2, respectively.

3.2.4.4 Mid Infrared Spectroscopy (MIR)

MIR spectra were measured using an Alpha FTIR spectrometer (Bruker Optik GmbH, Ettlingen, Germany), which collects spectra in the mid infrared (4000 – 500 cm^{-1}) region using diffuse reflectance mode (DRIFT) sampling. Each MIR spectrum was the average of 32 scans collected at a resolution of 4 cm^{-1}. Prior to scanning source and sediment samples, a reference gold standard was scanned as the background. The purpose of the background measurement is to detect the influence of the ambient conditions (e.g., humidity, temperature, etc.) and the spectrometer itself on the spectroscopic measurements. After measurements, the instrument's OPUS software automatically calculates the final spectrum by dividing the sample spectrum by the background spectrum. As such, spectral bands that resulted from the ambient conditions and/or the spectrometer are eliminated. Using corrections based on SNV + D, standard normal variate and detrending, MIR spectral regions of tracer properties (Table 3) were selected (MADEJOVÁ; GATES; PETIT, 2017; TIECHER et al., 2017a; ASTORGA et al., 2018) and linear interpolation was performed using equation 1.

Table 3. Spectral regions selected of soil constituent properties

ID	Property	Wave (cm^{-1})	ID	Property	Wave (cm^{-1})	ID	Property	Wave (cm^{-1})
Mp1_1	Kaolinite	3695	Mp3_31	Muscovite	753	Mp7_61	Quartz	1878
Mp1_2	Kaolinite	3694	Mp3_32	Muscovite	692	Mp7_62	Quartz	1790
Mp1_3	Kaolinite	3690	Mp3_33	Muscovite	535	Mp7_63	Quartz	1628
Mp1_4	Kaolinite	3669	Mp4_34	Vermiculite	3676	Mp7_64	Quartz	1527
Mp1_5	Kaolinite	3652	Mp4_35	Vermiculite	3607	Mp7_65	Quartz	814
Mp1_6	Kaolinite	3620	Mp4_36	Vermiculite	3436	Mp8_66	HIV	1628
Mp1_7	Kaolinite	1628	Mp4_37	Vermiculite	1004	Mp8_67	HIV	1157
Mp1_8	Kaolinite	1157	Mp4_38	Vermiculite	816	Mp8_68	HIV	1111
Mp1_9	Kaolinite	1111	Mp4_39	Vermiculite	652	Mp8_69	HIV	1018
Mp1_10	Kaolinite	1018	Mp4_40	Vermiculite	527	Mp8_70	HIV	814
Mp1_11	Kaolinite	915	Mp5_41	Micas	3620	Mp8_71	HIV	702
Mp1_12	Kaolinite	814	Mp5_42	Micas	1628	Mp9_72	Gibbsite	1111
Mp1_13	Kaolinite	702	Mp5_43	Micas	1157	Mp9_73	Gibbsite	814
Mp1_14	Kaolinite	600	Mp5_44	Micas	1111	Mp10_74	Clay	3644
Mp2_15	Smectite	3680	Mp5_45	Micas	1018	Mp10_75	Clay	3666
Mp2_16	Smectite	3650	Mp5_46	Micas	702	Mp10_76	Clay	3668
Mp2_17	Smectite	3630	Mp6_47	Ilite	3623	Mp11_77	Carbonates	1445
Mp2_18	Smectite	3620	Mp6_48	Ilite	1100	Mp11_78	Carbonates	1798
Mp2_19	Smectite	1628	Mp6_49	Ilite	1030	Mp11_79	Carbonates	2534
Mp2_20	Smectite	1157	Mp6_50	Ilite	916	Mp11_80	Carbonates	2881
Mp2_21	Smectite	1111	Mp6_51	Ilite	831	Mp11_81	Carbonates	2997
Mp2_22	Smectite	1018	Mp6_52	Ilite	801	Mp12_82	Iron oxides	600
Mp2_23	Smectite	915	Mp6_53	Ilite	780	Mp12_83	Iron oxides	700
Mp2_24	Smectite	702	Mp6_54	Ilite	756	Mp13_84	Iron oxyhydroxide	3100
Mp3_25	Muscovite	3659	Mp6_55	Ilite	693	Mp13_85	Iron oxyhydroxide	900
Mp3_26	Muscovite	3627	Mp6_56	Ilite	524	Mp13_86	Iron oxyhydroxide	800
Mp3_27	Muscovite	1028	Mp7_57	Quartz	1994			
Mp3_28	Muscovite	933	Mp7_58	Quartz	1975			
Mp3_29	Muscovite	831	Mp7_59	Quartz	1801			
Mp3_30	Muscovite	804	Mp7_60	Quartz	1867			

HIV, hydroxy-interlayered vermiculite

3.2.4.5 Tracer data processing for sediment source discrimination and apportionment

The first critical step in the processing of the tracer data involved checking the conservativeness of the optical tracers using exploratory data analysis such as boxplots. A

stepwise discriminant function analysis (DFA), based on the minimization of Wilks' lambda at the 0.05 level of significance, was then used to determine which conservative tracers were capable of discriminating between the potential sampled sediment sources on the basis of their integration into composite signatures.

The estimation of source contributions to the target SS and BS samples was undertaken for the catchment-wide and sub-catchment scales (Figure 1) using the MixSIAR model. The Markov Chain Monte Carlo (MCMC) parameters in MixSIAR were set as follows: number of chains = 3; chain length = 3,000,000; burn = 2,700,000; thin = 300. Convergence of un-mixing models was evaluated using the Gelman-Rubin diagnostic, rejecting the model output if any variable was above 1.0.

We use virtual mixtures to measure the effectiveness of sediment mix samples in predicting the contribution to sediment sources. The virtual mix models were found by calculating the results of the MixSIAR model for mixtures of sediments with the given source and tracers selected by the discriminant analysis and added with the other sources thus obtaining 1 (one) virtual sample (PHILLIPS; GREGG, 2003), equation 2.

$$y = \sum_{i=1}^{n} k_i f_i \tag{2}$$

where y = Virtual mixture, k = result from specific source MixSIAR model using mixtures of sediments, n = number of tracers, i =tracer and f = source. Furthermore, the virtual mixtures tests were assessed using root mean squared error (RMSE) and mean absolute error (MAE).

$$RMSE = \sqrt{\frac{\sum_{i=1}^{n}(Ypredicted - Yknown)^2}{n}} \tag{3}$$

$$\text{MAE} = \frac{\sum_{t=1}^{n}|Ypredicted - Yknown|}{n} \tag{4}$$

where YPredicted is the percentage source contribution predicted by the model, YKnown is the known percentage source contribution in the artificial mixture, and n represents the number of sediment sources (n = 3). This step is important to evaluate the

ability of the models to predict the optical properties measured in the target SS or BS samples. All statistical analyses and un-mixing modelling were carried out using R software (version 3.6.1, R Core team, 2019) with the klaR (ROEVER et al., 2018), MASS (VENABLES; RIPLEY, 2002) and MixSIAR (STOCK; SEMMENS, 2016) packages in the library.

3.3 Results and Discussion

3.3.1 Particle size distributions

The d_{90} of the target sediment samples (Figure 2) was used to select the appropriate particle size fraction for sieving the source material samples for comparison of optical tracer properties. These data suggested that the <32 µm (nearest sieve mesh size to 38 µm available to the research team) fraction was most appropriate for comparing the optical tracers in source materials and both target sediment types.

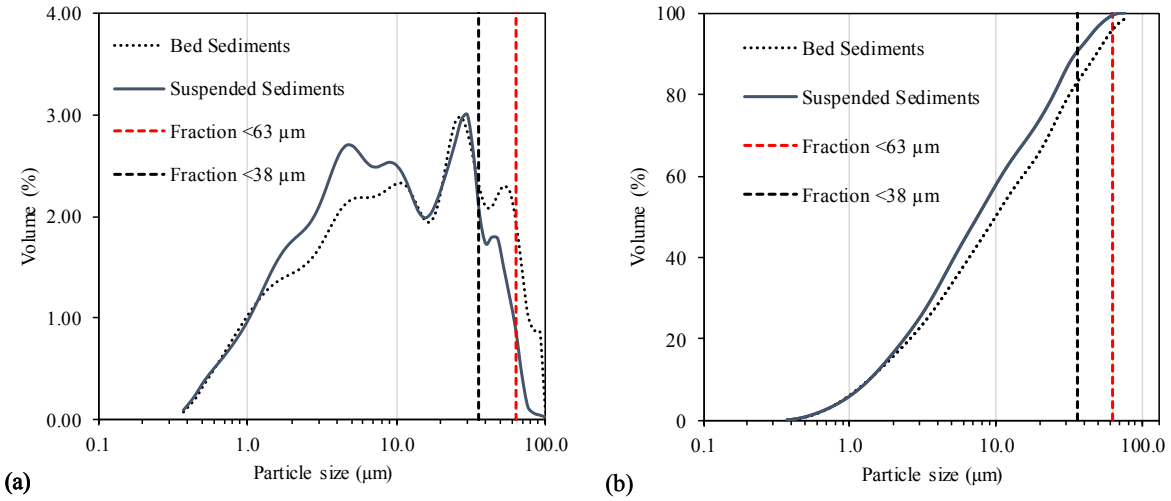

Figure 3. Average (a) and cumulative (b) particle size distributions of BS (n=4) samples and SS (n= 4) samples

3.4 Comparisons of tracer properties to assess conservative behaviour

3.4.1 Colour tracers

Non-conservative colour tracers were removed from further analysis based on the boxplot range test. At catchment-wide scale (Figure 4), all tracers were conservative. At sub-

catchment scale, the tracer y was removed due to evidence for non-conservative behaviour. Supplementary results for sub-catchment scale are presented in Figure S1 and S2.

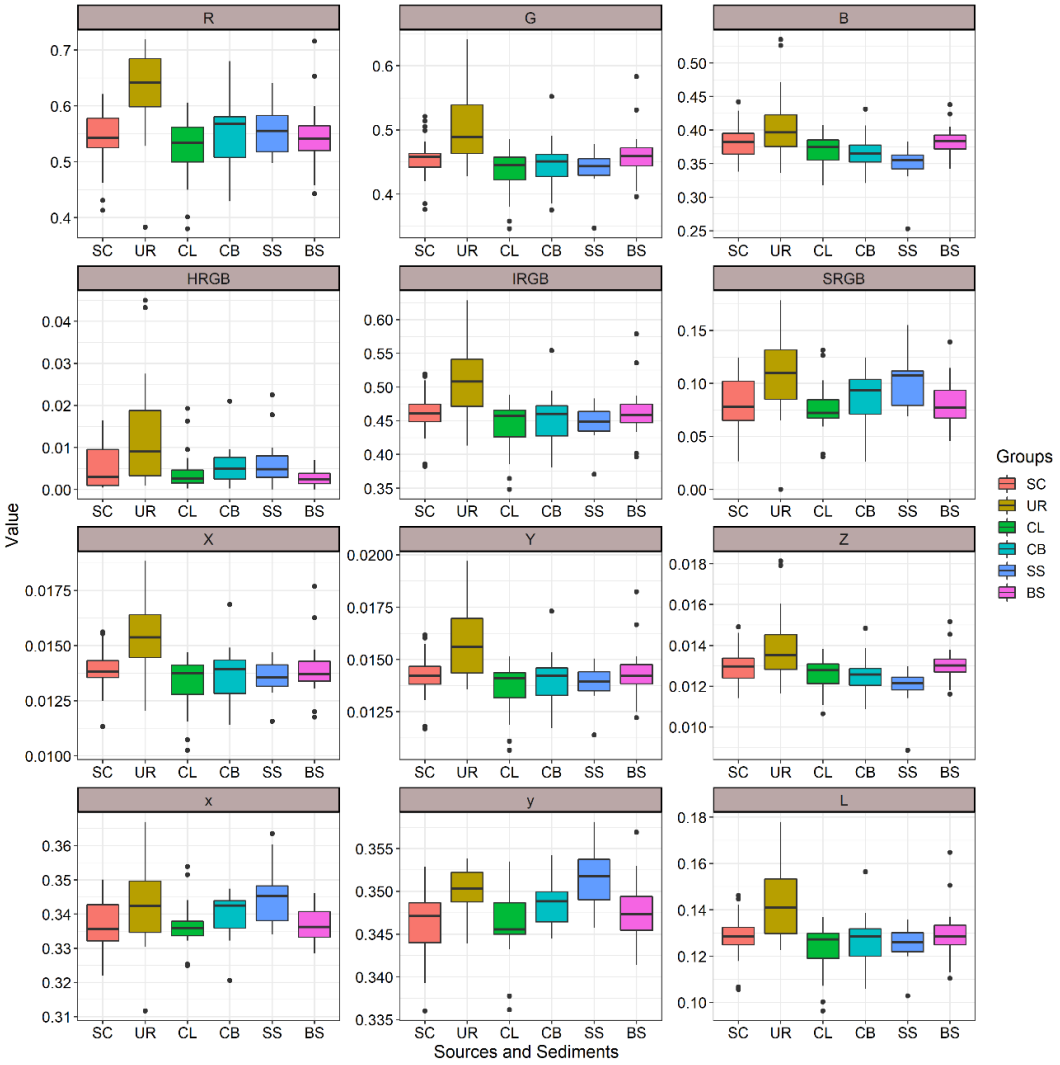

Figure 4. Example comparison of distributions of colour tracers for assessing conservative behaviour at catchment-wide scale. The median is shown by the central line, the interquartile range by the box, the range by the vertical line and outliers by the circles.

3.4.2 Near Infrared Spectroscopy (NIR)

Figure 5 presents a comparison of example NIR tracers (Np1_1, Cellulose property (1), wavelength 2352 cm^{-1} scans 1 to 3) at catchment-wide scale. At this scale, 12 tracers (Np1_1, Np1_3, Np2_7, Np3_16, Np3_20, Np5_22, Np7_35, Np8_37, Np11_50, Np11_52 and Np14_59) were removed due to evidence for non-conservatism. At sub-catchment scale, 14 tracers were ruled out (Np1_1, Np1_3, Np2_7, Np3_16, Np5_22, Np5_29, Np5_30, Np6_31, Np7_35, Np11_50, Np11_51, Np14_59, Np16_64). It should be noted that many of the

tracers removed belong to the wavelength present in the combination band area (1900 - 2500 nm). Fig. S3 and S4 provide the full dataset for the assessment of NIR tracer conservative behaviour.

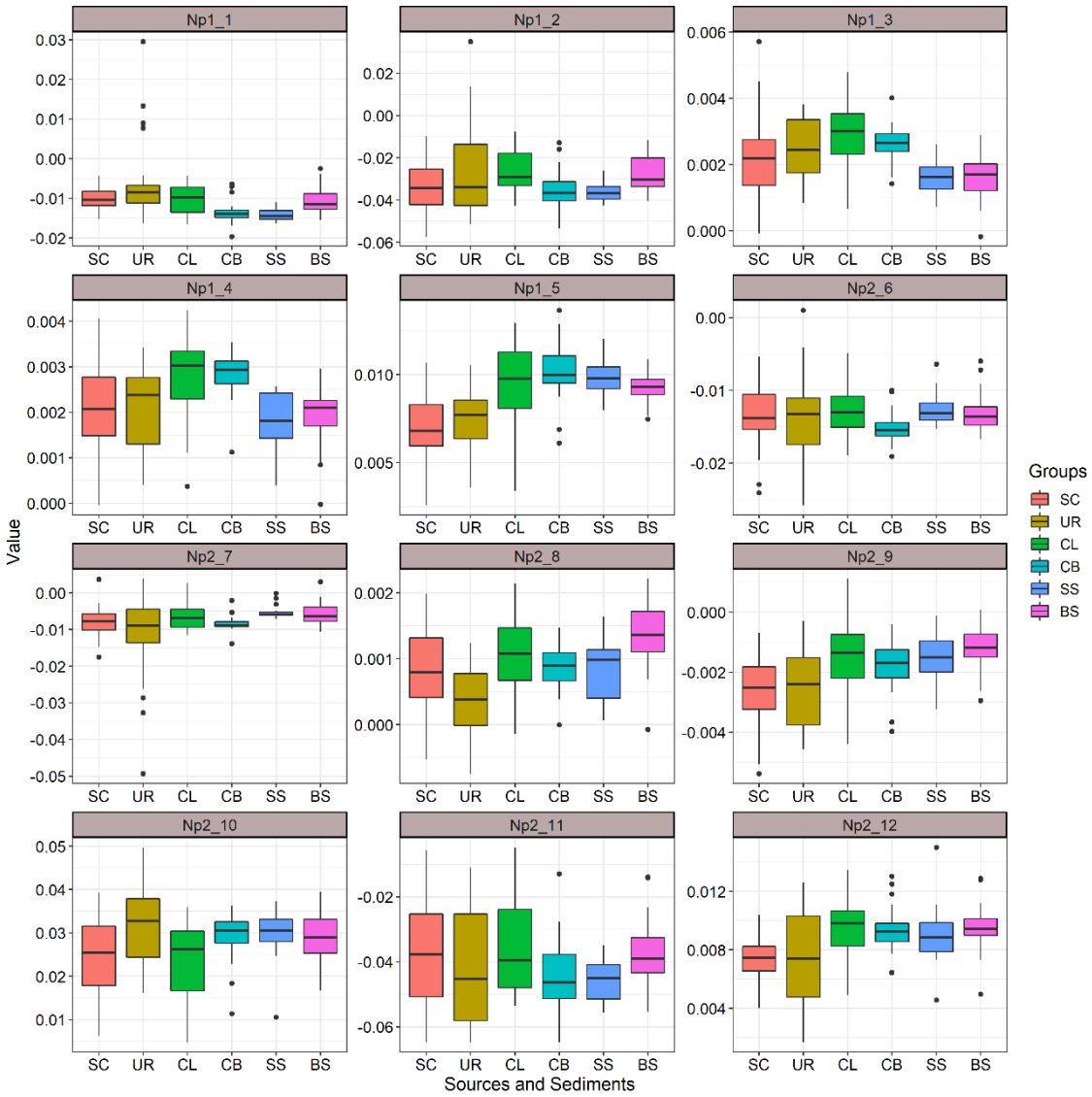

Figure 5. Example comparison of distributions of NIR tracers for assessing conservative behaviour at catchment-wide scale

The properties of organic constituents showed more marked variations in the CL sediment source. This was especially the case for carboxylate (C=H), starch + glucose, starch, protein, amide ($CONH_2$), carbohydrates and aromatic amine ($ArNH_2$) which are present in the formation of organo-mineral complexes (soil aggregates). These organic compounds are located at wavelength region 1460 to 1920 nm occurring in overtone ($\nu 1$) characterised by low electron excitation energy.

3.4.3 Mid Infrared Spectroscopy (MIR)

The evaluation of conservative behaviour of MIR tracers (Figure 6) showed that the Mp1_14 and Mp4_35 tracers at catchment-wide scale and Mp12_82 at the sub-catchment scale should be discarded from further analysis. The full MIR dataset is provided in Figure S5 and S6.

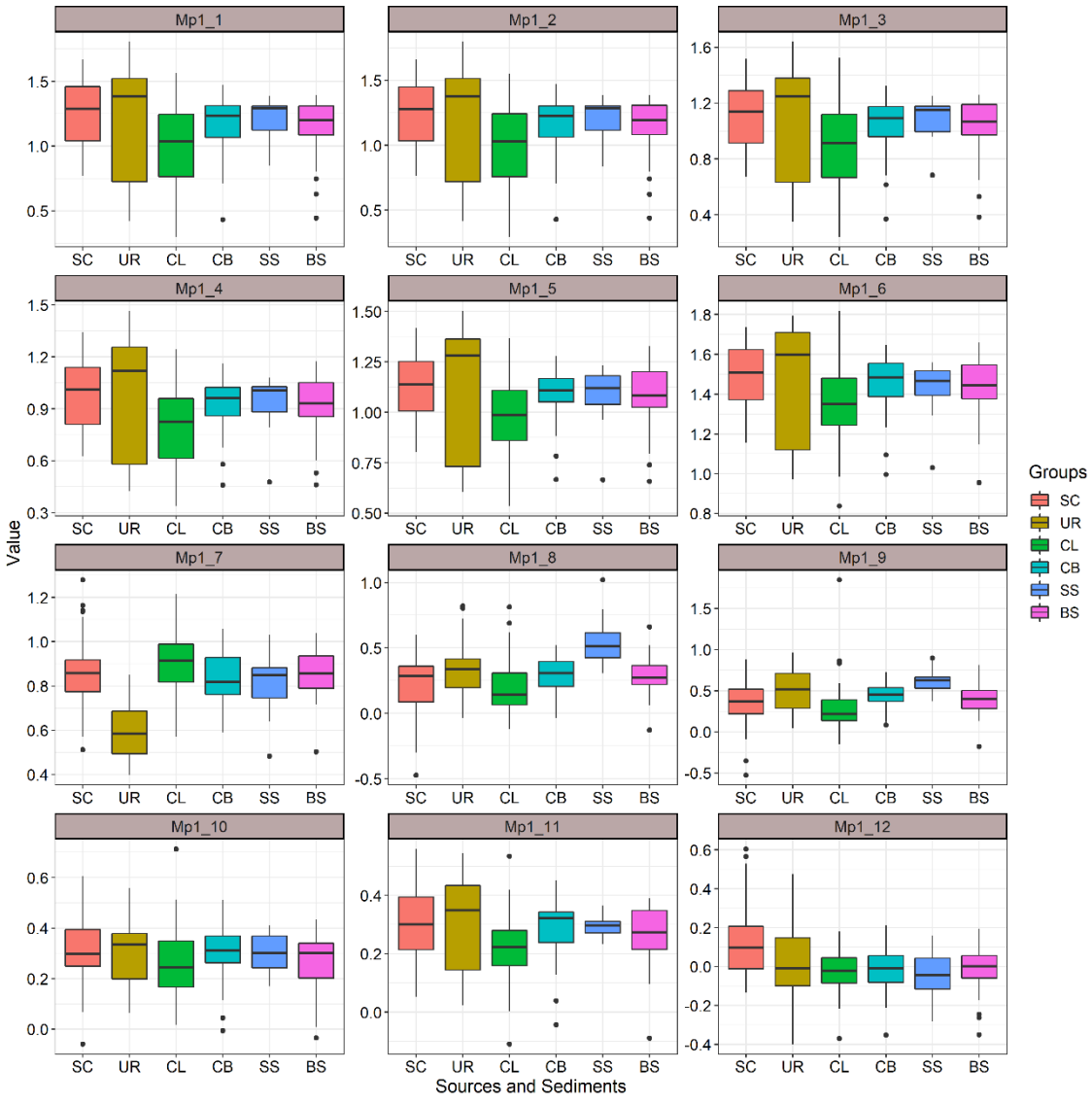

Figure 6. Example comparison of MIR tracers for assessing conservative behaviour at catchment-wide scale

The most pronounced MIR tracer variations were observed for the UR sediment source and especially for kaolinite (3695, 3694, 3690, 3669, 3652, 3620 and 915 cm^{-1}), smectite (3680, 3650, 3630 and 3620 cm^{-1}), muscovite (3659, 933 and 692 cm^{-1}), micas (3620 cm^{-1}), illite (3623 and 801 cm^{-1}) and clay (3666 and 3644 cm^{-1}).

3.5 Discrimination between sediment sources

3.5.1 Colour parameters

The forward stepwise DFA showed that a combination of X, Dw, HRGB and y discriminated the sediment sources at catchment-wide scale (Table 4), with an overall accuracy of 61% (95% confidence intervals for discriminatory power - 0.52, 0.69). At sub-catchment scale (Table 4), a composite signature combining R, HRGB, Pe and C was selected for discriminating between the individual sediment sources, yielding an overall accuracy of 67% (95% confidence intervals for discriminatory power - 0.54, 0.78) (Figure S7).

Table 4. Forward stepwise linear discriminant function analysis results using colour tracers

Properties	Wilks' lambda	F-value	p-value	Error Rates
Catchment-wide scale				
X	0.70	17.8	0.000	0.50
DWnm	0.59	7.9	0.000	0.45
HRGB	0.49	8.9	0.000	0.40
y	0.43	5.7	0.001	0.39
Sub-catchment scale				
R	0.61	13.6	0.000	0.52
HRGB	0.46	6.5	0.000	0.52
Pe	0.35	6.5	0.000	0.37
C	0.28	4.6	0.006	0.33

DFA using the colour tracers suggested that SC, CL and CB were the most similar sources at both catchment-wide and sub-catchment scales (see Figure S7).

3.5.2 Near Infrared Spectroscopy (NIR)

At catchment-wide scale (Table 4), 10 properties and 14 wavelengths were selected based on DFA as follows: cellulose (1780 nm), CH_2 (1053 nm), CH_3 (1705 and 2280 nm), $CONH_2$ (1960, 2030 and 2050 nm), CONH-CONHR (2000 nm), HC=CH (1510 nm), protein (2380 nm), starch (2276 and 2461 nm), AROH (1000 nm) and starch, glucose (1580 nm). The final composite signature correctly discriminated 89% (95% confidence intervals for

discriminatory power – 0.81, 0.93) of the source material samples. At sub-catchment scale, the final composite signature combined 8 properties and 12 wavelengths: cellulose (1780 nm), CH_3 (1705 and 2280 nm), $CONH_2$ (1960 nm), CONH-CONHR (2110 nm), HC=CH (1510, 1940 and 2180 nm), starch (1540 and 2461 nm), aromatic (1446 nm) and CH (1225 nm). This composite signature (Table 4) correctly distinguished 93% (95% confidence intervals for discriminatory power - 0.83, 0.98) (see supplementary information, Figure S8).

Table 4. Forward stepwise linear discriminant function analysis results using NIR tracers

Property	Wilks' lambda	F-value	p-value	Error Rates
Catchment-wide scale				
Np8_42	0.58	30.7	0.000	0.44
Np11_49	0.35	26.7	0.000	0.39
Np11_48	0.24	20.9	0.000	0.30
Np13_58	0.15	22.1	0.000	0.22
Np5_24	0.11	15.0	0.000	0.18
Np1_4	0.09	13.2	0.000	0.18
Np2_13	0.08	4.8	0.003	0.17
Np6_31	0.07	4.4	0.005	0.16
Np3_17	0.06	5.0	0.001	0.15
Np5_25	0.06	3.6	0.015	0.13
Np9_44	0.05	4.0	0.009	0.14
Np3_14	0.05	3.9	0.011	0.15
Np18_69	0.04	3.1	0.031	0.13
Np5_23	0.04	6.0	0.001	0.11
Sub-catchment scale				
Np14_60	0.57	15.5	0.000	0.42
Np8_42	0.35	12.9	0.000	0.36
Np11_48	0.28	5.6	0.000	0.28
Np3_14	0.18	10.1	0.000	0.27
Np11_53	0.14	7.1	0.000	0.24
Np1_4	0.11	4.0	0.012	0.21
Np16_65	0.08	6.5	0.001	0.18
Np8_40	0.07	4.9	0.004	0.16
Np5_23	0.05	3.8	0.015	0.15
Np8_36	0.04	4.8	0.005	0.10
Np3_17	0.04	4.1	0.011	0.10
Np6_32	0.03	4.3	0.009	0.07

The DFA showed overlap between the CB and CL sources on the basis of the NIR tracers, while SC and UR sources were better discriminated (Figure S8).

3.5.3 Mid Infrared Spectroscopy (MIR)

Forward stepwise DFA at catchment-wide scale using MIR tracers selected a final composite signature (Table 5) comprising of 13 tracers, 6 properties and 13 wavelengths; (smectite (3630, 3620 and 1628 cm^{-1}), muscovite (3659 and 804 cm^{-1}), vermiculite (3436 cm^{-1}), quartz (1801 and 1521 cm^{-1}), clay (3666 and 3668 cm^{-1}) and carbonates (1445, 1798, 2534 cm^{-1}). This composite signature correctly discriminated 84% (95% confidence intervals for discriminatory power – 0.77, 0.90) of the source samples. Six tracers were selected for the final composite signature at sub-catchment scale, comprising 4 properties and 7 wavelengths - (muscovite (3627 and 756 cm^{-1}), micas (1157 cm^{-1}), quartz (1974 cm^{-1}), carbonates (1445 and 2534 cm^{-1}). This signature correctly discriminated 72% (95% confidence intervals for discriminatory power – 0.59, 0.82) of the source samples (Table 5) (See supplementary information, Figure S9).

Table 5. Forward stepwise linear discriminant function analysis results using MIR tracers.

Properties	Wilks' lambda	F-value	p-value	Error Rates
Catchment-wide scale				
Mp2_19	0.64	22.9	0.000	0.54
Mp4_36	0.43	20.9	0.000	0.34
Mp7_59	0.34	11.4	0.000	0.34
Mp11_78	0.27	9.8	0.000	0.28
Mp11_80	0.22	8.4	0.000	0.25
Mp2_18	0.18	9.1	0.000	0.22
Mp3_25	0.16	5.3	0.002	0.21
Mp10_76	0.14	6.3	0.000	0.19
Mp10_75	0.12	6.4	0.000	0.19
Mp2_17	0.11	4.6	0.004	0.20
Mp3_30	0.10	2.8	0.044	0.21
Mp7_64	0.09	3.0	0.031	0.20
Mp11_77	0.07	8.2	0.000	0.16
Sub-catchment scale				
Mp7_58	0.67	10.4	0.000	0.45
Mp3_31	0.52	5.7	0.002	0.49
Mp11_79	0.43	4.5	0.006	0.45
Mp11_77	0.34	5.1	0.003	0.31
Mp3_26	0.24	8.3	0.000	0.28
Mp5_43	0.19	4.8	0.005	0.28

3.5.4 Colour + NIR + MIR tracers combined (CNM)

The combination of colour, NIR and MIR tracers generated the most powerful composite signatures at both catchment scales. At catchment-wide scale, the composite signature (Table 6) discriminated 95% (95% confidence intervals for discriminatory power - 0.90, 0.98) of the source material samples correctly, compared with 91% (0.81, 0.96) at sub-catchment scale.

Table 6. Forward stepwise linear discriminant function analysis results using Colour + NIR + MIR tracers

Properties	Wilks' lambda	F-value	p-value	Error Rates
Catchment-wide scale				
Np14_60	0.61	26.8	0.000	0.43
IRGB	0.36	28.1	0.000	0.33
Np11_48	0.27	13.3	0.000	0.28
Np3_14	0.18	20.6	0.000	0.22
Np1_4	0.13	16.5	0.000	0.17
Np13_58	0.10	13.4	0.000	0.18
Np5_24	0.08	7.9	0.000	0.16
Mp2_17	0.07	8.2	0.000	0.16
Np9_44	0.06	7.0	0.000	0.14
Np18_69	0.05	5.3	0.002	0.12
Mp2_16	0.04	4.8	0.004	0.11
Mp2_23	0.04	5.0	0.003	0.11
Mp7_64	0.03	4.3	0.006	0.12
Np6_31	0.03	5.5	0.001	0.09
Np5_25	0.03	4.5	0.005	0.09
Np5_23	0.02	4.6	0.004	0.08
RI	0.02	3.2	0.027	0.08
Np11_49	0.02	3.4	0.019	0.06
Mp10	0.02	3.2	0.027	0.06
Mp6_50	0.02	3.7	0.014	0.05
y	0.02	3.9	0.011	0.05
Mp3_28	0.01	3.4	0.020	0.05
Np8_40	0.01	2.7	0.049	0.05
Sub-Catchment scale				
Np5_24	0.53	19.0	0.000	0.37
X	0.33	12.2	0.000	0.33
Np11_48	0.24	8.2	0.000	0.30
Np1_4	0.14	12.6	0.000	0.19
Np13_58	0.10	8.4	0.000	0.13
Np6_31	0.08	5.5	0.002	0.13
Np1_3	0.06	4.9	0.004	0.12
V	0.05	4.5	0.007	0.10
DWnm	0.04	4.0	0.012	0.09

The CB and CL sediment sources were more difficult to discriminate at both catchment scales studied whereas SC and UR were the most clearly discriminated (Supplementary Information, Figure S10).

3.5.5 Sources source apportionment

Source type contributions to SS and BS samples estimated by MixSIAR modelling exhibited substantial uncertainties and strong negative correlations at both scales (Supplementary Information, Figure S11 and S12). The negative correlations revealed an aspect of collinearity between the optical tracers. The CB source showed the highest negative correlations with CL (-0.80) using NIR tracers at catchment-wide scale.

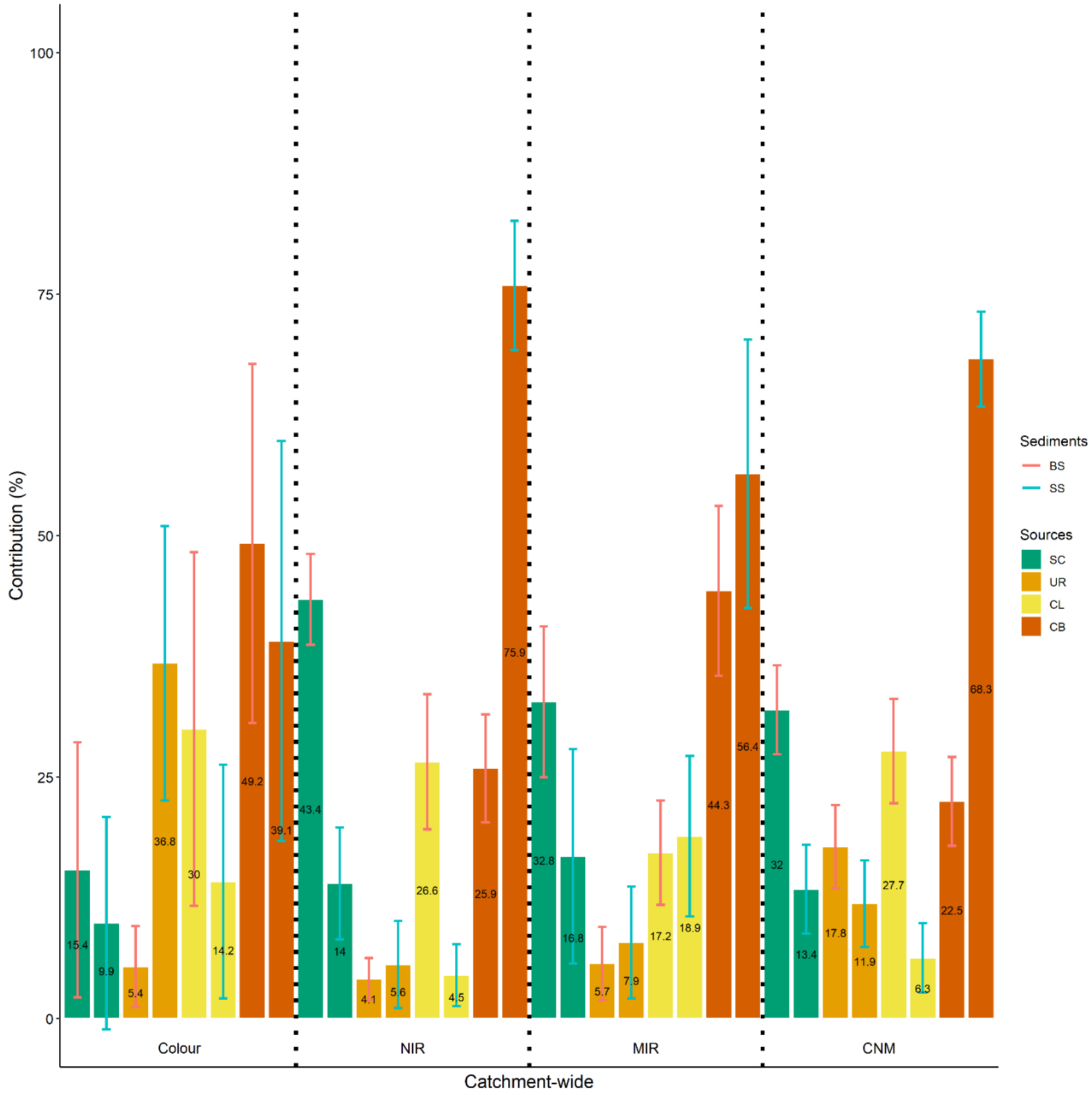

Figure 7. Source contributions to target sediment samples at catchment-wide scale, estimated using MixSIAR and the different final composite signatures. Sources: sugarcane (SC) unpaved road (UR), cropland (CL) and channel bank (CB). Sediments: bed sediments (BS) and suspended sediments (SS)

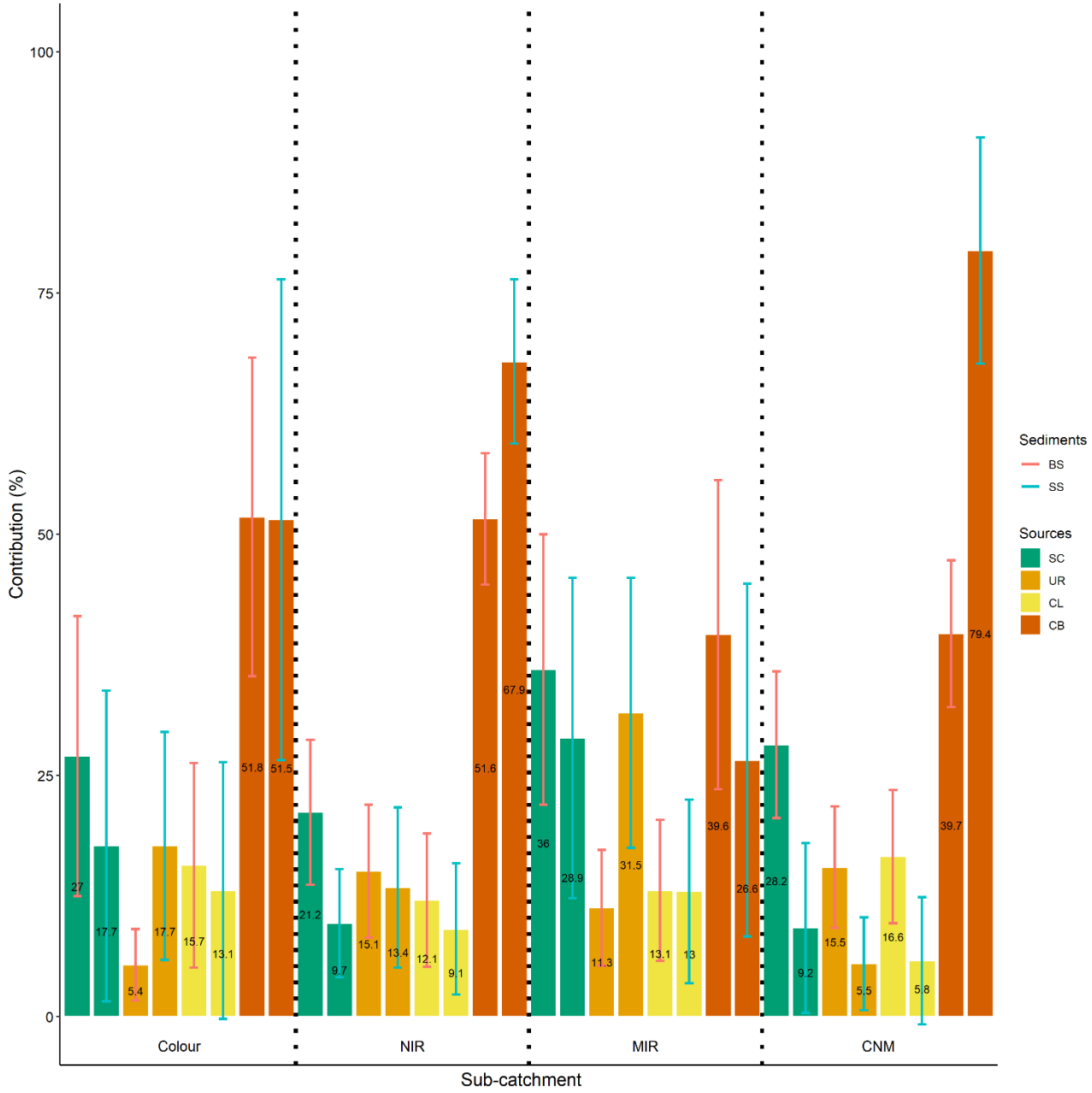

Figure 8. Source contributions to target sediment samples at sub-catchment scale, estimated using MixSIAR and the different composite signatures. Sources: sugarcane (SC) unpaved road (UR), cropland (CL) and channel bank (CB). Sediments: bed sediments (BS) and suspended sediments (SS)

The estimated average relative contribution of each source for SS and BS at catchment-wide and sub-catchment scale (Figure 7 and Figure 8) indicates that the dominant sources were CB and SC using each set of optical properties. For catchment-wide, the dominant CB source contributed 49 ± 19% of BS and 39 ± 21% of SS using a composite signature of colour properties, 26 ± 5.6% of BS and 76 ± 6.7% of SS using a signature of NIR

properties, 44 ± 8% of BS and 56 ± 14% of SS using a signature comprising MIR properties and 68.3 ± 4.9% of SS using a composite signature combining all optical property types . At sub-catchment scale, the colour, NIR and CNM composite signatures all suggested that the dominant source was CB, contributing an average of >50% to both BS and SS. The MIR composite signature predicted approximately equal contributions from SC and CB at sub-catchment scale.

All MixSIAR models passed the Gelman-Rubin convergence test as all the potential scale reduction factor (PSRF) values were < 1.05, thereby demonstrating that the Markov chains were sufficiently long. Relative mean errors of approximately 15% suggest a good fit (COLLINS et al., 2001) between source-contribution weighted and measured tracer properties in target sediment samples. Table 7 RMSE and MAE estimates based on the virtual mixing tests show values below 15% on a sub-catchment scale for all sets of tracers in the bed sediment. In the suspended sediment for the Colour, MIR and CNM tracers the values were above 15%, showing that they are not optimal sets of tracers for this basin size. In general, the NIR property estimates were 7.6% and 3.6 for SS and 4.7% and 2.0% for BS in catchment-wide, for sub-catchment in SS they were 4.6% and 2.4, for BS they were 1.5% and 0.7%. This indicates that using the spectra of organic compounds from the NIR as tracers proved to be robust and suitable for discrimination between sediment sources in both sediments and basin scale size, with errors below 8%.

Table 7. Virtual mixture comparisons of the predicted and known relative contributions sediment sources using two sediments

Properties	Sediments	Source proportions	Sediments sources					
			CB	CL	UR	SC	RMSE	MAE
Colour Catchment-wide	SS	Predict	39.1	14.2	36.8	9.9	19.5	9.1
		Known	2	1.8	31.6	64.7		
	BS	Predict	49.2	30	5.4	15.4	1.7	0.8
		Known	50.1	33.3	6.1	10.5		
Colour Sub catchment 1	SS	Predict	51.5	13.1	17.7	17.7	10.1	4.9
		Known	80.9	10.1	2.5	6.5		
	BS	Predict	51.8	15.7	5.4	27	10.4	4.9
		Known	81.1	8.7	2.6	7.6		
NIR Catchment-wide	SS	Predict	75.9	4.5	5.6	14	7.6	3.6
		Known	54.4	7.3	9.7	28.6		
	BS	Predict	25.9	26.6	4.1	43.4	4.7	2.0
		Known	36.8	14.7	4.3	44.1		
NIR Sub catchment 1	SS	Predict	67.9	9.1	13.4	9.7	4.6	2.4
		Known	55.6	16.2	11.4	16.9		
	BS	Predict	51.6	12.1	15.1	21.2	1.5	0.7
		Known	52	16.1	12.1	19.9		
MIR Catchment-wide	SS	Predict	56.4	18.9	7.9	16.8	31.7	15.2
		Known	0.4	0.5	98.9	0.2		
	BS	Predict	44.3	17.2	5.7	32.8	23.2	11.0
		Known	10.4	14.8	71.9	2.9		
MIR Sub catchment 1	SS	Predict	26.6	13	31.5	28.9	9.3	4.6
		Known	54.1	7.9	18.3	19.6		
	BS	Predict	39.6	13.1	11.3	36	6.8	3.6
		Known	54.1	8	18.3	19.6		
CNM Catchment-wide	SS	Predict	68.3	6.3	11.9	13.4	20.3	8.2
		Known	0.607	0.14	0.113	0.14		
	BS	Predict	22.5	27.7	17.8	32	14.6	8.3
		Known	0.477	0.189	0.144	0.19		
CNM Sub catchment 1	SS	Predict	79.4	5.8	5.5	9.2	17.9	7.7
		Known	35	49.1	8.2	7.7		
	BS	Predict	39.7	16.6	15.5	28.2	5.8	2.9
		Known	32.2	33.7	11.9	22.2		

Sources: cropland (CL), sugarcane (SC) unpaved road (UR) and channel bank (CB). Sediments: bed sediments (BS) and suspended sediments (SS)

3.5.6 Sediment source discrimination using the tracers

The selected colour tracers (R, HRGB, X, y, C, Dw and Pe) exhibited pronounced variability and yielded the weakest discrimination of the sediment source category samples; 61% at catchment-wide and 67% at sub-catchment scale. These results suggest that colour parameters can be influenced by the catchment size and overlapping fingerprints for different sources, reducing the capacity to discriminate between land uses and channel banks. In spite of the highest redness rates and iron content in UR, the low organic matter content contributed to the lighter colours in the UR source (Figure 4 and SI (Figure S3) (MARTÍNEZ-CARRERAS et al., 2010; TIECHER et al., 2015; PULLEY; ROWNTREE, 2016).

The MID-IR region of the main absorption peaks are between 3695 and 3620 cm^{-1}, which correspond to clay and clay minerals silicate 2:1 (smectite), 1:1 (kaolinite), and muscovite originated from the vibrations in the radicals Al-OH and Si-O. In addition, the absorption peaks between 1445 and 2881 cm^{-1} for quartz and carbonates were found in the samples at both catchment-wide and sub-catchment scale, due to the CO_3^{2-} stretching vibration (Figure 6 and SI (Figure S5 and S6). The higher variation in maximum and minimum clay values, clay minerals, and quartz in UR samples is related to the characteristics of the main soils in the study catchment, i.e., Acrisols (~ 56%) and Nitisols (~ 20%) with very clayey texture, composed of minerals such as kaolinite, smectite, mica (muscovite), illite and quartz (COSTA et al., 2019; ALMEIDA et al., 2019).

Cropland areas, especially those cultivated with bananas, often in steep sloping areas, produce large amounts of organic material that protects the soil from major rainy events that transport large amounts of waste and intra-aggregate roots. The organic compounds HC=CH, CH_3 starch, CONH.CONHR, cellulose, protein and starch + Glucose (Table 5), found in greater abundance in the 2000 nm spectral range, are formed by the hydrogen-linked elongation bands OH, attributed to unconjugated C=O, C=C of aromatic skeletal vibrations, carbohydrates including C–O–C and C–O stretch, C–H symmetric and asymmetric stretching and N-H and S-H bands, as observed by Fourty et al. (1996), Ben-Dor, Inbar and Chen (1997), Guimarães et al. (2009) and Rodríguez-Zúñiga et al. (2014), for the compounds cellulose, hemicellulose, starch, lignin and sugar in the same spectral range. Cellulose and lignin are the most abundant components of vascular plant tissues, constituting 10 to 70% of crop residues; cellulose is considered more labile and generally decomposes faster than lignin due to its higher molecular weight and stability and three-dimensional chemical structure (SAHA et al., 2005; TORRES et al., 2014; CHEN et al., 2018).

On average, the litter of banana crops has 5 - 17% lignin and 50-65% cellulose and sugarcane 19-25% lignin and 32-55% (GUIMARÃES et al., 2009; MENDES et al., 2010; THEVENOT; DIGNAC; RUMPEL, 2010). The cellulose and lignin content may provide different decomposition rates and organic matter accumulation, which affects soil stabilization (RASSE et al., 2006; THEVENOT; DIGNAC; RUMPEL, 2010; COTRUFO et al., 2013, 2019; STACY et al., 2019). Thus, the mechanisms of stabilization of organic matter in the soil matrix related to texture, cation bridges, Fe oxides, Al and Mn, expandable and non-expandable phyllosilicates play a prominent role in the protection of intra-aggregate organic matter and disintegration during erosive processes (KLEBER; SOLLINS; SUTTON, 2007; COTRUFO et al., 2013; STACY et al., 2019).

3.5.7 Source contributions for different types of target sediment

The most important relative contributions to SS and BS were from CB and SC sources (Figure 7 and Figure 8). Previous research has reported the significance of farm land as a sediment source (COLLINS; WALLING, 2006, 2007; GELLIS; FULLER; VAN METRE, 2017; LAMBA; KARTHIKEYAN; THOMPSON, 2015; TIECHER et al., 2018; LIM; KIM; KIM, 2019). The cultivation of sugarcane, the largest cultivated area (65%) in the study catchment, occurs without targeted management practices that reduce the impacts caused by the trafficking of machines. High rainfall totals and intense rainstorms in the study area frequently coincide with the period of initial growth of sugarcane, when protective vegetation cover is lower and soil losses are enhanced (COUTO JUNIOR et al., 2019; GOMES et al., 2019). Intense machinery trafficking, cultivation in riparian areas, widespread surface washing in rainy seasons, development of gullies and the slopes of the SC and CL areas combine to increase the propensity for such areas to contribute substantially as sediment sources.

The high contributions of CB to the sampled SS is likely to reflect a number of factors and controls including the uncontrolled river channel access for irrigation in the SC areas, the numerous sand extraction points along the riverbanks and the erosion resulting from high water discharges during rainy seasons. Indiscriminate river sand extraction can produce an average sediment yield of ~ 5,000 - 85,400 t $year^{-1}$ (78% as bed sediments). This activity damages river channel banks, triggers the loss of protective bank vegetation, generates siltation and, thus, is a threat to trophic structure (RINALDI; WYŻGA; SURIAN, 2005; WALLING, 2006; SURIAN; CISOTTO, 2007; PADMALAL et al., 2008; ASHRAF et al., 2011; SREEBHA; PADMALAL, 2011). Sediment samples collected from an agricultural

catchment in southern Brazil showed that 90% and 56% of the fine channel BS and SS, respectively, originated from eroding channel banks, due to the erosive impacts of severe flooding (TIECHER et al., 2018).

In Brazil, agricultural roads are mostly unpaved and the high trafficking rates by vehicles can produce on average 43.2 t ha^{-1} yr^{-1} of sediment (RAMOS-SCHARRÓN; MAC DONALD, 2007; RIJSDIJK; BRUIJNZEEL; SUTOTO, 2007; RAMOS-SCHARRÓN, 2010; SANTOS et al., 2017; FARIAS et al., 2019). For UR with steep slopes, the sediment yield can be ~ 14 times higher (RAMOS-SHARRON; MAC DONALD, 2007). However, despite the widespread unpaved roads and direct connectivity between these and the river channel system, especially in the SC areas, in general, the UR contribution did not exceed 10% at either study catchment scales or for either target sediment type sampled. The only exceptions were in the case of the composite signature based on colour properties at catchment-wide scale (36.5 ± 14.2%) and based on MIR properties (31.5 ± 14.0%) at sub-catchment scale. At catchment-wide scale, in other studies, the contributions of UR to sampled target sediment have been reported as being very important or even dominant, with examples including 59% (COOPER et al., 2014), 67% (NOSRATI et al., 2019) and 75% (BRAVO-LINARES et al., 2018).

3.5.8 Implications for management of the sediment problem in the study catchment

Our results, regardless of optical property, target sediment type or study catchment scale, suggest that CB represents the primary source of the sediment problem in the study catchment. The occurrence of channel bank collapse, sand extraction, and animals along the legal protection areas also contributed to the instability of stream channels in the Goiana watershed. Targeted remedial actions therefore need to deliver protection for eroding channel banks. Here, options used in Brazil include well-designed and maintained vegetative filter strips wherein riparian tree roots improve the mass stability of riverbanks (ABERNETHY et al., 2000). Vegetative filter strips are currently absent along the Goiana River meaning that there is ample opportunity for such features to be installed for sediment management.

The second most important sediment source, regardless of tracer or target sediment type, or catchment scale, was SC. Potential mitigation measures implemented by farmers in Brazil to tackle elevated soil erosion and sediment loss from SC include keeping crop residues on topsoils after harvest. Landscape disturbance such as fire often increases soil erosion and sediment and contaminant transfer to water resources (SMITH et al., 2011; EMELKO et al.,

2016) and fire can be an issue for SC farming in the study area. The use of crop residues therefore needs to be considered carefully in the context of fire risk.

The study of more conventional geochemical properties may bring additional perspectives for the application of best management practices, not only in relation to sediment source areas, but also to environmental impacts. The SC area represents about 65% of the study catchment. Many pesticides are applied during the crop cycle. Here, the main herbicides used include Diuron, Hexazinone, Mesotrione, Diclosulam, Amicarbazona, Clomazone, Picloran, 2,4-D, Flumioxazin, Glifosato, Halosulfuron-methyl, Metribuzin, Picloram-trietanolamina, Imazapique, Fluroxipir and Isoxaflutole and the management of these contaminants should be borne in mind when devising holistic catchment management strategies for water quality protection in general rather than for sediment alone.

3.6 Conclusions

The study showed that low-cost optical properties are effective for identifying sediment sources. A composite signature of colour properties generated the lowest discriminatory power but yielded the lowest relative errors between predicted and measured tracer content in target sediment samples. We demonstrated the use of a simple interpolation of NIRS and MIRS results for using specific spectra of organic compounds or soil components to help quantify sediment source contributions. CB was identified as the dominant sediment source at both sub-catchment and catchment-wide scales. Further work is required is continue testing the low-cost optical tracers applied in this study in different environmental settings and using different target sediment types. Such work will help to inform investigators more generally of the potential for optical tracers to deliver robust source apportionment results.

REFERENCES

ABERNETHY, B.; RUTHERFURD, I. D. The effect of riparian tree roots on the mass-stability of riverbanks. **Earth Surface Processes and Landforms**, v. 25, p. 921–937, 2000. https://doi.org/10.1002/1096-9837(200008)25:9%3C921::AID-ESP93%3E3.0.CO;2-7

ALMEIDA, M. D. C. D.; ARAÚJO, J. K. S.; RIBEIRO FILHO, M. R.; SOUZA JÚNIOR, V. S. D. Relief Position and Soil Properties under Continuous Banana Cropping in Subhumid Climate in Northeast Brazil. **Revista Brasileira de Ciência do Solo**, v. 43, p. e0180207, 2019. https://doi.org/10.1590/18069657rbcs20180207

ASHRAF, M. A.; MAAH, M. J.; YUSOFF, I.; WAJID, A.; MAHMOOD, K. Sand mining effects, causes and concerns: A case study from Bestari Jaya, Selangor, Peninsular Malaysia. **Scientific Research and Essays**, v. 6, n. 6, p. 1216-1231, 2011. https://doi.org/10.5897/SRE10.690

ASTORGA, R. T.; DE LOS SANTOS VILLALOBOS, S.; VELASCO, H.; DOMÍNGUEZ-QUINTERO, O.; CARDOSO, R. P.; DOS ANJOS, R. M.; DIAWARA, Y.; DERCON, G.; MABIT, L. Exploring innovative techniques for identifying geochemical elements as fingerprints of sediment sources in an agricultural catchment of Argentina affected by soil erosion. **Environmental Science and Pollution Research**, v. 25, n. 21, p. 20868-20879, 2018. https://doi.org/10.1007/s11356-018-2154-4

BEN-DOR, E.; INBAR, Y.; CHEN, Y. The reflectance spectra of organic matter in the visible near-infrared and short wave infrared region (400–2500 nm) during a controlled decomposition process. **Remote Sensing of Environment**, v. 61, n. 1, p. 1-15, 1997. https://doi.org/10.1016/S0034-4257(96)00120-4

BRAVO-LINARES, C.; SCHULLER, P.; CASTILLO, A.; OVANDO-FUENTEALBA, L.; MUÑOZ-ARCOS, E.; ALARCÓN, O; BUSTAMANTE-ORTEGA, R. First use of a compound-specific stable isotope (CSSI) technique to trace sediment transport in upland forest catchments of Chile. **Science of the Total Environment**, v. 618, p. 1114-1124, 2018. https://doi.org/10.1016/j.scitotenv.2017.09.163

CALICIOGLU, O.; FLAMMINI, A.; BRACCO, S.; BELLÙ, L.; SIMS, R. The future challenges of food and agriculture: An integrated analysis of trends and solutions. **Sustainability**, v.11, n. 1, p. 222, 2019. https://doi.org/10.3390/su11010222

CHEN, X.; HU, Y.; FENG, S.; RUI, Y.; ZHANG, Z.; HE, H., GE, T., WU, J.; SU, Y. Lignin and cellulose dynamics with straw incorporation in two contrasting c;opping soils. **Scientific Reports**, v. 8, n. 1, p. 1633, 2018. https://doi.org/10.1038/s41598-018-20134-5

COLLINS, A. L.; WALLING, D. E. Investigating the remobilization of fine sediment stored on the channel bed of lowland permeable catchments in the UK. **IAHS PUBLICATION**, v. 306, p. 471, 2006.

COLLINS, A. L.; WALLING, D. E. Sources of fine sediment recovered from the channel bed of lowland groundwater-fed catchments in the UK. **Geomorphology**, v. 88, n. 1-2, p. 120-138, 2007. https://doi.org/10.1016/j.geomorph.2006.10.018

COLLINS, A. L.; WALLING, D. E.; WEBB, L.; KING, P. Apportioning catchment scale sediment sources using a modified composite fingerprinting technique incorporating property weightings and prior information. **Geoderma**, v. 155, n. 3-4, p. 249-261, 2010. https://doi.org/10.1016/j.geoderma.2009.12.008

COLLINS, A. L.; WILLIAMS, L. J.; ZHANG, Y. S.; MARIUS, M.; DUNGAIT, J. A. J., SMALLMAN, D. J.; DIXON, E. R.; STRINGFELLOW, A.; SEAR, D. A.; JONES, J. I; NADEN, P. S. Catchment source contributions to the sediment-bound organic matter degrading salmonid spawning gravels in a lowland river, southern England. **Science of the Total Environment**, v. 456, p. 181-195, 2013. https://doi.org/10.1016/j.scitotenv.2013.03.093

COLLINS, A. L.; WILLIAMS, L. J.; ZHANG, Y. S.; MARIUS, M.; DUNGAIT, J. A. J.; SMALLMAN, D. J.; DIXON, E. R.; STRINGFELLOW, A.; SEAR, D. A.; JONES, J. I.; NADEN, P. S. Sources of sediment-bound organic matter infiltrating spawning gravels during the incubation and emergence life stages of salmonids. **Agriculture, Ecosystems & Environment**, v. 196, p. 76-93, 2014. https://doi.org/10.1016/j.agee.2014.06.018

COLLINS, A.L.; PULLEY, S.; FOSTER, I.D.L.; GELLIS, A.; PORTO, P.; HOROWITZ, A.J. Sediment source fingerprinting as an aid to catchment management: a review of the current state of knowledge and a methodological decision-tree for end-users. **Journal of Environmental Management**, v. 194, p. 86-108, 2017. https://doi.org/10.1016/j.jenvman.2016.09.075

COOPER, R. J.; KRUEGER, T.; HISCOCK, K. M.; RAWLINS, B. G. Sensitivity of fluvial sediment source apportionment to mixing model assumptions: A Bayesian model comparison. **Water Resources Research**, v. 50, n. 11, p. 9031-9047, 2014. https://doi.org/10.1590/18069657rbcs20180101

COSTA, E. U. C. D;, ARAUJO, J. K. S.; NEVES, L. V. D. M. W.; ARAÚJO FILHO, J. C. D.; SOUSA, J. E. S. D.. CORRÊA, M. M.; RIBEIRO FILHO, M. R; SOUZA JÚNIOR, V. S. D. Genesis and Classification of Nitisols from Volcano-Sedimentary Lithology in Northeastern Brazil. **Revista Brasileira de Ciência do Solo**, v. 43. p. 748 749, 2019. https://doi.org/10.1038/s41561-019-0484-6

COTRUFO, M. F.; RANALLI, M. G.; HADDIX, M. L.; SIX, J.; LUGATO, E. Soil carbon storage informed by particulate and mineral-associated organic matter. **Nature Geoscience**, v. 12, n. 12, p. 989- 751 994, 2019. https://doi.org/10.1111/gcb.12113

COTRUFO, M. F.; WALLENSTEIN, M. D.; BOOT, C. M.; DENEF, K.; PAUL, E. The microbial Efficiency- matrix stabilization (MEMS) framework integrates plant litter decomposition with soil organic matter stabilization: do labile plant inputs form stable soil organic matter? **Global Change Biology**, v. 19, n. 4, p. 988-995, 2013. https://doi.org/10.1016/j.catena.2018.09.001

COUTO JÚNIOR, A. A.; CONCEIÇÃO, F. T.; FERNANDES, A. M.; SPATTI JUNIOR, E. P.; LUPINACCI, C. M.; MORUZZI, R. B. Land use changes associated with the expansion of sugar cane crops and their influences on soil removal in a tropical watershed in São Paulo State (Brazil). **Catena**, v. 172, p. 313-323, 2019. https://doi.org/10.1111/gcb.13073

EMELKO, M. B.; STONE, M.; SILINS, U.; ALLIN, D.; COLLINS, A. L.; WILLIAMS, C. H. S.; MARTENS, A. M.; BLADON, K. D. Sediment-phosphorus dynamics can shift aquatic ecology and cause downstream legacy effects after wildfire in large river systems. **Global Change Biology**, v. 22, p. 1168-1184, 2016. https://doi.org/10.1007/s11368-019-02302-w

EVRARD, O.; DURAND, R.; FOUCHER, A;, TIECHER, T.; SELLIER, V.; ONDA, Y;, LEFÈVRE, I.; CERDAN, O.; LACEBY, J. P. Using spectrocolourimetry to trace sediment source dynamics in coastal catchments draining the main Fukushima radioactive pollution plume (2011–2017). **Journal of Soils and Sediments**, v.19, p. 3290–3301, 2019. https://doi.org/10.1016/j.ijsrc.2019.03.002

FARIAS, T. R. L.; MEDEIROS, P. H. A.; NAVARRO-HEVIA, J.; DE ARAÚJO, J. C. Unpaved rural roads as source areas of sediment in a watershed of the Brazilian semi-arid region. **International Journal of Sediment Research**, v. 34, n. 5, p. 475-485, 2019. https://doi.org/10.1016/0034-4257(95)00234-0

FOURTY, T.; BARET, F.; JACQUEMOUD, S.; SCHMUCK, G.; VERDEBOUT, J. Leaf optical properties with explicit description of its biochemical composition: direct and inverse problems. **Remote Sensing of Environment**, v. 56, n. 2, p.104-117, 1996. https://doi.org/10.1016/j.jenvman.2016.06.018

GELLIS, A. C.; FULLER, C. C.; VAN METRE, P. C.. Sources and ages of fine-grained sediment to streams using fallout radionuclides in the Midwestern United States. **Journal of Environmental Management**, v. 194, p. 73-85, 2017. https://doi.org/10.1016/j.catena.2019.104083

GOMES, T. F.; VAN DE BROEK, M.; GOVERS, G.; SILVA, R. W.; MORAES, J. M.; CAMARGO, P. B.; MAZZI, E. A.; MARTINELLI, L. A.. Runoff, soil loss, and sources of particulate organic carbon delivered to streams by sugarcane and riparian areas: An isotopic approach. **Catena**, v. 181, p. 104083, 2019. https://doi.org/10.1016/j.indcrop.2009.07.013

GUIMARÃES, J. L.; FROLLINI, E.; DA SILVA, C. G.; WYPYCH, F.; SATYANARAYANA, K. G. Characterization of banana, sugarcane bagasse and sponge gourd fibers of Brazil. **Industrial Crops and Products**, v. 30, n. 3, p. 407-415, 2009. https://doi.org/10.2134/jeq1975.00472425000400010016x

KLAGES, M. G.; HSIEH, Y. P. Suspended Solids Carried by the Gallatin River of Southwestern Montana: II. Using Mineralogy for Inferring Sources. **Journal of Environmental Quality**, v. 4, n. 1, p. 68-73, 1975.

KLEBER, M.; SOLLINS, P.; SUTTON, R. A conceptual model of organo-mineral interactions in soils: self-assembly of organic molecular fragments into zonal structures on mineral surfaces. **Biogeochemistry**, v. 85, n. 1, p. 9-24, 2007. https://doi.org/10.1007/s10533-007-9103-5

KOITER, A. J.; LOBB, D. A.; OWENS, P. N.; PETTICREW, E. L.; TIESSEN, K. H. D.; LI, S. Investigating the role of connectivity and scale in assessing the sources of sediment in an agricultural watershed in the Canadian prairies using sediment source fingerprinting. **Journal Soils Sediments**, v. 13, p. 1676–1691, 2013. https://doi.org/10.1007/s11368-013-0762-7

LAMBA, J.; KARTHIKEYAN, K. G.; THOMPSON, A. M. Apportionment of suspended sediment sources in an agricultural watershed using sediment fingerprinting. **Geoderma**, v. 239, p. 25-33, 2015. https://doi.org/10.1016/j.geoderma.2014.09.024

LIM, Y. S.; KIM, J. W.; KIM, J. K. Suspended sediment source tracing at the Juksan Weir in the Yeongsan River using composite fingerprints. **Quaternary International**, v. 519, p. 245-254, 2019. https://doi.org/10.1016/j.quaint.2019.01.004

LIU, K.; LOBB, D. A.; MILLER, J. J.; OWENS, P. N.; CARON, M. E. Determining sources offine-grained sediment for a reach of the Lower Little Bow River, Alberta, using a colour-based sediment fingerprinting approach. **Canadian Journal of Soil Science**, v. 98, n. 1, p. 55-69, 2017. https://doi.org/10.1139/cjss-2016-0131

MADEJOVÁ, J.; GATES, W.P.; PETIT, S. IR spectra of clay minerals In: GATES, W., KLOPROGGE, J. T., MADEJOVA, J., & BERGAYA, F. **Infrared and Raman Spectroscopies of Clay Minerals**, v. 8, p. 107-149, 2017.

MARTÍNEZ-CARRERAS, N;, KREIN, A.; GALLART, F.; IFFLY, J. F.; PFISTER, L.; HOFFMANN, L.; OWENS, P. N. Assessment of different colour parameters for discriminating potential suspended sediment sources and provenance: a multi-scale study in Luxembourg. **Geomorphology**, v. 118, n. 1-2, p. 118-129, 2010. https://doi.org/10.1016/j.geomorph.2009.12.013

MENDES, F. M.; SIQUEIRA, G.; CARVALHO, W.; FERRAZ, A.; MILAGRES, A. M. Enzymatic hydrolysis of chemithermomechanically pretreated sugarcane bagasse and samples with reduced initial lignin content. **Biotechnology Progress**, v. 27, n. 2, p. 395-401, 2010. https://doi.org/10.1002/btpr.553

MINELLA, J. P. G.; MERTEN, G. H.; WALLING, D. E.; REICHERT, J. M. Changing sediment yield as an indicator of improved soil management practices in southern Brazil. **Catena**, v. 79, n. 3, p. 228-236, 2009. https://doi.org/10.1016/j.catena.2009.02.020

MINELLA, J. P.; MERTEN, G. H.; BARROS, C. A.; RAMON, R.; SCHLESNER, A.; CLARKE, R. T.; MORO, M.; DALBIANCO, L. Long-term sediment yield from a small catchment in southern Brazil affected by land use and soil management changes. **Hydrological Processes**, v. 32, n. 2, p. 200-211, 2018. https://doi.org/10.1002/hyp.11404

MUGGLER, C. C, PAPE, T.; BUURMAN, P. Laser grain-size determination in soil genetic studies 2. clay content, clay formation, and aggregation in some brazilian oxisols. **Soil Science**, v. 162, p. 219-228, 1997. https://doi.org/10.1097/00010694-199703000-00008

NOSRATI, K.; GOVERS, G.; SEMMENS, B. X.; WARD, E. J. A mixing model to incorporate uncertainty in sediment fingerprinting. **Geoderma**, v. 217, p. 173-180, 2014. https://doi.org/10.1016/j.geoderma.2013.12.002

NOSRATI, K.; COLLINS, A. L. Investigating the importance of recreational roads as a sediment source in a mountainous catchment using a fingerprinting procedure with different multivariate statistical techniques and a Bayesian un-mixing model. **Journal of Hydrology,** v. 569, p. 506-518, 2019. https://doi.org/10.1016/j.jhydrol.2018.12.019

OECD-FAO. OECD-FAO Agricultural Outlook 2018-2027, 2018. Retrieved from: <http://www.fao.org/publications/oecd-fao-agricultural-outlook/2018-2027/en/>. Accessed on November 15, 2019.

OWENS, P.; BLAKE, W.; GASPAR, L.; GATEUILLE, D.; KOITER, A.; LOBB, D., PETTICREW, E. L.; REIFFARTH, D. G.; SMITH, H. G.; WOODWARD, J. Fingerprinting and tracing the sources of soils and sediments: Earth and ocean science, geoarchaeological, forensic, and human health applications. **Earth-Science Reviews**, v. 162, p. 1-23, 2016. https://doi.org/10.1016/j.earscirev.2016.08.012

PADMALAL, D.; MAYA, K.; SREEBHA, S.; SREEJA, R. Environmental effects of river sand mining: a case from the river catchments of Vembanad lake, Southwest coast of India. **Environmental Geology**, v. 54, n. 4, p. 879-889, 2008. https://doi.org/10.1007/s00254-007-0870-z

PHILLIPS, J. M.; RUSSELL, M. A.; WALLING, D. E. Time-integrated sampling of fluvial suspended sediment: a simple methodology for small catchments. **Hydrological Processes**, v. 14, n. 14, p. 2589-2602, 2000. https://doi.org/10.1002/1099-1085(20001015)14:14%3C2589::AID-HYP94%3E3.0.CO;2-D

PHILLIPS, D.L.; AND J.W. GREGG. Source partitioning using stable isotopes: Coping with too many sources. **Oecologia**, v. 136, p. 261–269, 2003. https://doi.org/10.1007/s00442-003-1218-3

PULLEY, S.; ROWNTREE, K. The use of an ordinary colour scanner to fingerprint sediment sources in the South African Karoo. **Journal of Environmental Management**, v. 165, p. 253-262, 2016. https://doi.org/10.1016/j.jenvman.2015.09.037

PULLEY, S.; VAN DER WAAL, B.; ROWNTREE, K.; COLLINS, A. L. Colour as reliable tracer to identify the sources of historically deposited flood bench sediment in the Transkei, South Africa: A comparison with mineral magnetic tracers before and after hydrogen peroxide pre-treatment. **Catena**, v. 160, p. 242-251, 2018. https://doi.org/10.1016/j.catena.2017.09.018

RAMOS-SCHARRÓN, C. E.; MACDONALD, L. H. Runoff and suspended sediment yields from an unpaved road segment, St John, US Virgin Islands. **Hydrological Processes: An International Journal**, v. 21, n. 1, p. 35-50, 2007. https://doi.org/10.1002/hyp.6175

RAMOS-SCHARRÓN, C. E. Sediment production from unpaved roads in a sub-tropical dry setting—Southwestern Puerto Rico. **Catena**, v. 82, n. 3, p. 146-158, 2010. https://doi.org/10.1016/j.catena.2010.06.001

RASSE, D. P.; DIGNAC, M. F.; BAHRI, H.; RUMPEL, C.; MARIOTTI, A.; CHENU, C. Lignin turnover in an agricultural field: from plant residues to soil- protected fractions. **European Journal of Soil Science**, v. 57, n. 4, p. 530-538, 2006. https://doi.org/10.1111/j.1365-2389.2006.00806.x

RIJSDIJK, A.; BRUIJNZEEL, L. S.; SUTOTO, C. K. Runoff and sediment yield from rural roads, trails and settlements in the upper Konto catchment, East Java, Indonesia. **Geomorphology**, v. 87, n. 1-2, p. 28-37, 2007. https://doi.org/10.1016/j.geomorph.2006.06.040

RINALDI, M.; WYŻGA, B.; SURIAN, N. Sediment mining in alluvial channels: physical effects and management perspectives. **River Research and Applications**, v. 21, n. 7, p. 805-828, 2005. https://doi.org/10.1002/rra.884

RODRÍGUEZ-ZÚÑIGA, U. F.; FARINAS, C. S.; CARNEIRO, R. L.; DA SILVA, G. M.; CRUZ, A. J. G.; GIORDANO, R. D. L. C.; GIORDANO, R. C.; ARRUDA RIBEIRO, M. P. Fast determination of the composition of pretreated sugarcane bagasse using near-infrared spectroscopy. **BioEnergy Research**, v. 7, n. 4, p. 1441-1453, 2014. https://doi.org/10.1007/s12155-014-9488-7

ROEVER, C.; RAABE, N.; LUEBKE, K.; LIGGES, U.; SZEPANNEK, G.; ZENTGRAF, M.; SVMLIGHT, S. Package 'klaR': Classification and Visualization. Rpackage version 0.6-14, 2018. Available in:<https://cran.r project.org/web/packages/klaR/index.html> Accessed on October 15, 2019.

SANTOS, J. C. N.; DE ANDRADE, E. M.; MEDEIROS, P. H. A.; GUERREIRO, M. J. S.; DE QUEIROZ PALÁCIO, H. A. Effect of rainfall characteristics on runoff and water erosion for different land uses in a tropical semiarid region. **Water Resources Management**, v. 31, n. 1, p. 173-185, 2017. https://doi.org/10.1007/s11269-016-1517-1

SAHA, B. C.; ITEN, L. B.; COTTA, M. A.; WU, Y. V. Dilute acid pretreatment, enzymatic saccharification and fermentation of wheat straw to ethanol. **Process Biochemistry**, v. 40, n. 12, p. 3693-3700, 2005. https://doi.org/10.1016/j.procbio.2005.04.006

SHRESTHA, D. S.; STAAB, B. D.; DUFFIELD, J. A. Biofuel impact on food prices index and land use change. **Biomass and Bioenergy**, v. 124, p. 43-53, 2019. https://doi.org/10.13031/aim.201700835

SMITH B. J; SRINIVASAN S.; GOMEZ-HERAS, M; BASHEER, P. A. M.; VILES, H. A. Near-surface temperature cycling of stone and its implications for scales of surface deterioration. **Geomorphology**, v. 130, p. 76-82, 2011. https://doi.org/10.1016/j.geomorph.2010.10.005

SREEBHA, S.; PADMALAL, D. Environmental impact assessment of sand mining from the small catchment rivers in the southwestern coast of India: a case study. **Environmental Management**, v. 47, n. 1, p. 130-140, 2011. https://doi.org/10.1007/s00267-010-9571-6

STACY, E. M.; BERHE, A. A.; HUNSAKER, C. T.; JOHNSON, D. W.; MEDING, S. M.; HART, S. C. Stabilization mechanisms and decomposition potential of eroded soil organic matter pools in temperate forests of the Sierra Nevada, California. **Journal of Geophysical Research: Biogeosciences**, v. 124, n. 1, p. 2-17, 2019. https://doi.org/10.1029/2018JG004566

STOCK, B. C., SEMMENS, B. X. MixSIAR, User Manual Version 3.1.9, 2016. Available in:< https://doi.org/10.5281/zenodo.1209993>.Accessed on March 5, 2019.

SURIAN, N.; CISOTTO, A. Channel adjustments, bedload transport and sediment sources in a gravel- bed river, Brenta River, Italy. Earth Surface Processes and Landforms: **The Journal of the British Geomorphological Research Group**, v. 32, n. 11, p. 1641-1656, 2007. https://doi.org/10.1002/esp.1591

TANG, Q., FU, B.; WEN, A.; ZHANG, X.; HE, X.; COLLINS, A.L. Fingerprinting the sources of water-mobilized threatening agricultural and water resource sustainability: progress, challenges and prospects in China. **Science China Earth Sciences**, v. 62, p. 2017-2030, 2019. https://doi.org/10.1007/s11430-018-9349-0

THEVENOT, M.; DIGNAC, M. F.; RUMPEL, C. Fate of lignins in soils: a review. **Soil Biology and Biochemistry**, v. 42, n. 8, p. 1200-1211, 2010. https://doi.org/10.1016/j.soilbio.2010.03.017

TIECHER, T.; CANER, L.; MINELLA, J. P. G.; DOS SANTOS, D. R. Combining visible-based color parameters and geochemical tracers to improve sediment source discrimination and apportionment. **Science of the Total Environment**, v. 527, p. 135-149, 2015. https://doi.org/10.1016/j.scitotenv.2015.04.103

TIECHER, T.; MINELLA, J. P. G.; CANER, L.; EVRARD, O.; ZAFAR, M.; CAPOANE, V.; LE GALL, M.; DOS SANTOS, D. R. Quantifying land use contributions to suspended sediment in a large cultivated catchment of Southern Brazil (Guaporé River, Rio Grande do Sul). **Agriculture, Ecosystems & Environment**, v. 237, p. 95-108, 2017a. https://doi.org/10.1016/j.agee.2016.12.004

TIECHER, T; CANER, L.; MINELLA, J. P. G.; EVRARD, O.; MONDAMERT, L.; LABANOWSKI, J.; SANTOS, D. R. Tracing sediment sources using mid-infrared spectroscopy in Arvorezinha catchment, southern Brazil. **Land Degradation & Development**, v.28, n. 5, p.1603-1614, 2017b. https://doi.org/10.1002/ldr.2690

TIECHER, T.; RAMON, R.; LACEBY, J. P.; EVRARD, O.; MINELLA, J. P. G. Potential of phosphorus fractions to trace sediment sources in a rural catchment of Southern Brazil: Comparison with the conventional approach based on elemental geochemistry. **Geoderma**, v. 337, p. 1067-1076, 2019. https://doi.org/10.1016/j.geoderma.2018.11.011

TORRES, I. F.; BASTIDA, F.; HERNÁNDEZ, T.; BOMBACH, P.; RICHNOW, H. H.; GARCÍA, C. The role of lignin and cellulose in the carbon-cycling of degraded soils under semiarid climate and their relation to microbial biomass. **Soil Biology and Biochemistry**, v. 75, p. 152-160, 2014. https://doi.org/10.1016/j.soilbio.2014.04.007

TURNER, A., TAYLOR, A. On site determination of trace metals in estuarine sediments by field portable-XRF. **Talanta**, v. 190, p. 498-506, 2018. https://doi.org/10.1016/j.talanta.2018.08.024

UBER, M.; LEGOUT, C.; NORD, G.; CROUZET, C.; DEMORY, F.; POULENARD, J. Comparing alternative tracing measurements and mixing models to fingerprint suspended sediment sources in a mesoscale Mediterranean catchment. **Journal of Soils and Sediments**, v. 19, p. 3255-3273, 2019. https://doi.org/10.1007/s11368-019-02270-1

VALENTE, M. L.; REICHERT, J. M.; LEGOUT, C., TIECHER, T.; CAVALCANTE, R. B. L.; EVRARD, O. Quantification of sediment source contributions in two paired catchments of the Brazilian Pampa using conventional and alternative fingerprinting approaches. **Hydrological Processes**, v. 34, n. 13, p. 2965-2986, 2020. https://doi.org/10.1002/hyp.13768

VENABLES, W. N.; RIPLEY, B. D. **MASS library of functions**. Modern applied statistics with S, 4 ed., Springer, 2002, 495p.

VISCARRA ROSSEL, R. A. ColoSol. Executable software to perform colour space model transformation for soil colour, 2004. Available in: http://www.usyd.edu.au/su/agric/acpa/people/rvrossel/ soft02.htm. Accessed January 7, 2018.

VISCARRA ROSSEL, R. A.; MINASNY, B.; ROUDIER, P.; MCBRATNEY, A. B. Colour space models for soil science. **Geoderma**, v. 133, n. 3-4, p. 320-337, 2006. https://doi.org/10.1016/j.geoderma.2005.07.017

WALLING, D. E.; WOODWARD, J. C.; NICHOLAS, A. P. A multi-parameter approach to fingerprinting suspended-sediment sources. **IAHS Publication**, v. 215, p. 329-338, 1993.

WALLING, D. E. The evolution of sediment source fingerprinting investigations in fluvial systems. **Journal of Soils and Sediments**, v. 13, n. 10, p.1658-1675, 2013. https://doi.org/10.1007/s11368-013-0767-2

WALLING, D. E. Human impact on land–ocean sediment transfer by the world's rivers. **Geomorphology**, v. 79, n. 3-4, p. 192-216, 2006. https://doi.org/10.1016/j.geomorph.2006.06.019

ŽIVKOVIĆ, S.; VELJKOVIĆ, M. Environmental impacts the of production and use of biodiesel. **Environmental Science and Pollution Research**, v. 25, n. 1, p. 191-199, 2018. https://doi.org/10.1007/s11356-017-0649-z

ZHANG, Y.; COLLINS, A. L.; MCMILLAN, S.; DIXON, E. R.; CANCER- BERROYA, E.; POIRET, C.; STRINGFELLOW, A. Fingerprinting source contributions to bed sediment-associated organic matter in the headwater subcatchments of the River Itchen SAC, Hampshire, UK. **River Research and Applications**, v. 33, n. 10, p. 1515-1526, 2017. https://doi.org/10.1002/rra.3172

4 APPENDIX - SPECIFIC SPECTRA OF ORGANIC COMPOUNDS, INORGANIC CONSTITUENTS AND SOIL COLOURS FOR IDENTIFICATION OF SEDIMENT SOURCES IN A RURAL BRAZIL CATCHMENT

a)

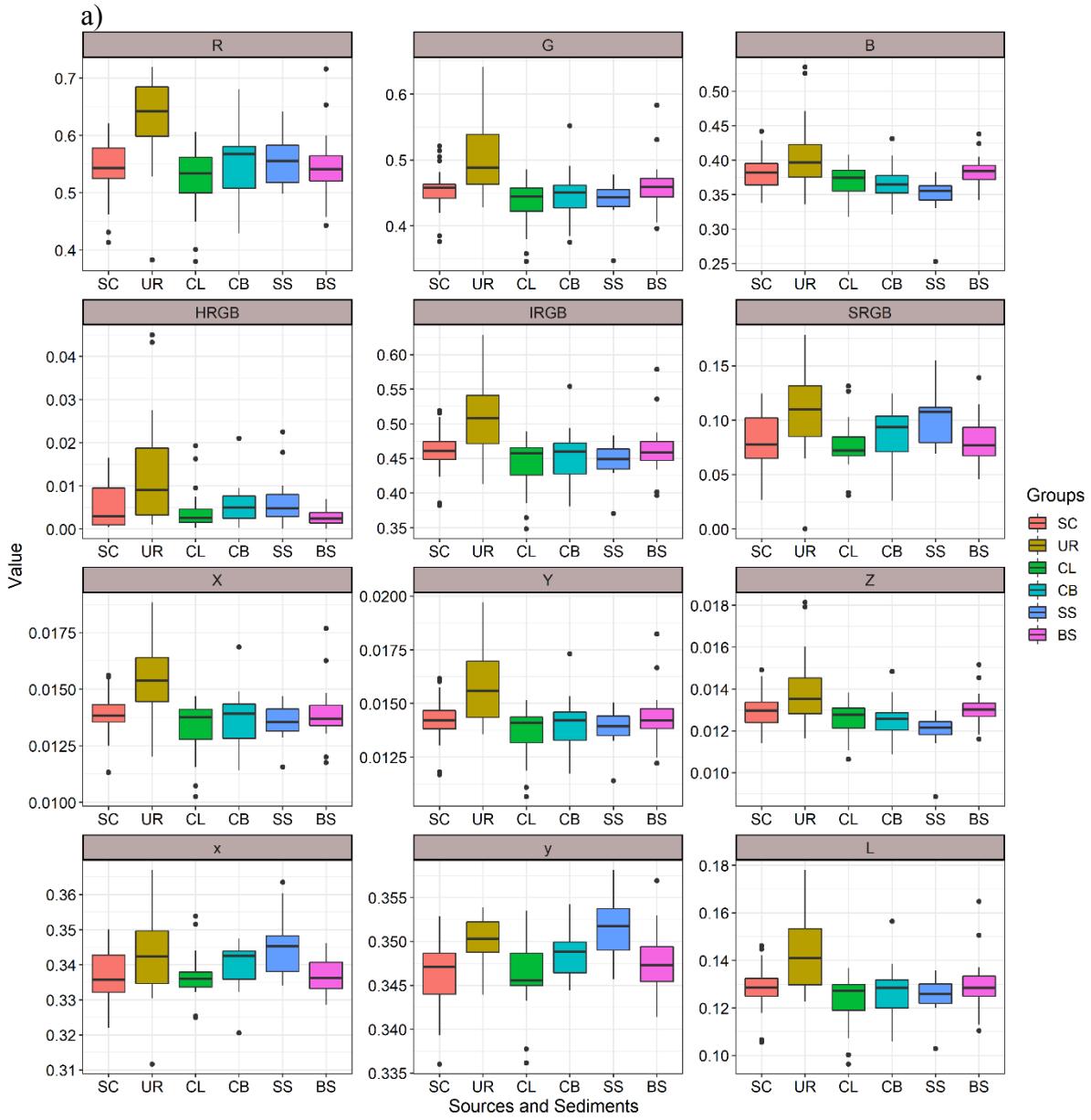

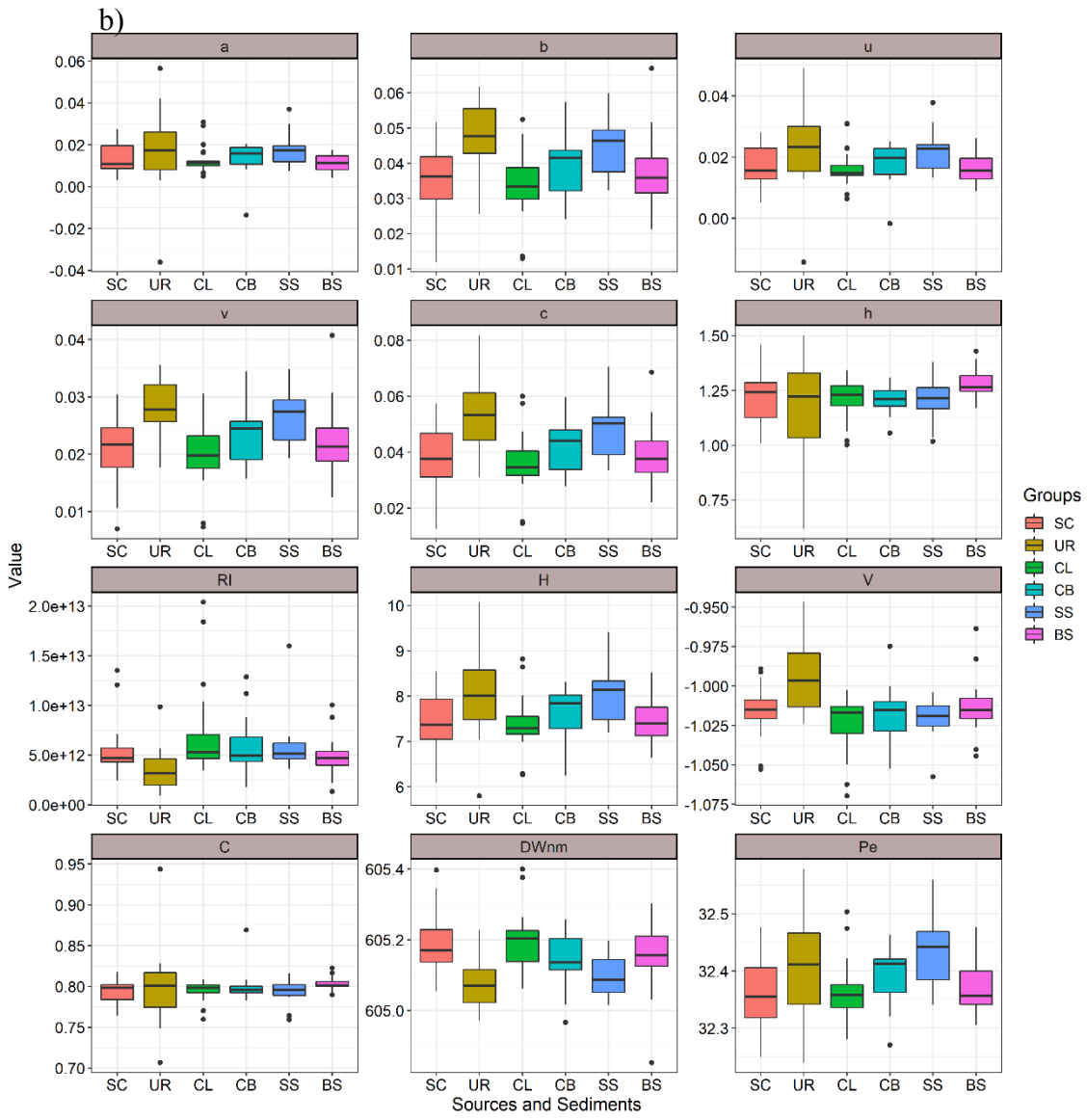

Figure S1. Distributions of colour tracers for assessing conservative behaviour at catchment-wide scale. The median is shown by the central line, the interquartile range by the box, and outliers by the circles

a)

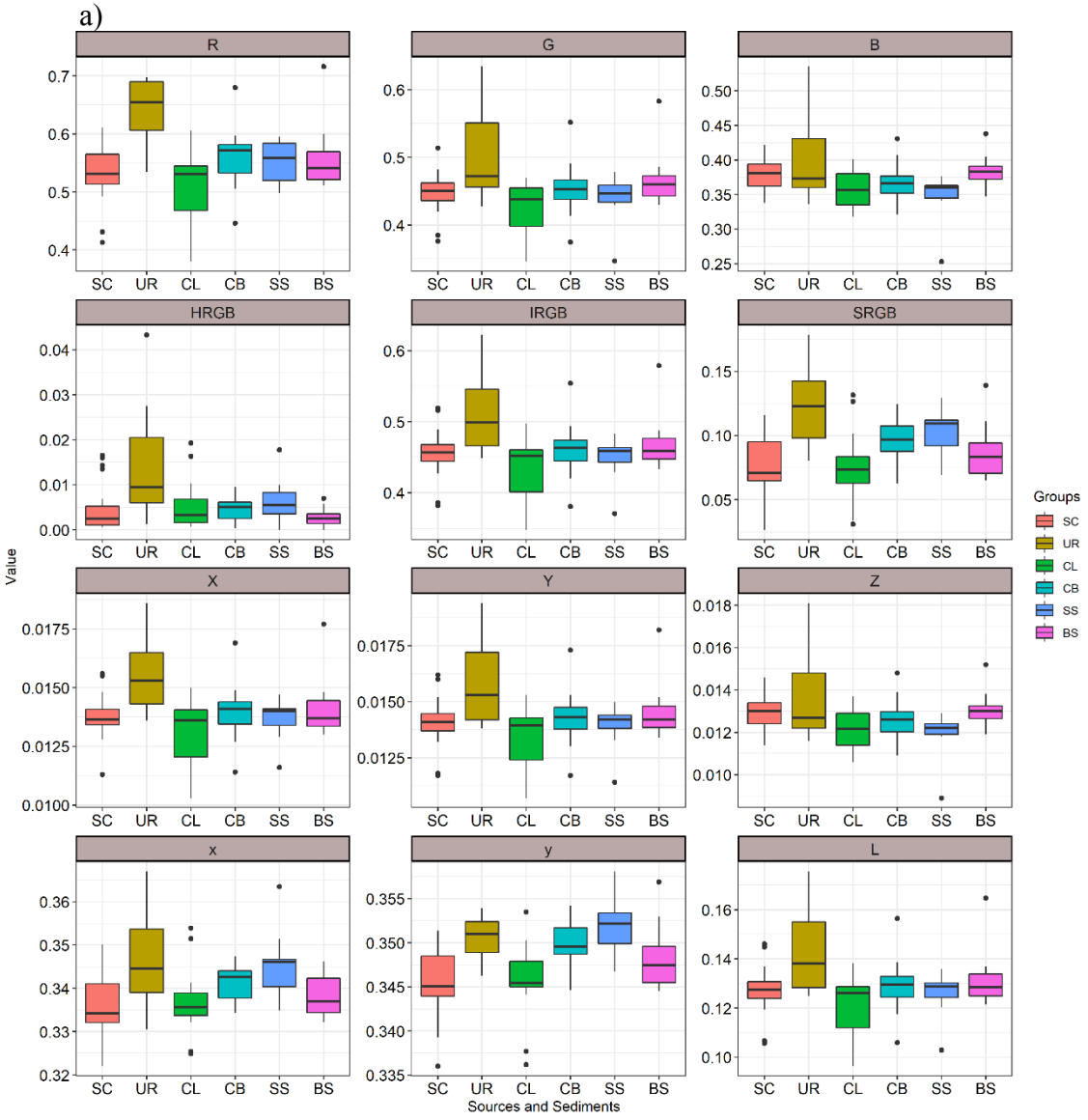
R
G
B
HRGB
IRGB
SRGB
X
Y
Z
x
y
L
SC
UR
CL
CB
SS
BS
Value
Sources and Sediments
Groups
SC
UR
CL
CB
SS
BS

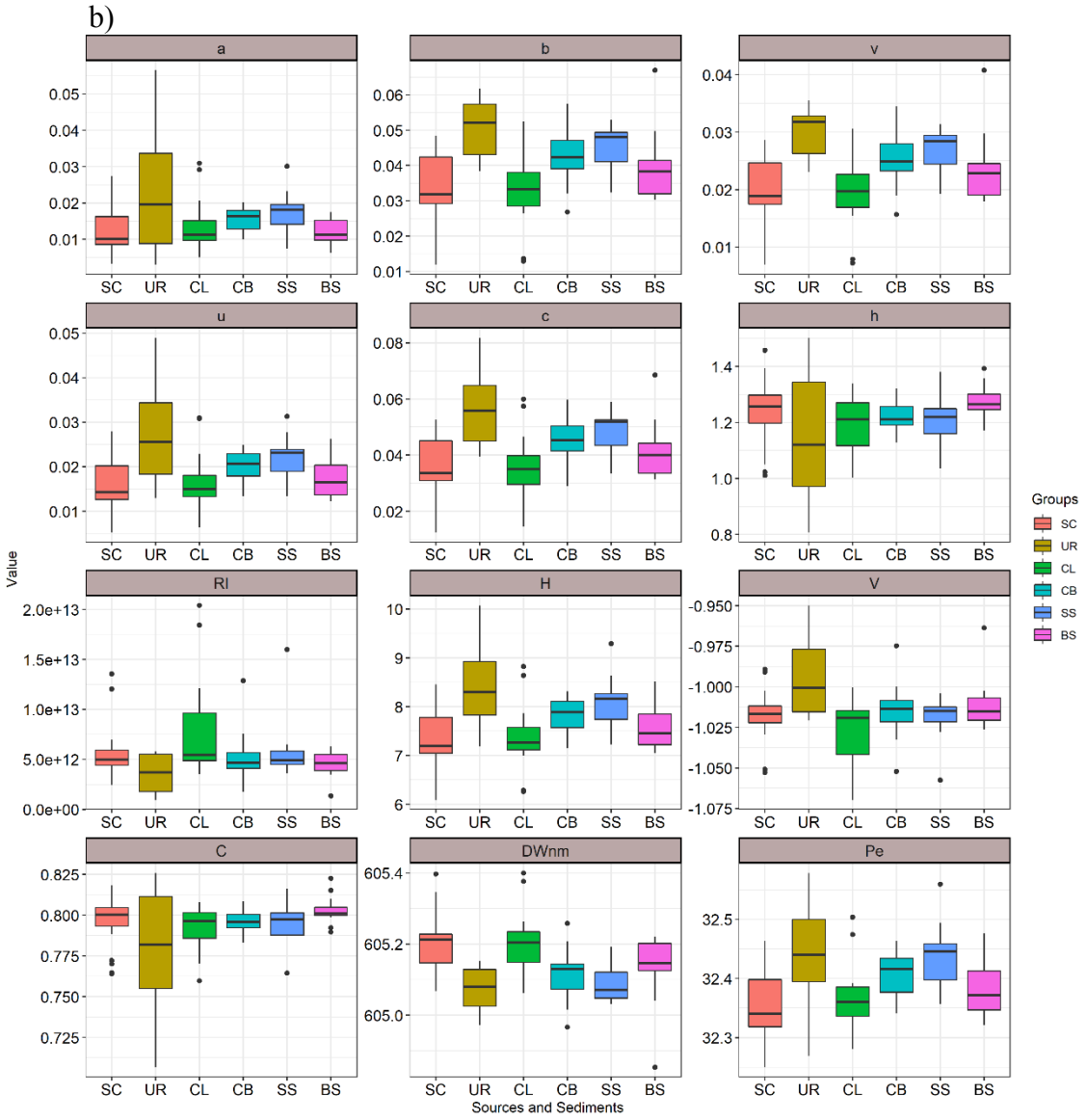

Figure S2. Distributions of colour tracers for assessing conservative behaviour at sub-catchment scale. The median is shown by the central line, the interquartile range by the box, and outliers by the circles

a)

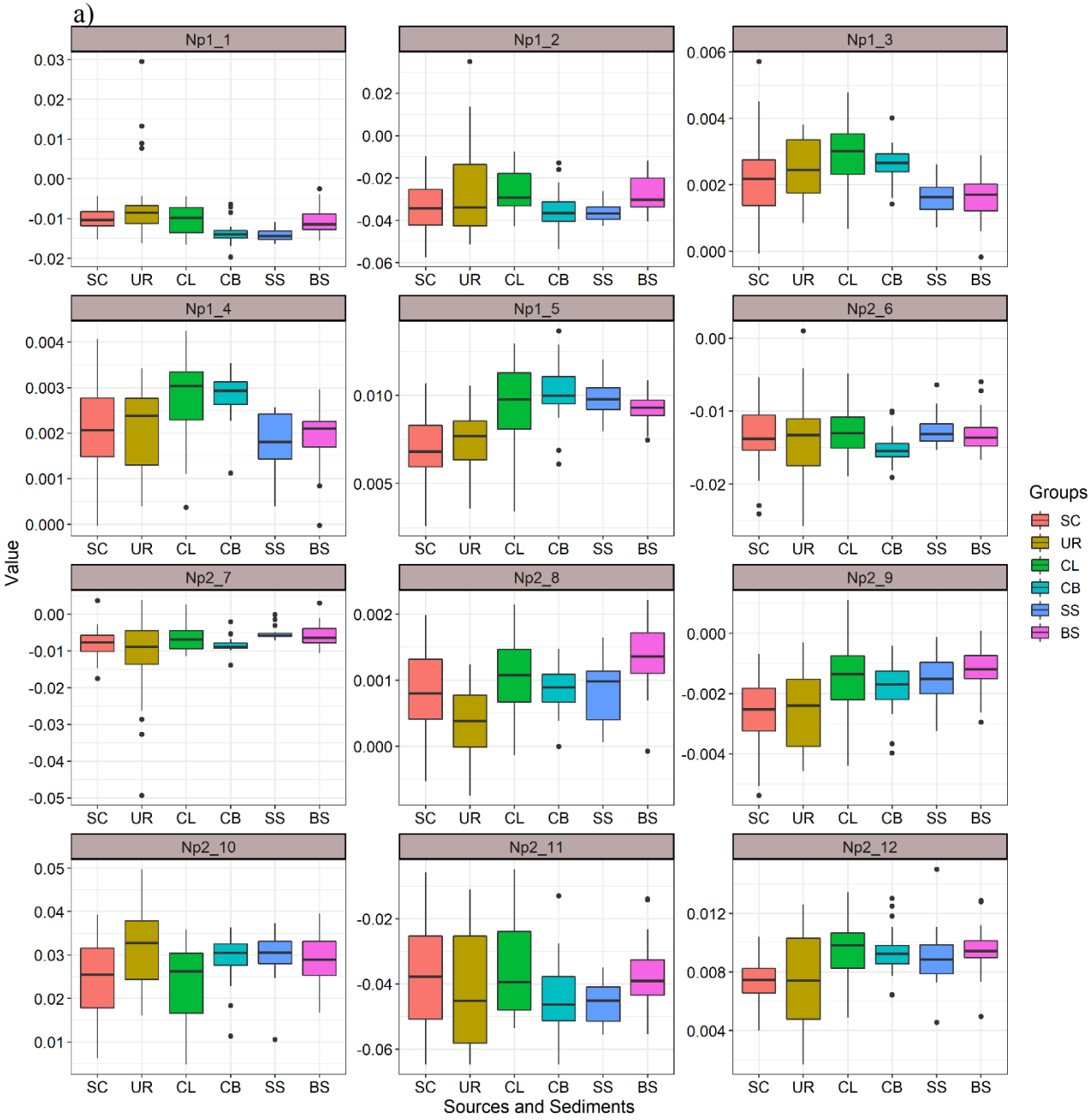
Np1_1
Np1_2
Np1_3
Np1_4
Np1_5
Np2_6
Np2_7
Np2_8
Np2_9
Np2_10
Np2_11
Np2_12
SC
UR
CL
CB
SS
BS
Value
Sources and Sediments
Groups

b)

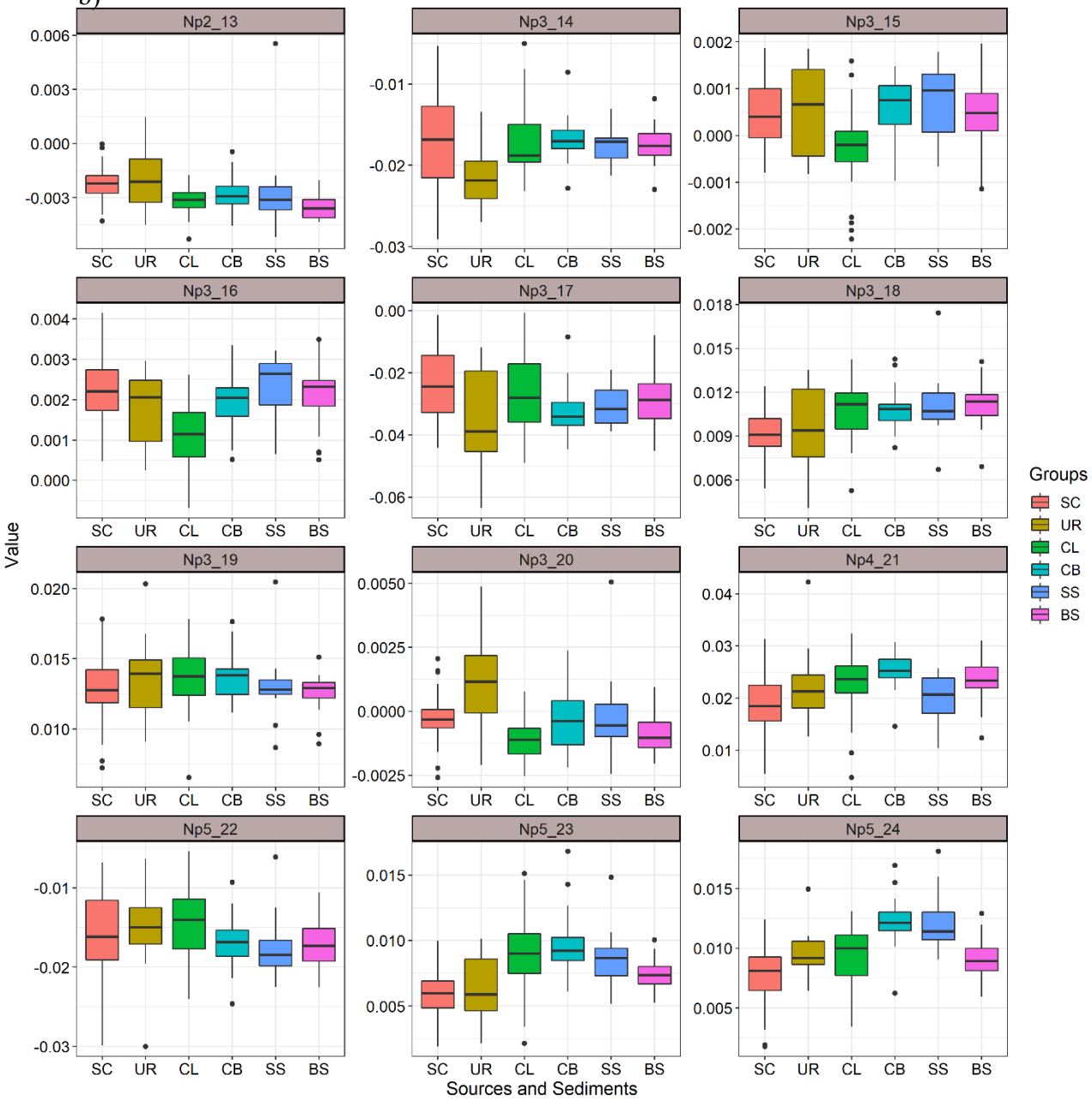
Np2_13
Np3_14
Np3_15
Np3_16
Np3_17
Np3_18
Np3_19
Np3_20
Np4_21
Np5_22
Np5_23
Np5_24
SC
UR
CL
CB
SS
BS
Value
Sources and Sediments
Groups

c)

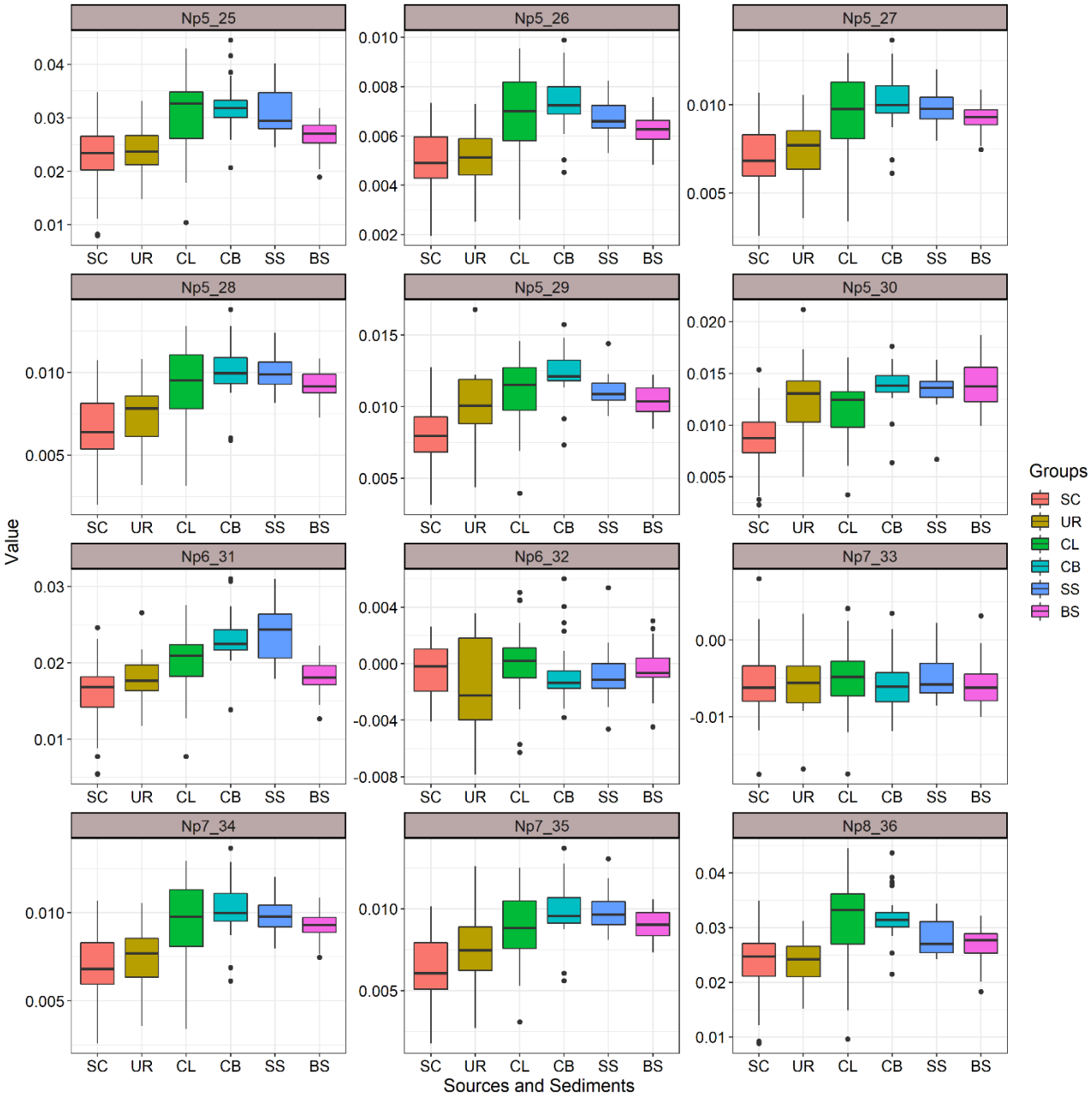
Np5_25
Np5_26
Np5_27
Np5_28
Np5_29
Np5_30
Np6_31
Np6_32
Np7_33
Np7_34
Np7_35
Np8_36
SC
UR
CL
CB
SS
BS
Value
Sources and Sediments
Groups

d)

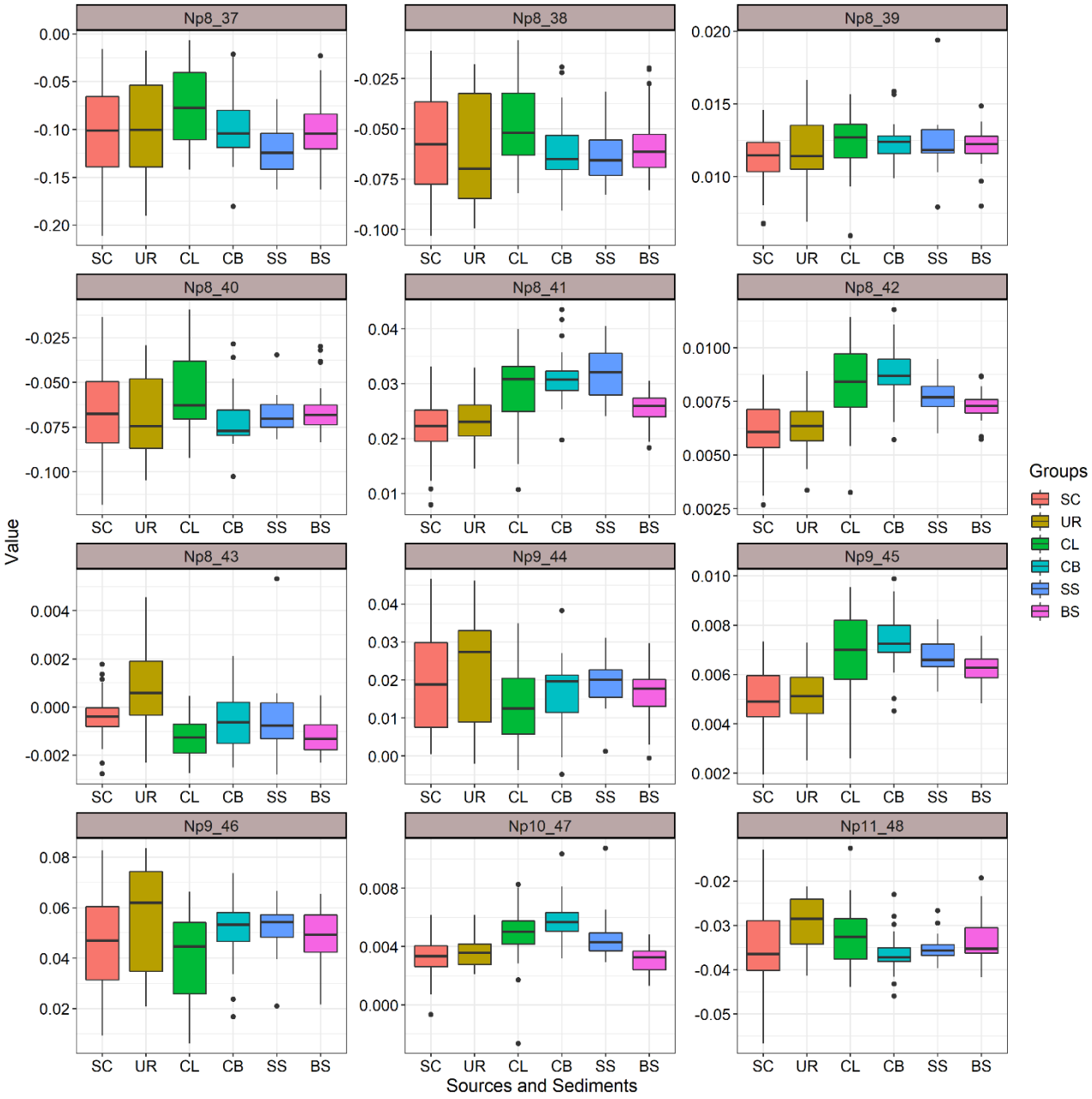
Np8_37
Np8_38
Np8_39
Np8_40
Np8_41
Np8_42
Np8_43
Np9_44
Np9_45
Np9_46
Np10_47
Np11_48
SC
UR
CL
CB
SS
BS
Value
Sources and Sediments
Groups

e)

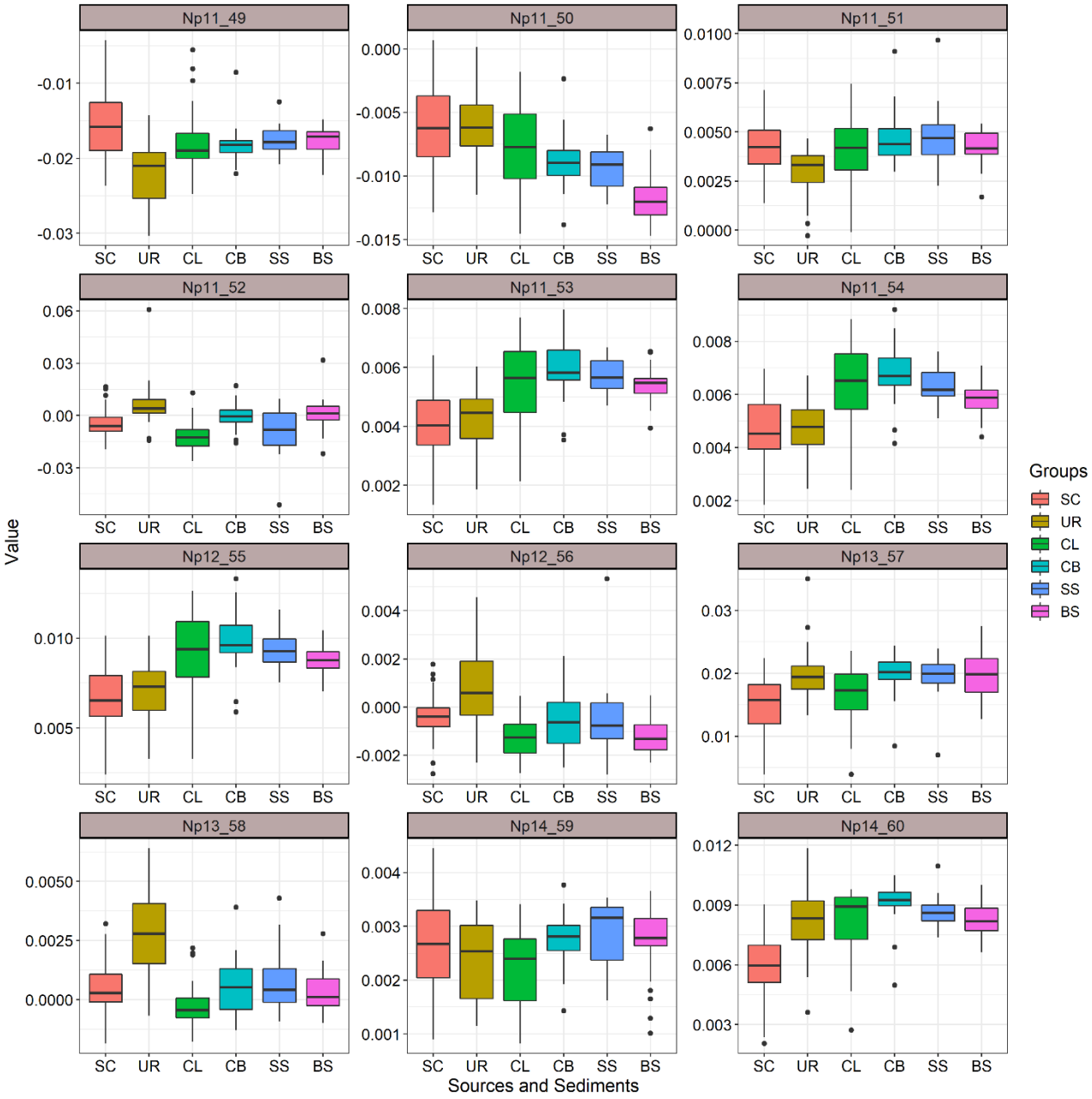
Np11_49
Np11_50
Np11_51
Np11_52
Np11_53
Np11_54
Np12_55
Np12_56
Np13_57
Np13_58
Np14_59
Np14_60
SC
UR
CL
CB
SS
BS
Value
Sources and Sediments
Groups

f)

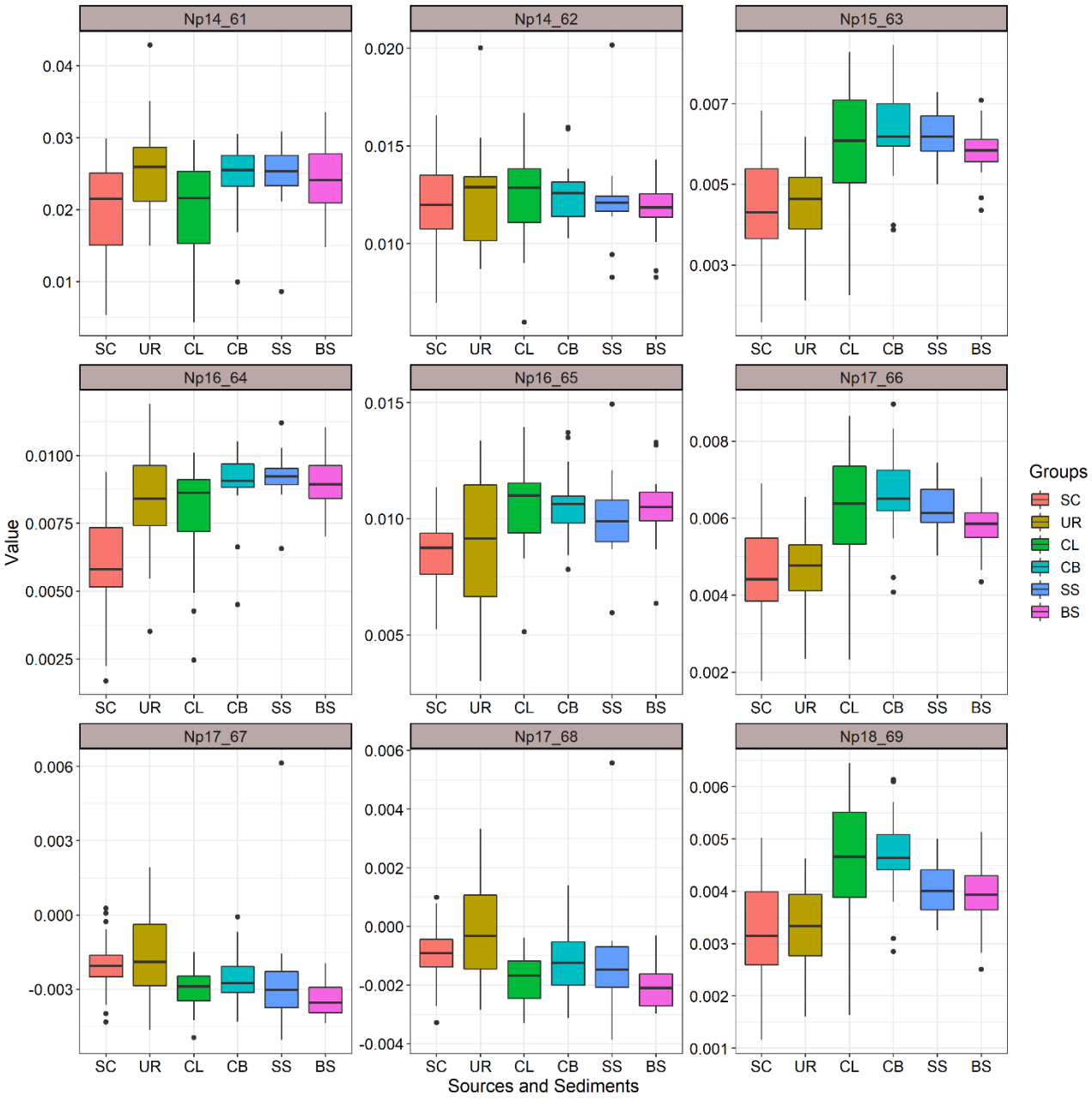

Figure S3. Distributions of NIR tracers for assessing conservative behaviour at catchment-wide scale. The median is shown by the central line, the interquartile range by the box, and outliers by the circles

a)

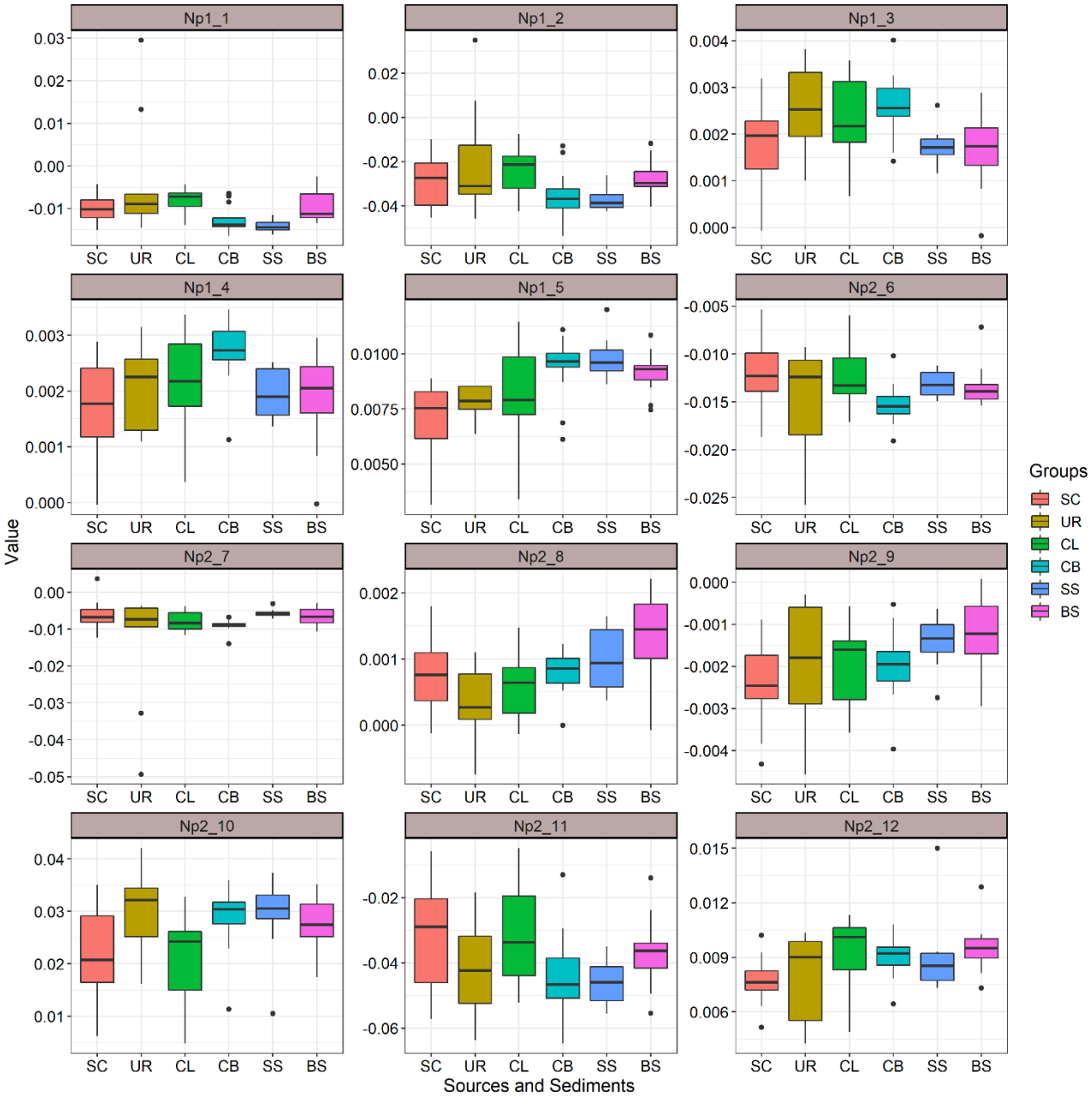
Np1_1
Np1_2
Np1_3
Np1_4
Np1_5
Np2_6
Np2_7
Np2_8
Np2_9
Np2_10
Np2_11
Np2_12
SC
UR
CL
CB
SS
BS
Value
Sources and Sediments
Groups

b)

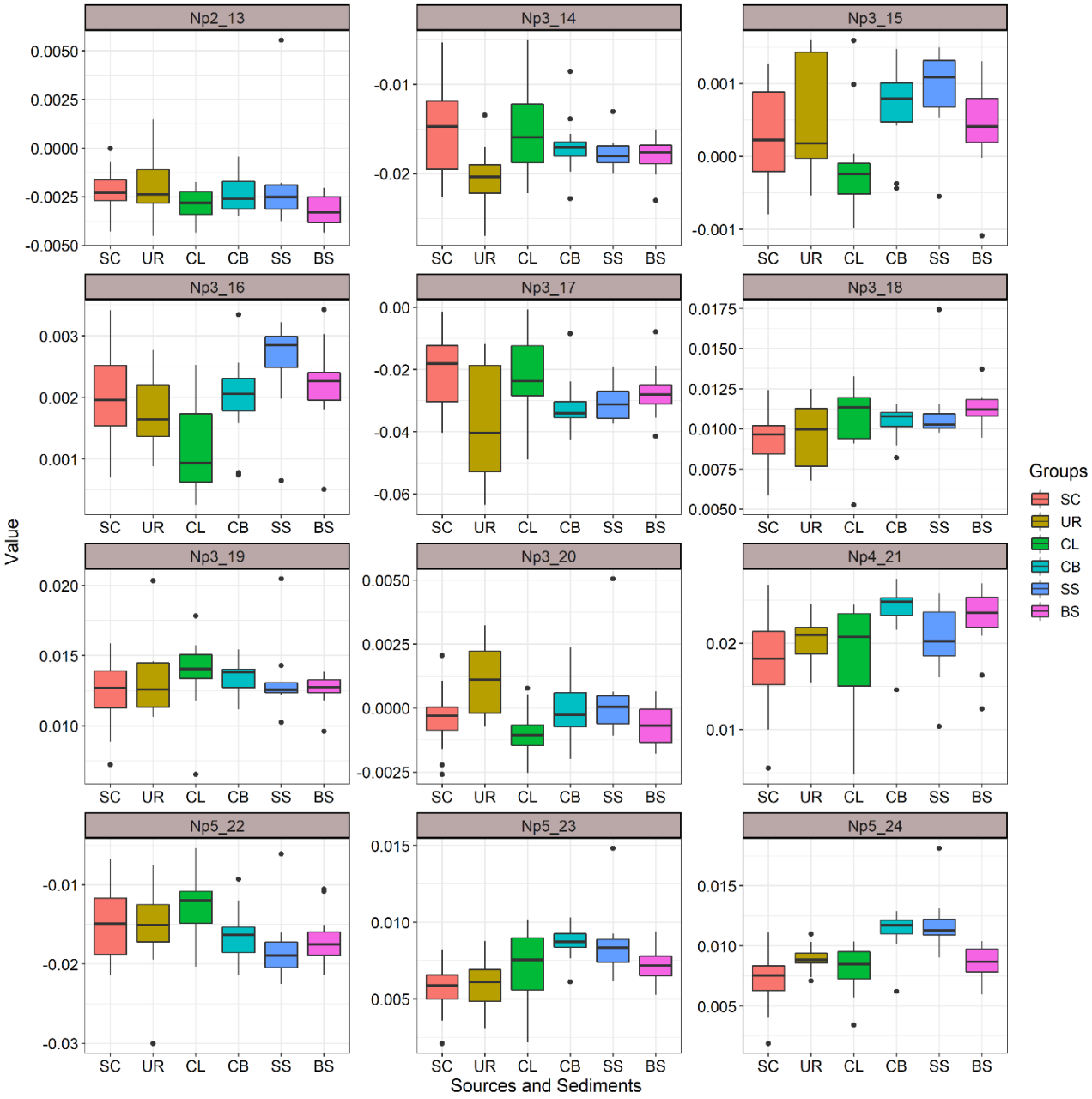
Np2_13
Np3_14
Np3_15
Np3_16
Np3_17
Np3_18
Np3_19
Np3_20
Np4_21
Np5_22
Np5_23
Np5_24
SC
UR
CL
CB
SS
BS
Value
Sources and Sediments
Groups

c)

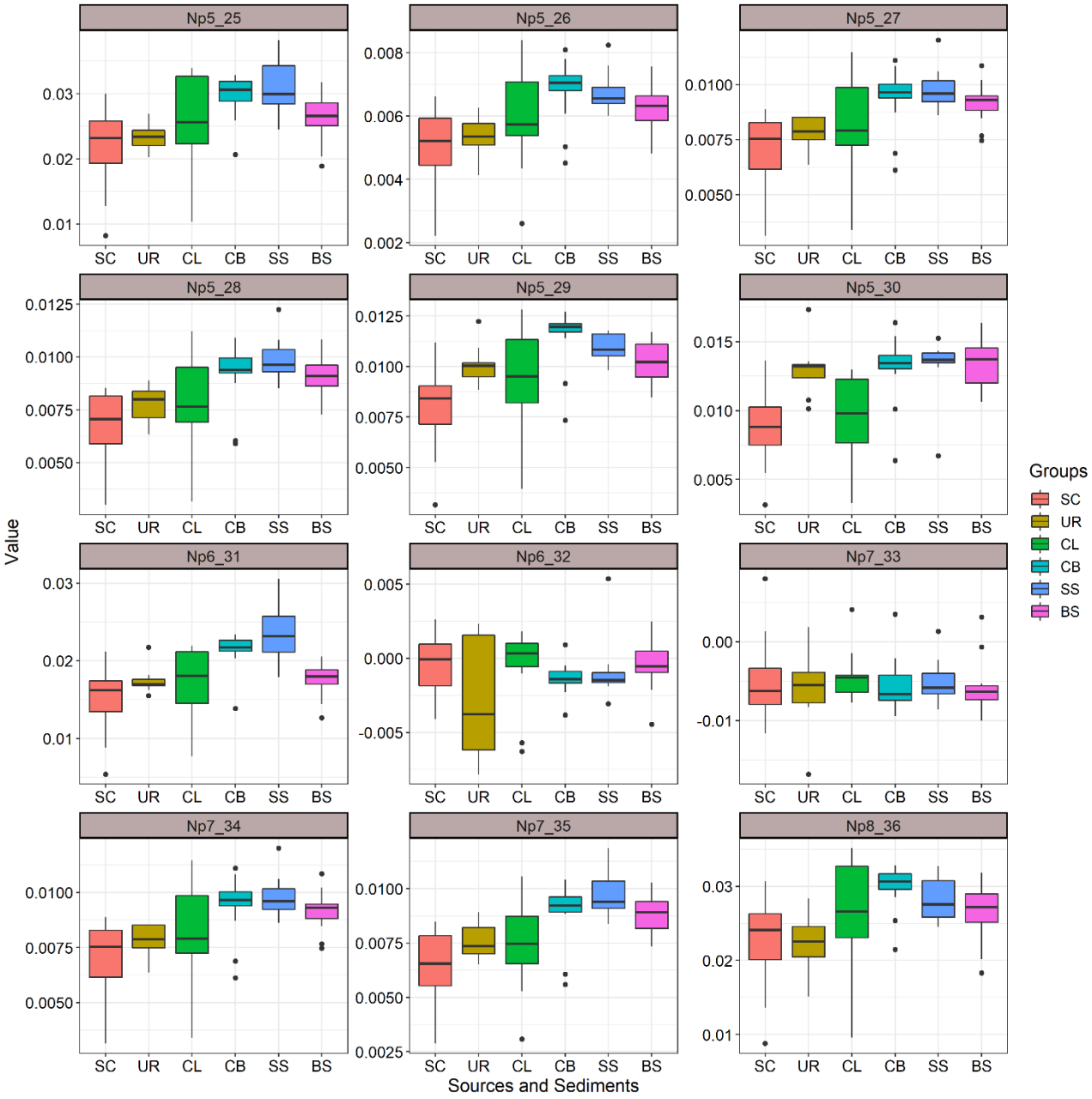
Np5_25
Np5_26
Np5_27
Np5_28
Np5_29
Np5_30
Np6_31
Np6_32
Np7_33
Np7_34
Np7_35
Np8_36
SC
UR
CL
CB
SS
BS
Value
Sources and Sediments
Groups

d)

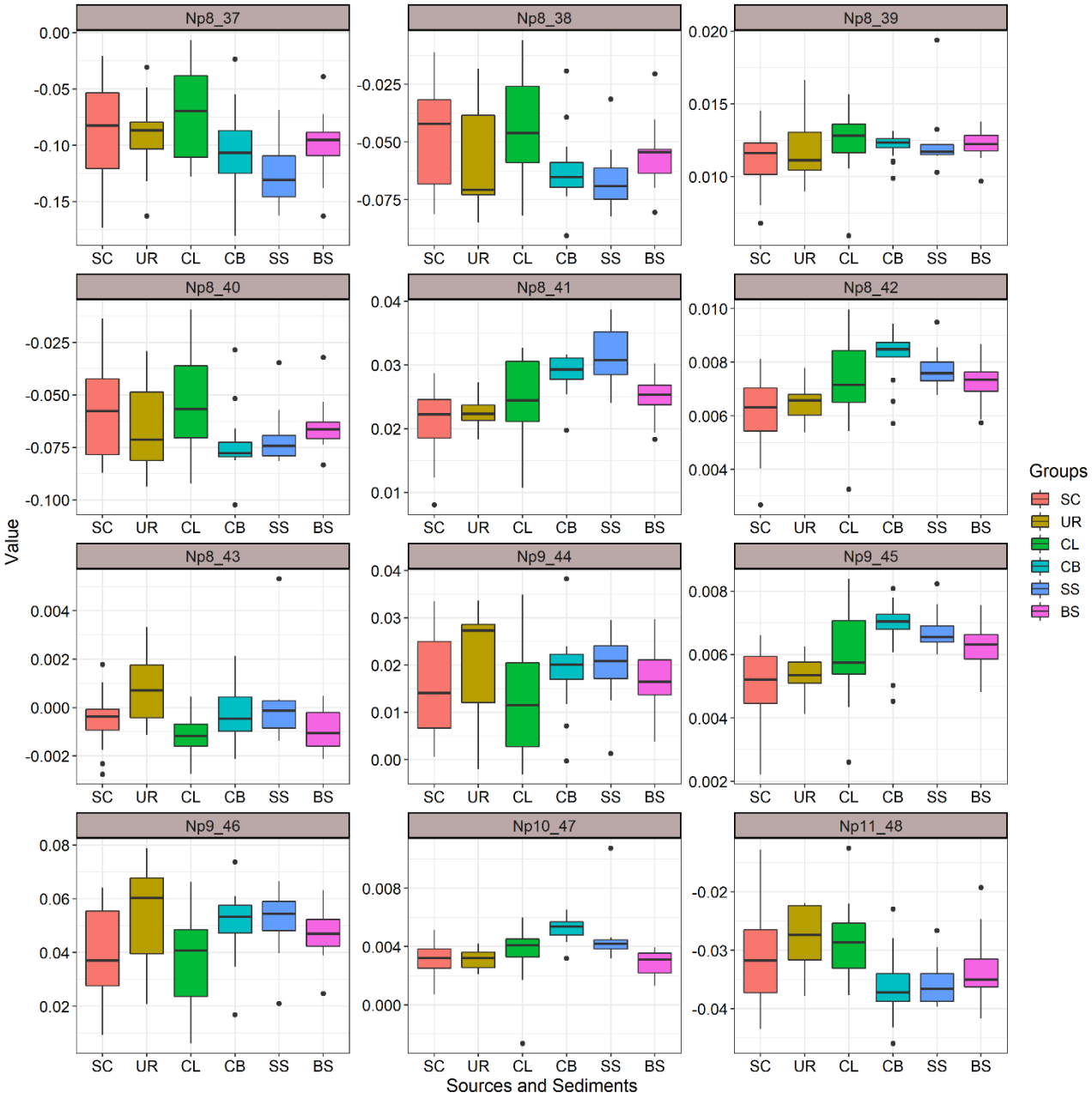
Np8_37
Np8_38
Np8_39
Np8_40
Np8_41
Np8_42
Np8_43
Np9_44
Np9_45
Np9_46
Np10_47
Np11_48
SC
UR
CL
CB
SS
BS
Value
Sources and Sediments
Groups

e)

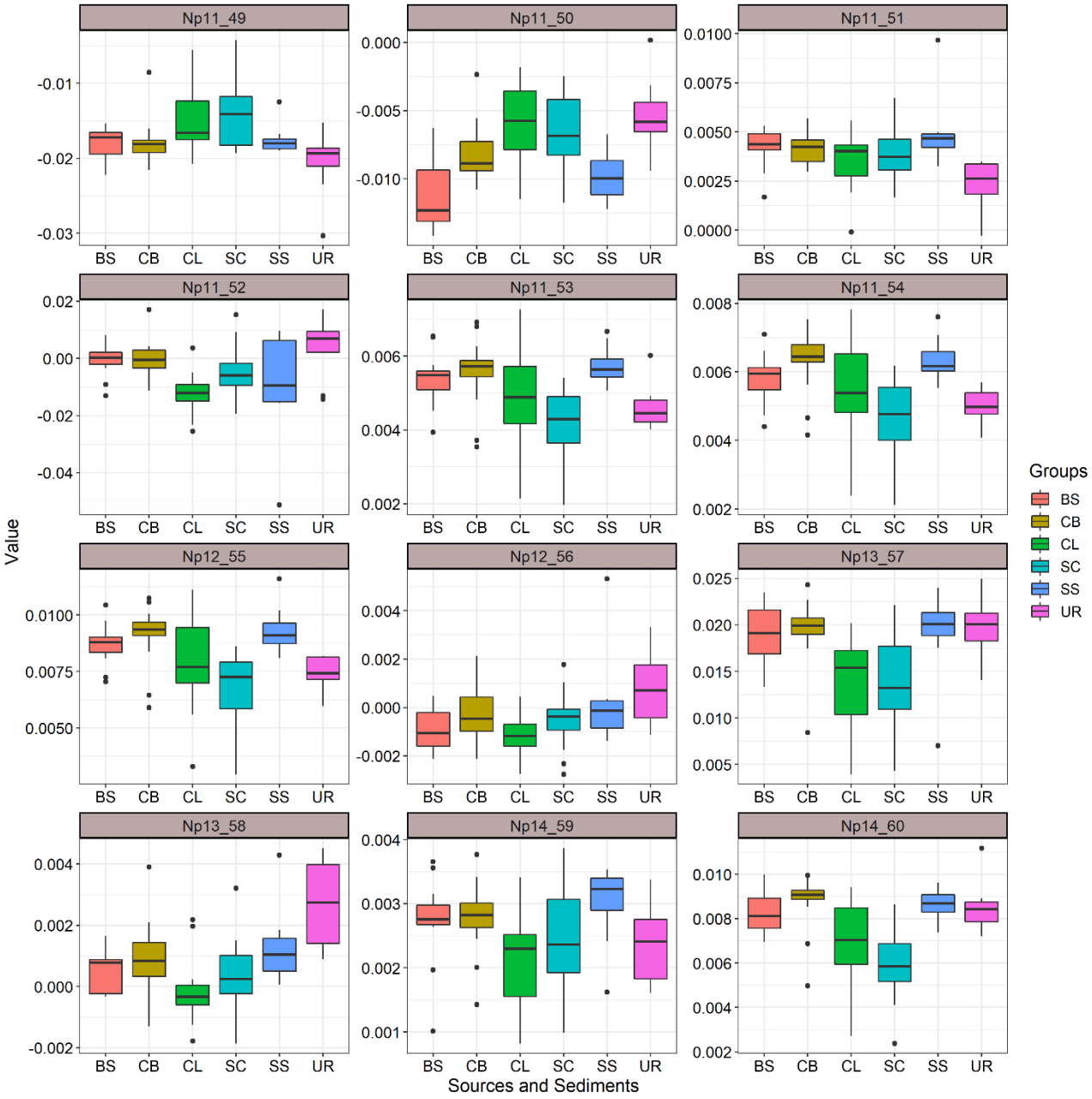
Np11_49
Np11_50
Np11_51
Np11_52
Np11_53
Np11_54
Np12_55
Np12_56
Np13_57
Np13_58
Np14_59
Np14_60
BS
CB
CL
SC
SS
UR
Value
Sources and Sediments
Groups

f)

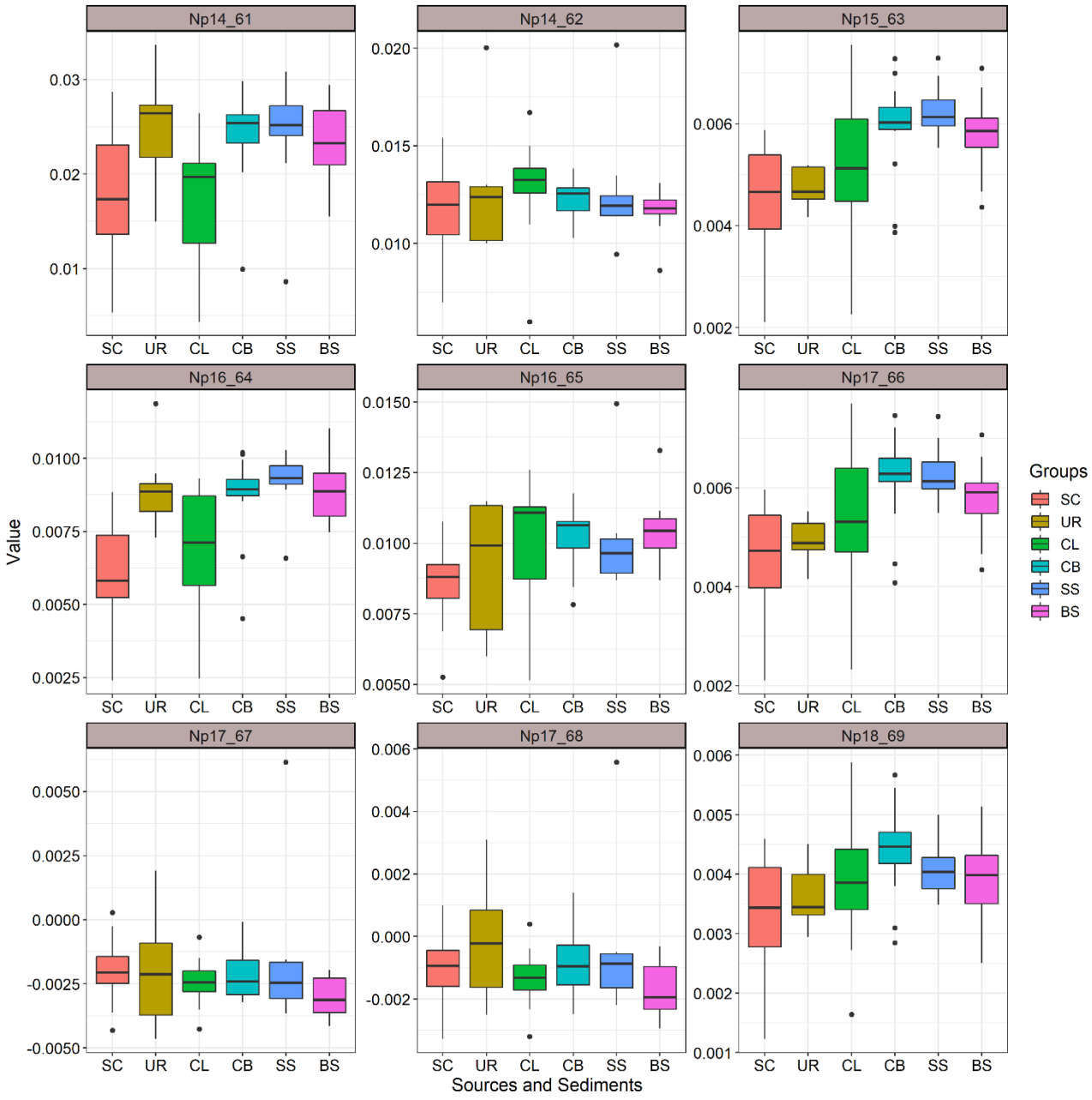

Figure S4. Distributions of NIR tracers for assessing conservative behaviour at sub-catchment scale. The median is shown by the central line, the interquartile range by the box, and outliers by the circles

a)

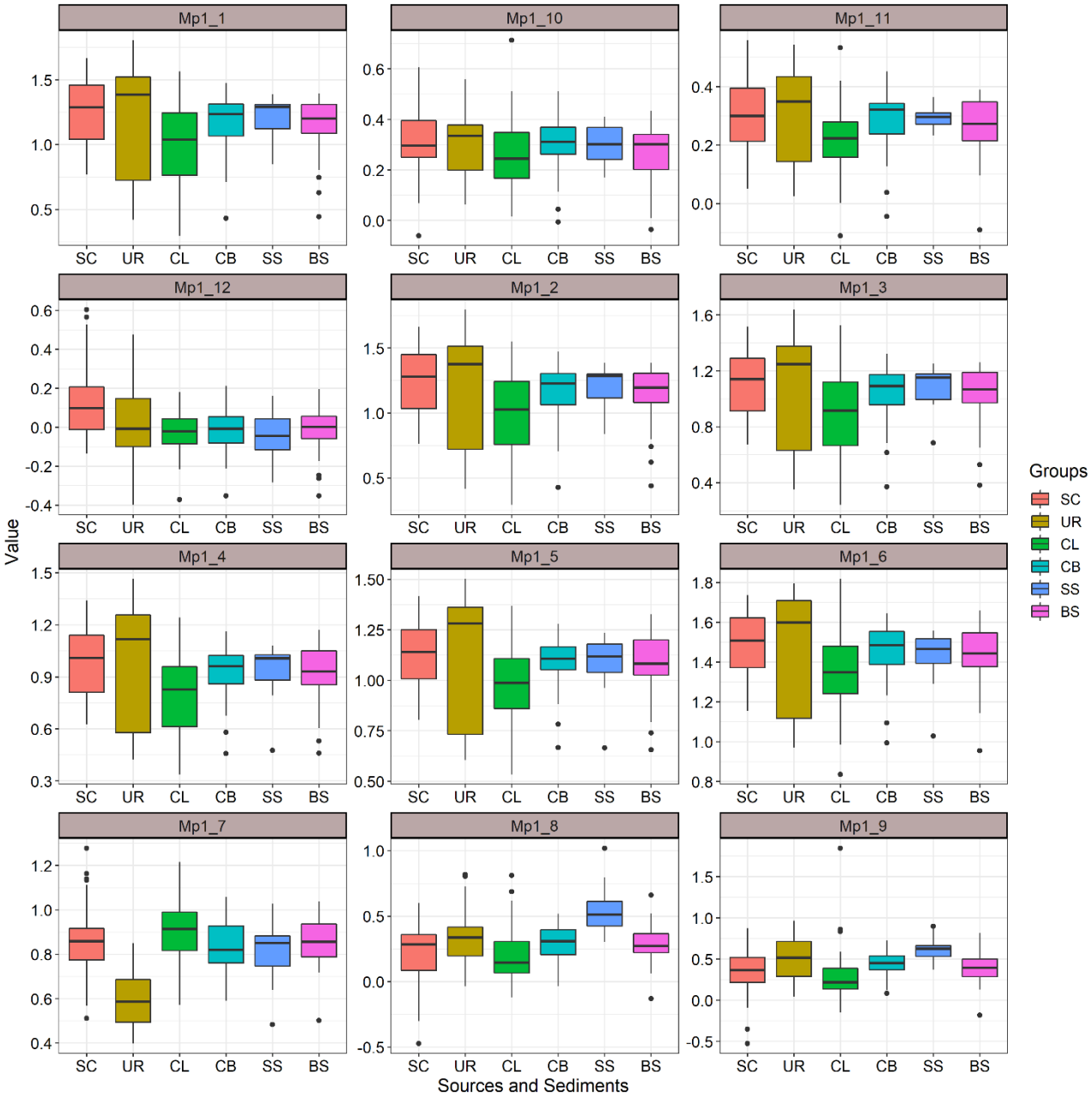
Mp1_1
Mp1_10
Mp1_11
Mp1_12
Mp1_2
Mp1_3
Mp1_4
Mp1_5
Mp1_6
Mp1_7
Mp1_8
Mp1_9
SC
UR
CL
CB
SS
BS
Value
Sources and Sediments
Groups

b)

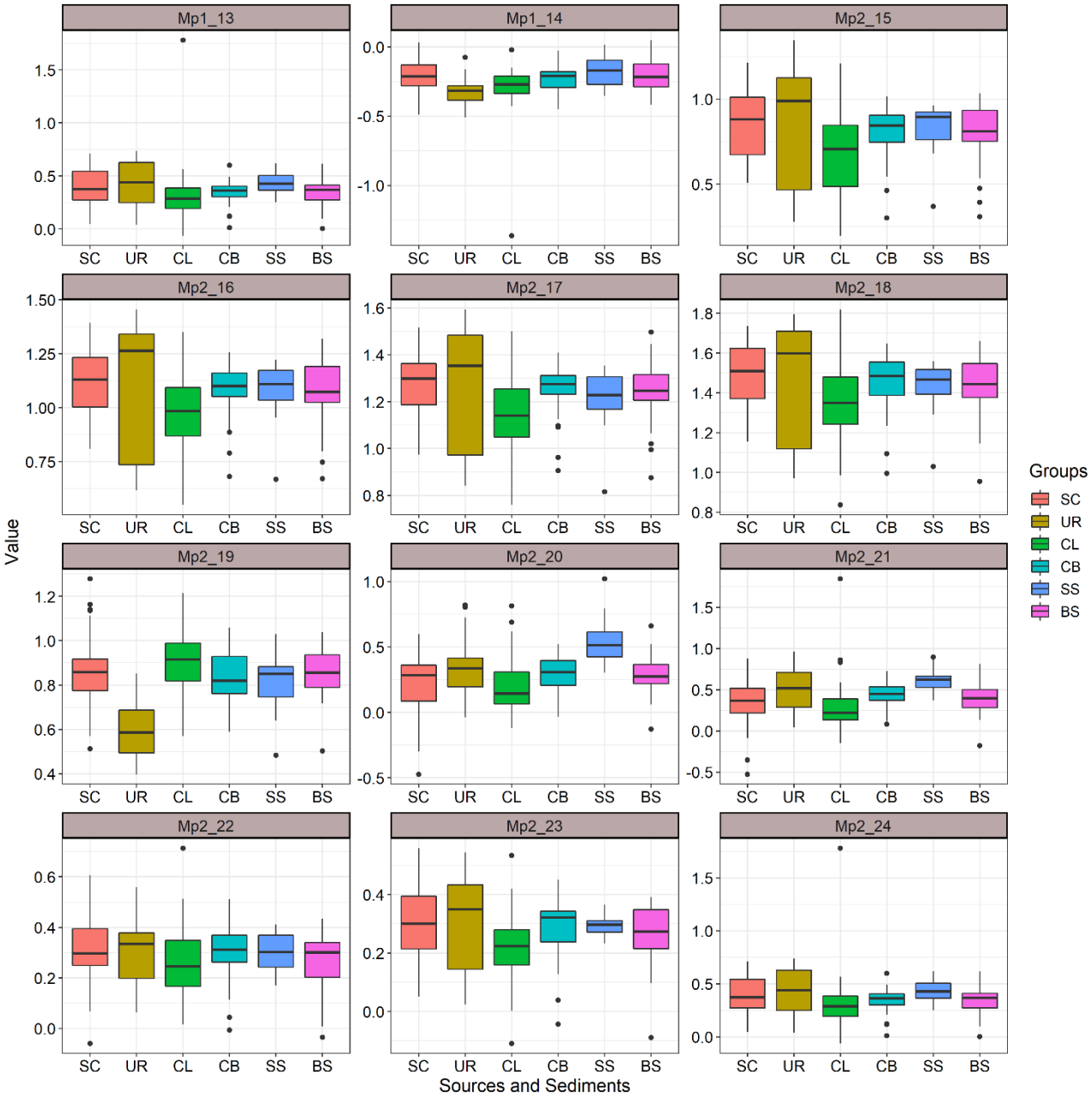
Mp1_13
Mp1_14
Mp2_15
Mp2_16
Mp2_17
Mp2_18
Mp2_19
Mp2_20
Mp2_21
Mp2_22
Mp2_23
Mp2_24
SC
UR
CL
CB
SS
BS
Value
Sources and Sediments
Groups

c)

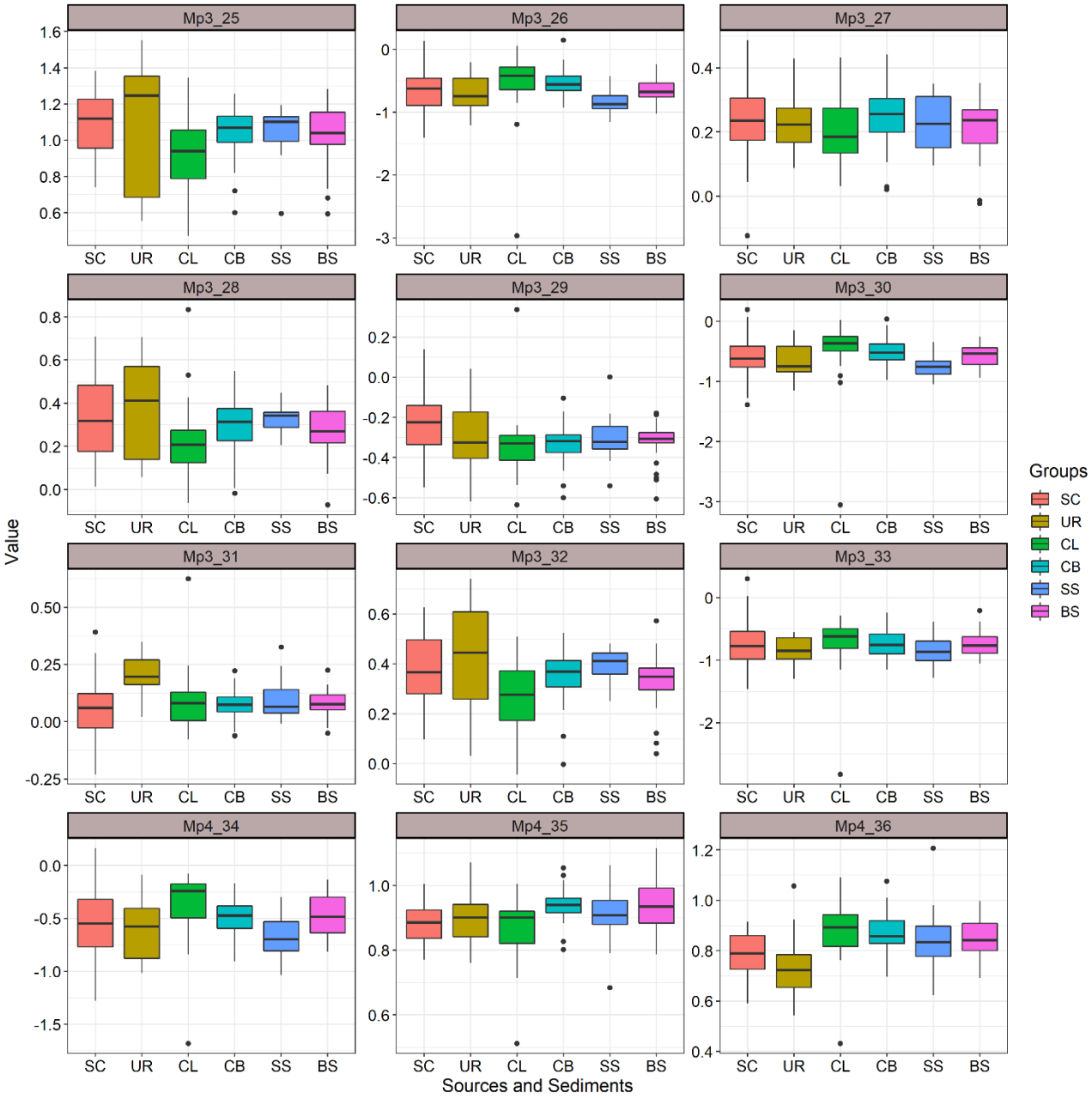
Mp3_25
Mp3_26
Mp3_27
Mp3_28
Mp3_29
Mp3_30
Mp3_31
Mp3_32
Mp3_33
Mp4_34
Mp4_35
Mp4_36
SC
UR
CL
CB
SS
BS
Value
Sources and Sediments
Groups

d)

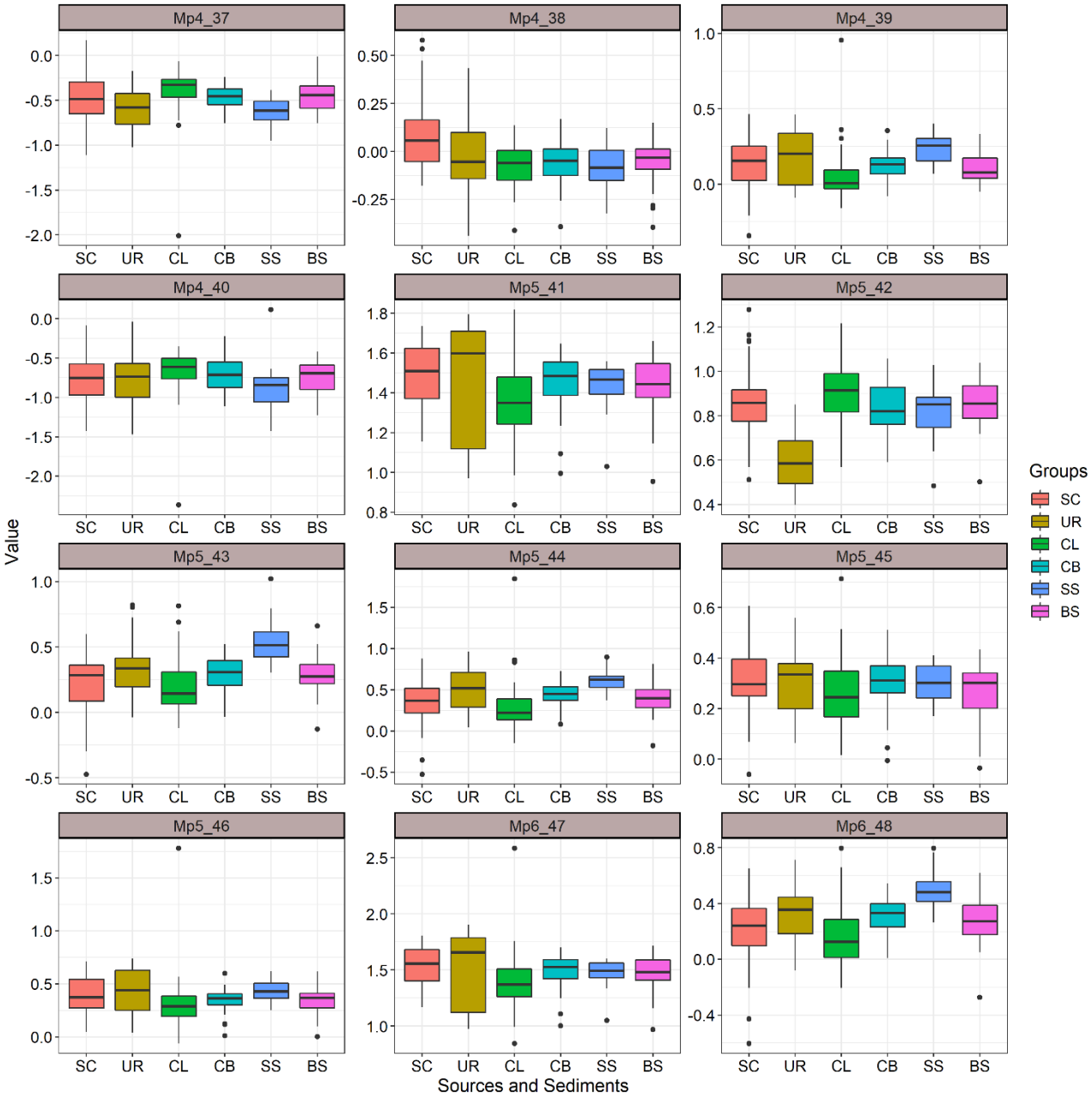
Mp4_37
Mp4_38
Mp4_39
Mp4_40
Mp5_41
Mp5_42
Mp5_43
Mp5_44
Mp5_45
Mp5_46
Mp6_47
Mp6_48
SC
UR
CL
CB
SS
BS
Value
Sources and Sediments
Groups

e)

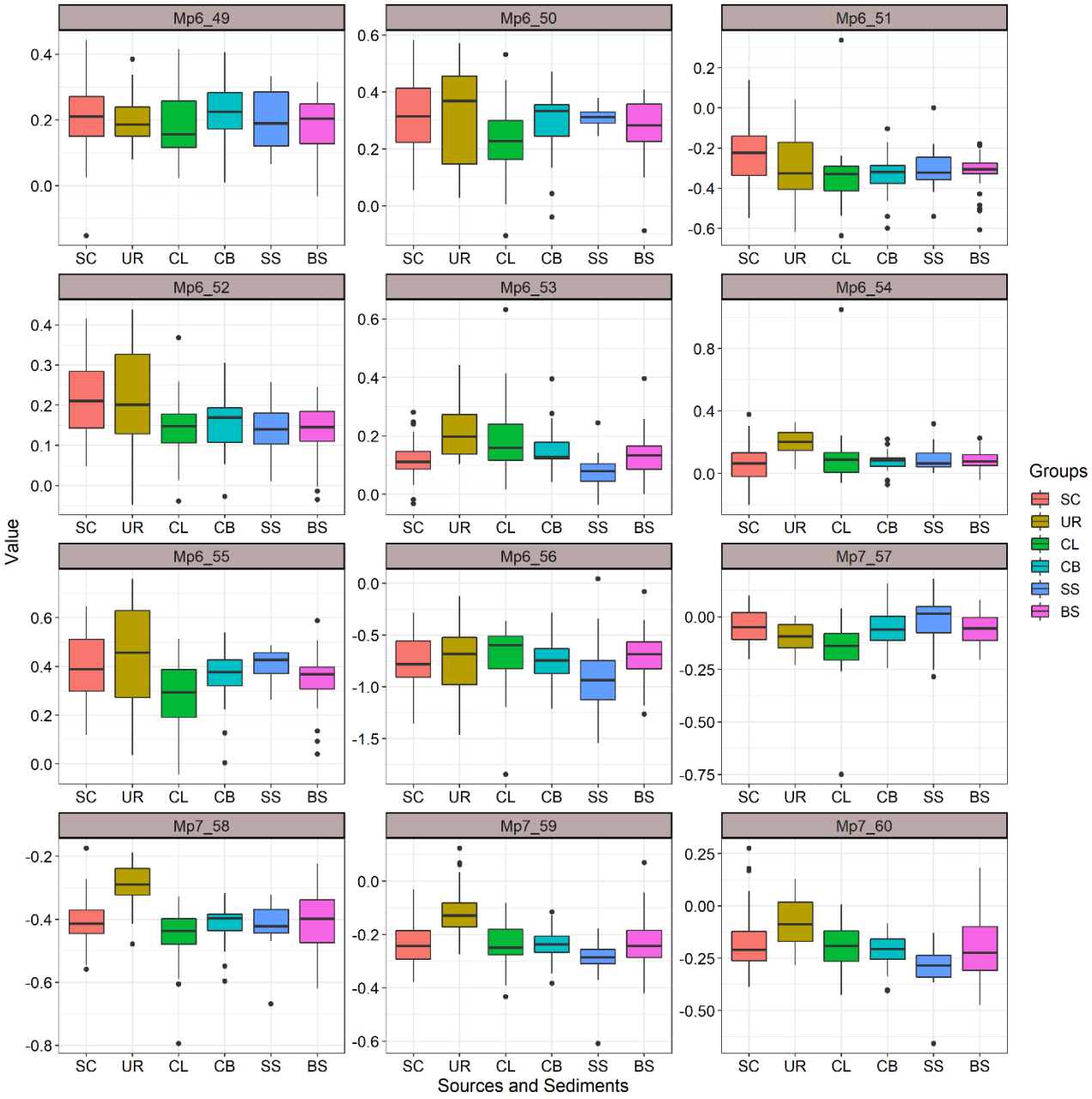
Mp6_49
Mp6_50
Mp6_51
Mp6_52
Mp6_53
Mp6_54
Mp6_55
Mp6_56
Mp7_57
Mp7_58
Mp7_59
Mp7_60
SC
UR
CL
CB
SS
BS
Value
Sources and Sediments
Groups

f)

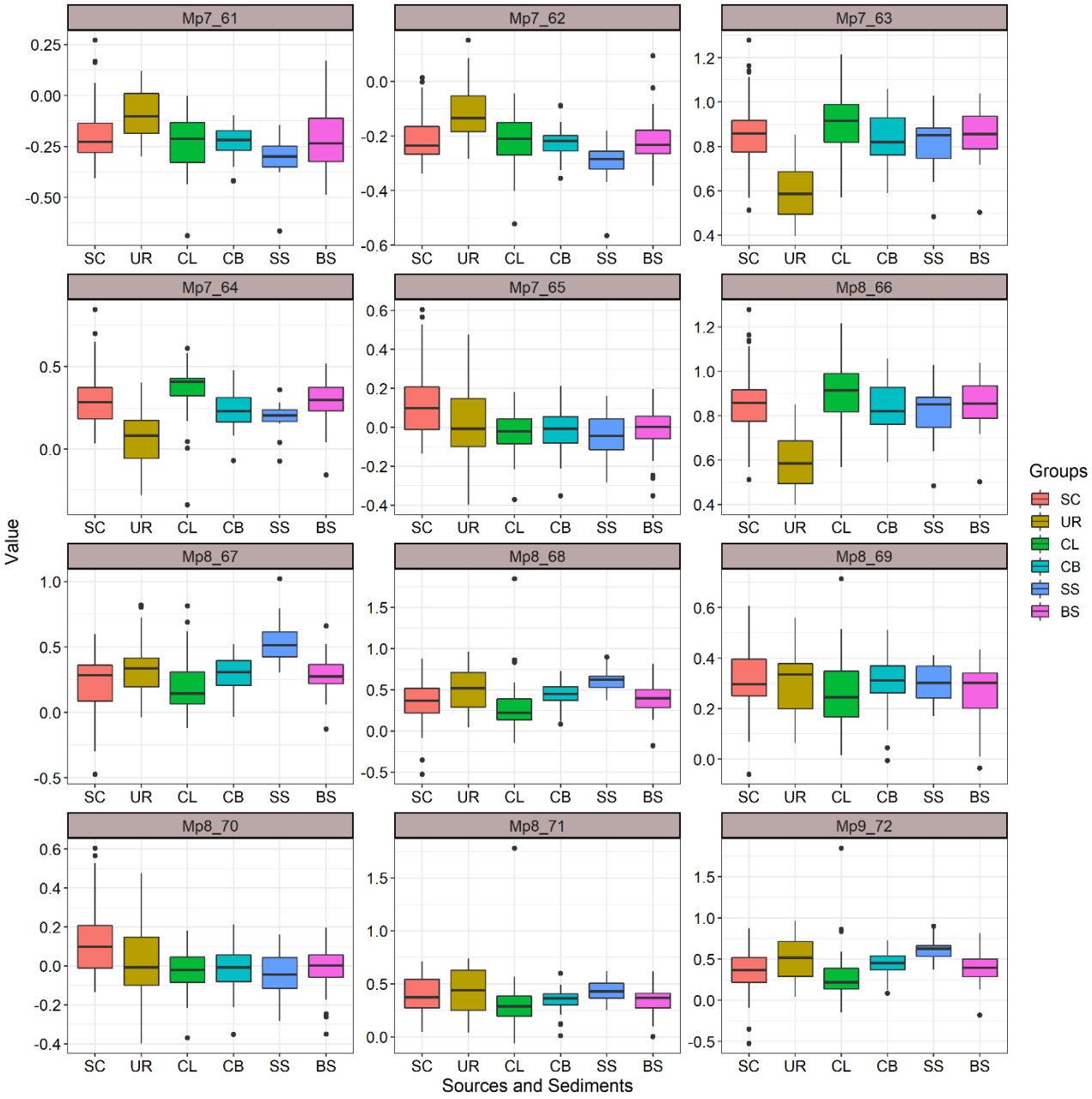
Mp7_61
Mp7_62
Mp7_63
Mp7_64
Mp7_65
Mp8_66
Mp8_67
Mp8_68
Mp8_69
Mp8_70
Mp8_71
Mp9_72
SC
UR
CL
CB
SS
BS
Value
Sources and Sediments
Groups

g)

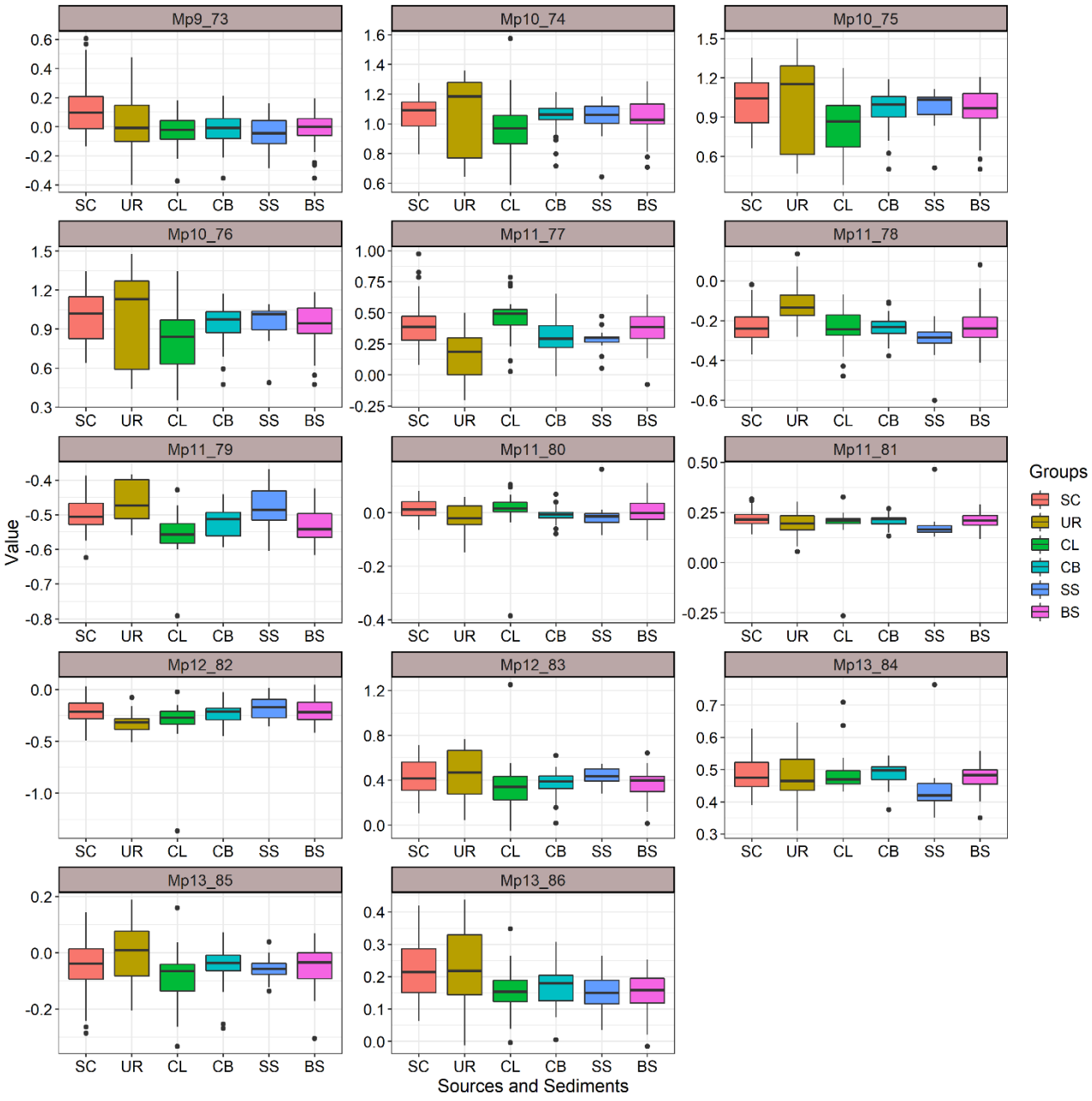

Figure S5. Distributions of MIR tracers for assessing conservative behaviour at catchment-wide scale. The median is shown by the central line, the interquartile range by the box, and outliers by the circles

a)

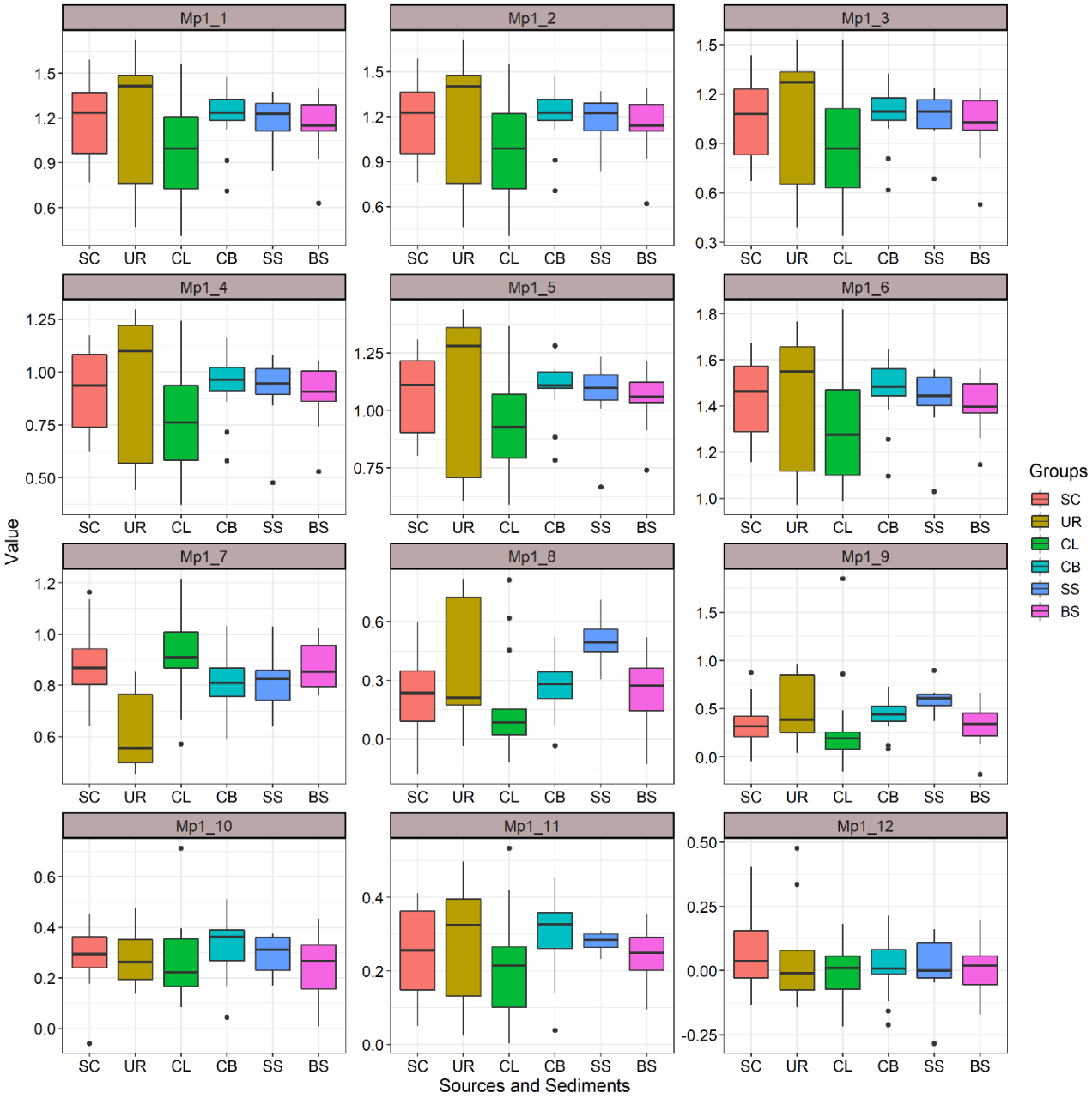
Mp1_1
Mp1_2
Mp1_3
Mp1_4
Mp1_5
Mp1_6
Mp1_7
Mp1_8
Mp1_9
Mp1_10
Mp1_11
Mp1_12
SC
UR
CL
CB
SS
BS
Value
Sources and Sediments
Groups

b)

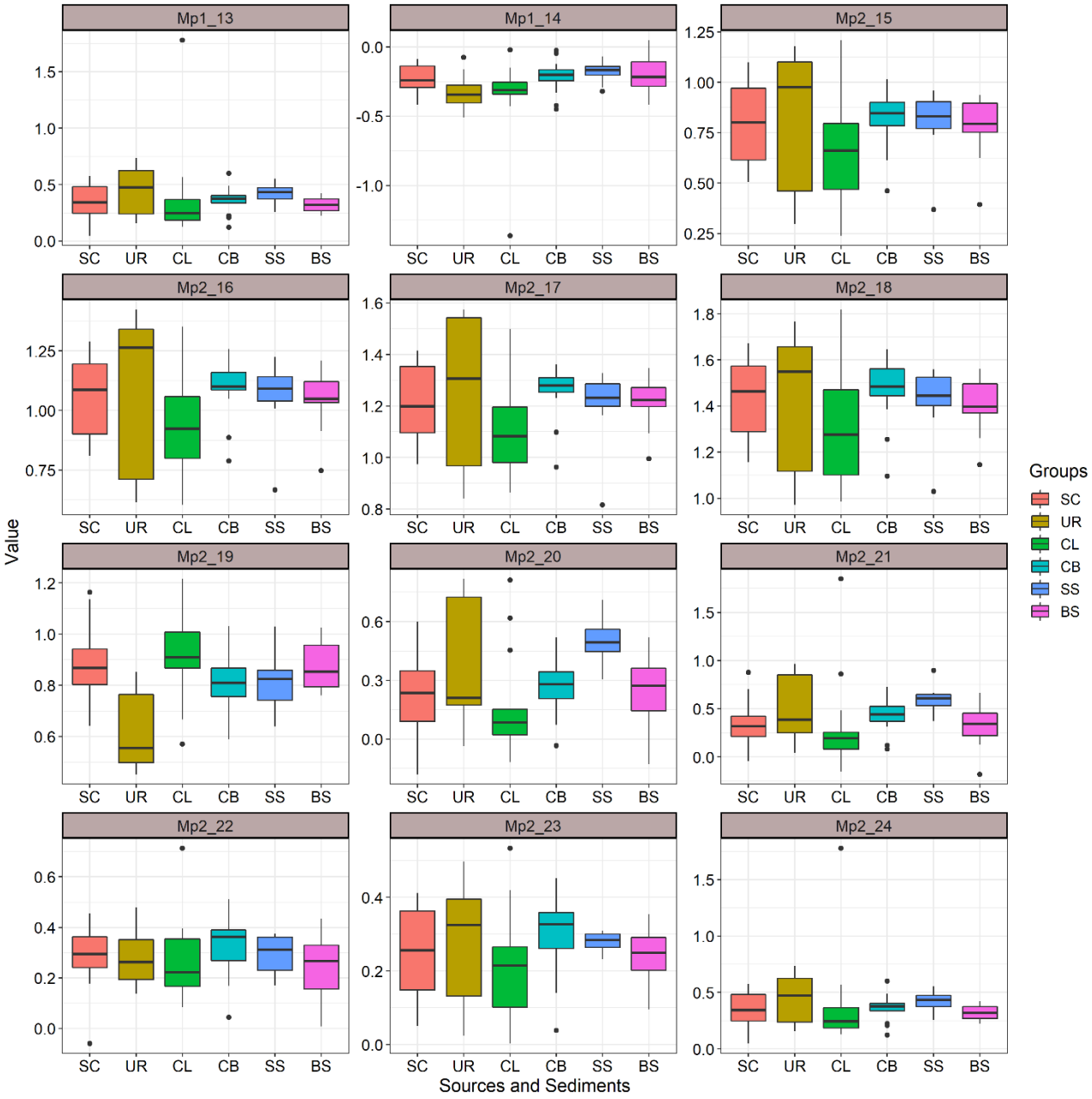
Mp1_13
Mp1_14
Mp2_15
Mp2_16
Mp2_17
Mp2_18
Mp2_19
Mp2_20
Mp2_21
Mp2_22
Mp2_23
Mp2_24
SC
UR
CL
CB
SS
BS
Value
Sources and Sediments
Groups

c)

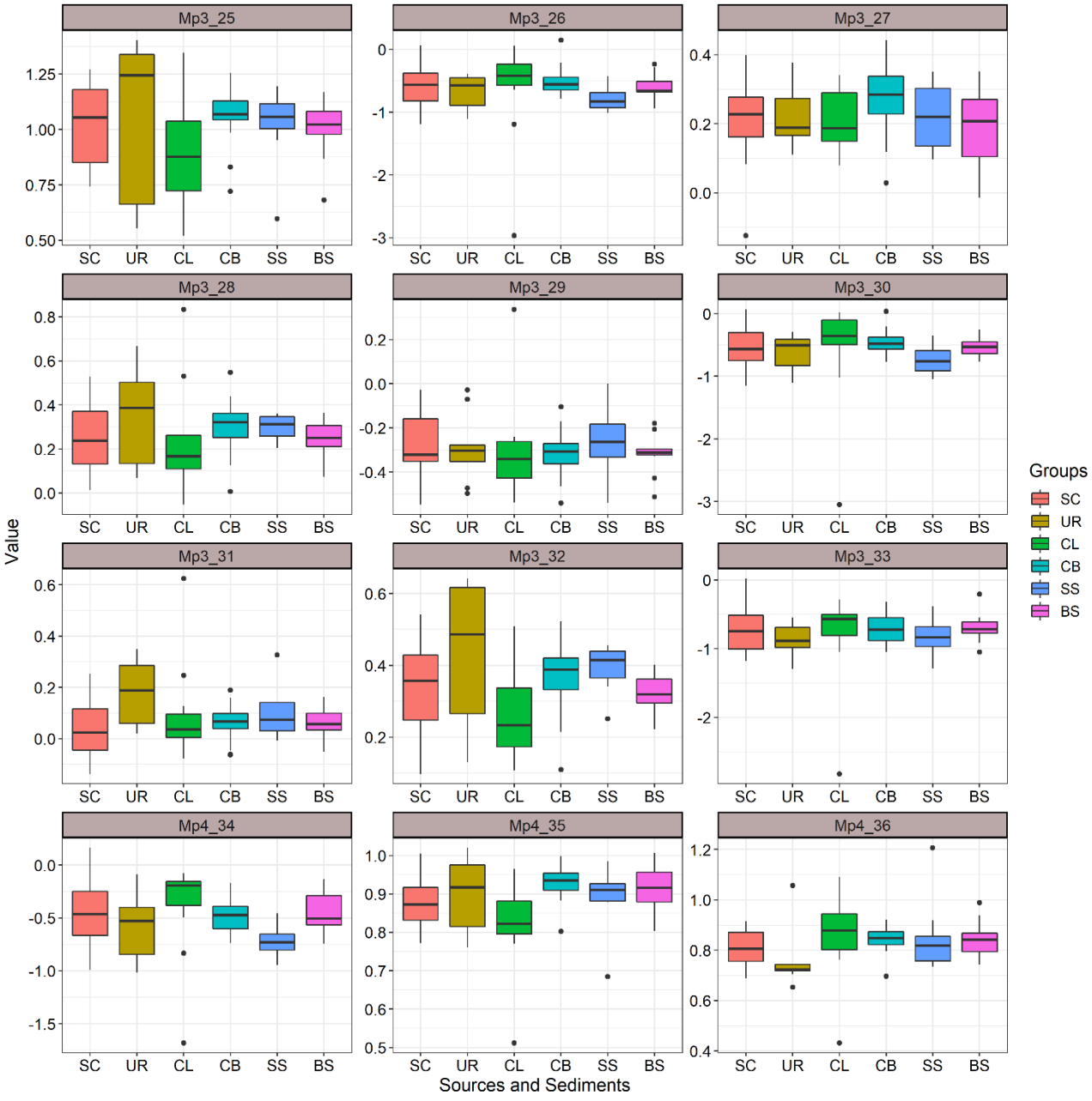
Mp3_25
Mp3_26
Mp3_27
Mp3_28
Mp3_29
Mp3_30
Mp3_31
Mp3_32
Mp3_33
Mp4_34
Mp4_35
Mp4_36
SC
UR
CL
CB
SS
BS
Value
Sources and Sediments
Groups

d)

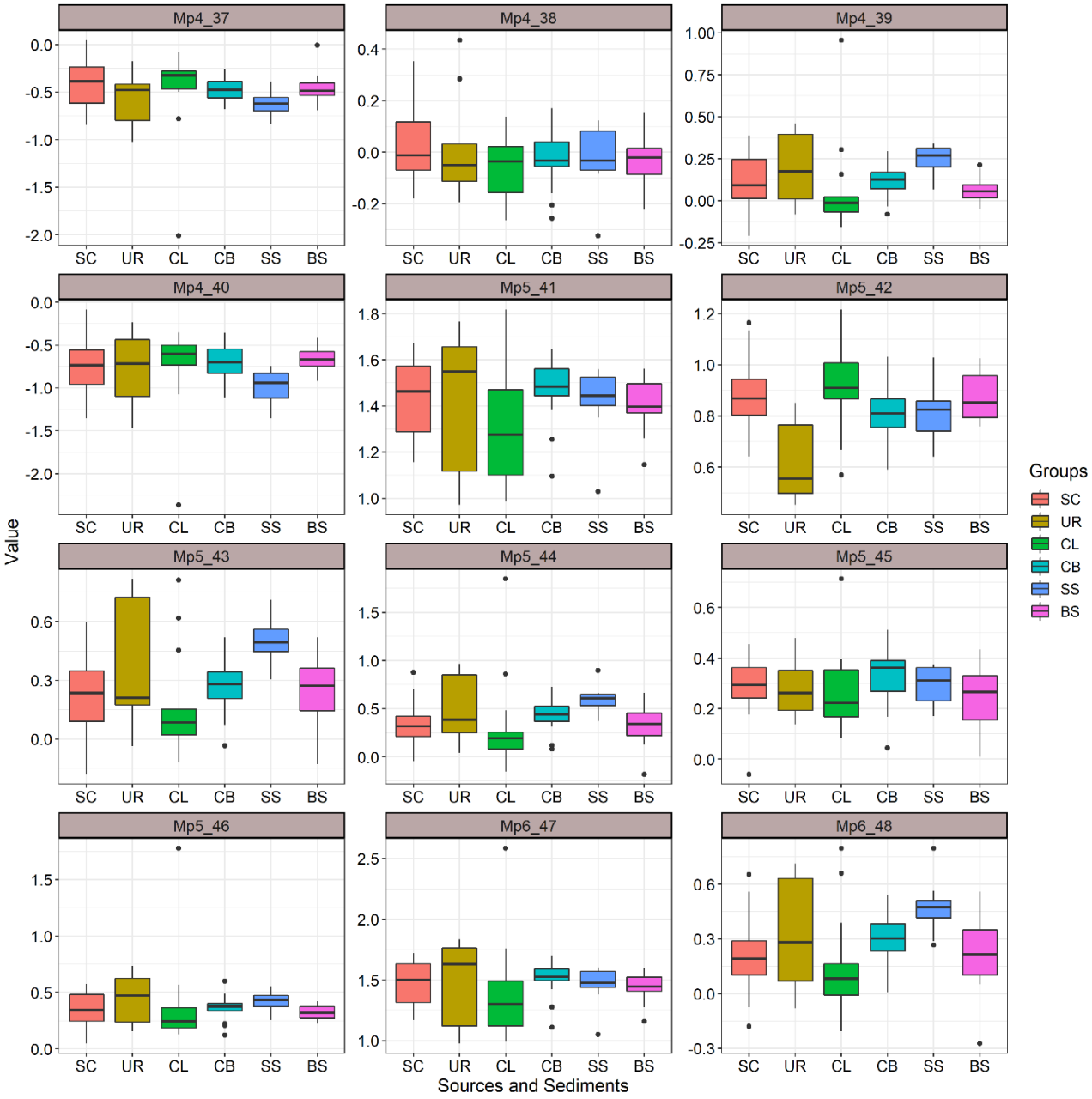
Mp4_37
Mp4_38
Mp4_39
Mp4_40
Mp5_41
Mp5_42
Mp5_43
Mp5_44
Mp5_45
Mp5_46
Mp6_47
Mp6_48
SC
UR
CL
CB
SS
BS
Value
Sources and Sediments
Groups

e)

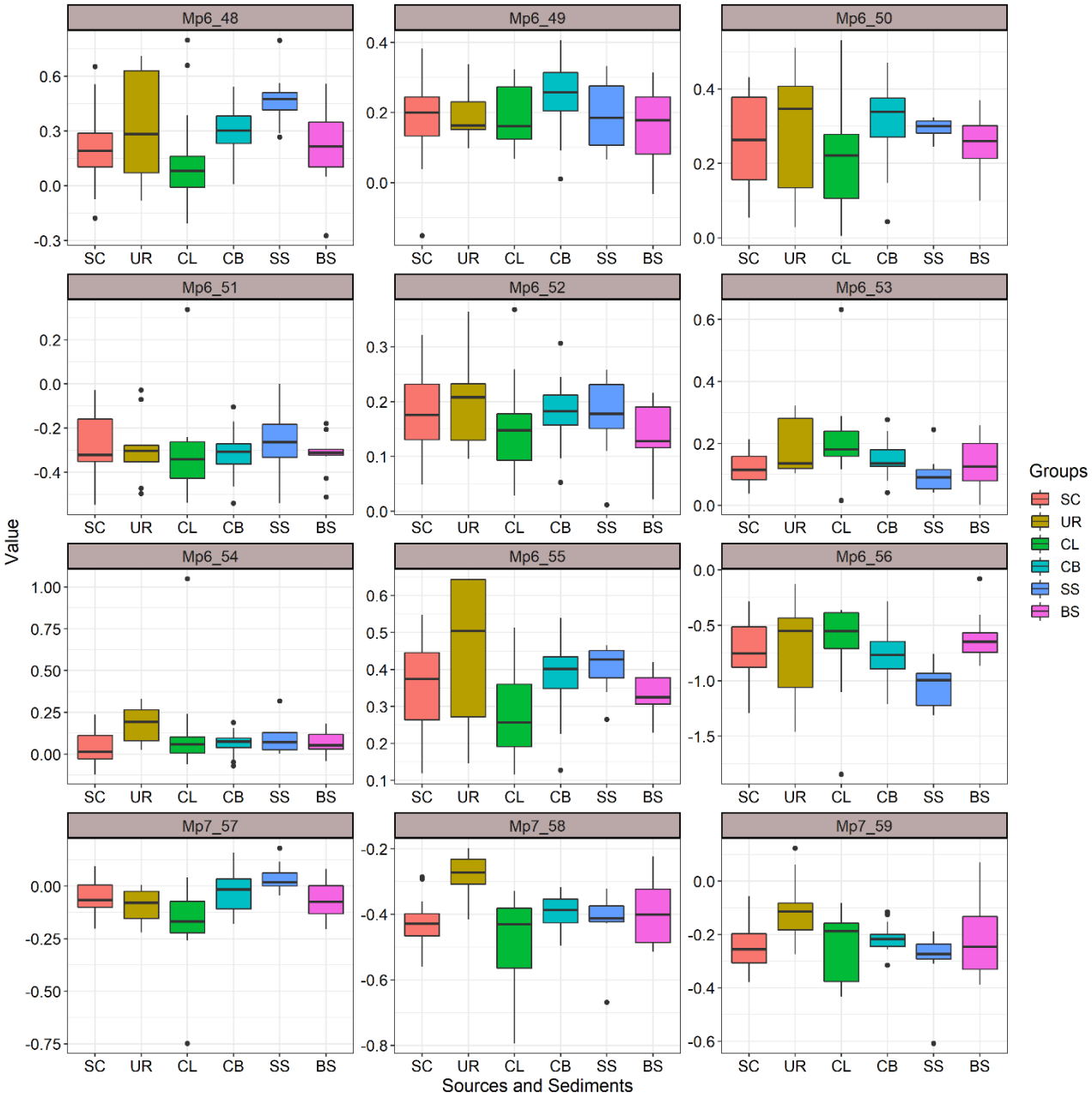
Mp6_48
Mp6_49
Mp6_50
Mp6_51
Mp6_52
Mp6_53
Mp6_54
Mp6_55
Mp6_56
Mp7_57
Mp7_58
Mp7_59
SC
UR
CL
CB
SS
BS
Value
Sources and Sediments
Groups

f)

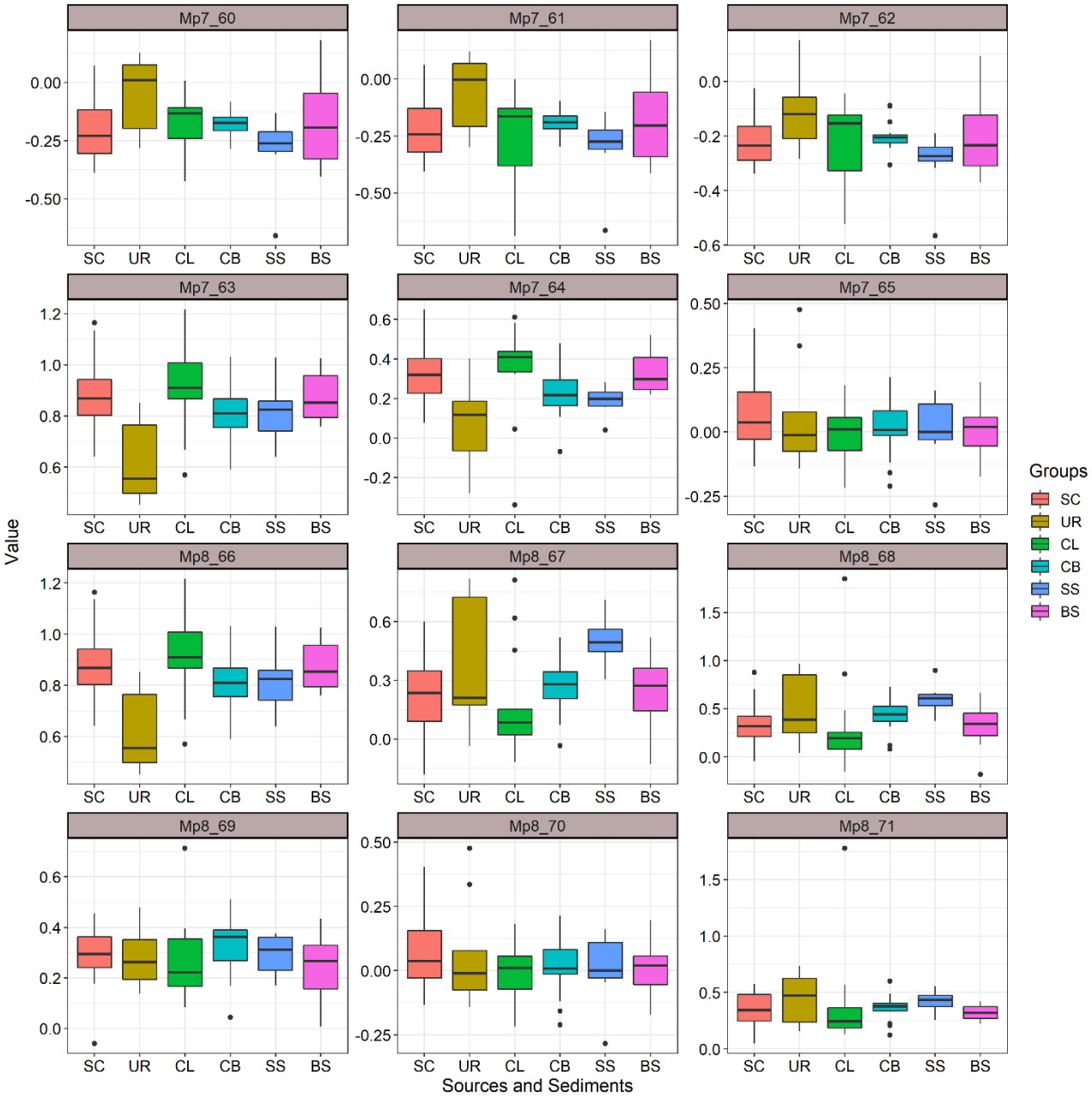
Mp7_60
Mp7_61
Mp7_62
Mp7_63
Mp7_64
Mp7_65
Mp8_66
Mp8_67
Mp8_68
Mp8_69
Mp8_70
Mp8_71
SC
UR
CL
CB
SS
BS
Value
Sources and Sediments
Groups

g)

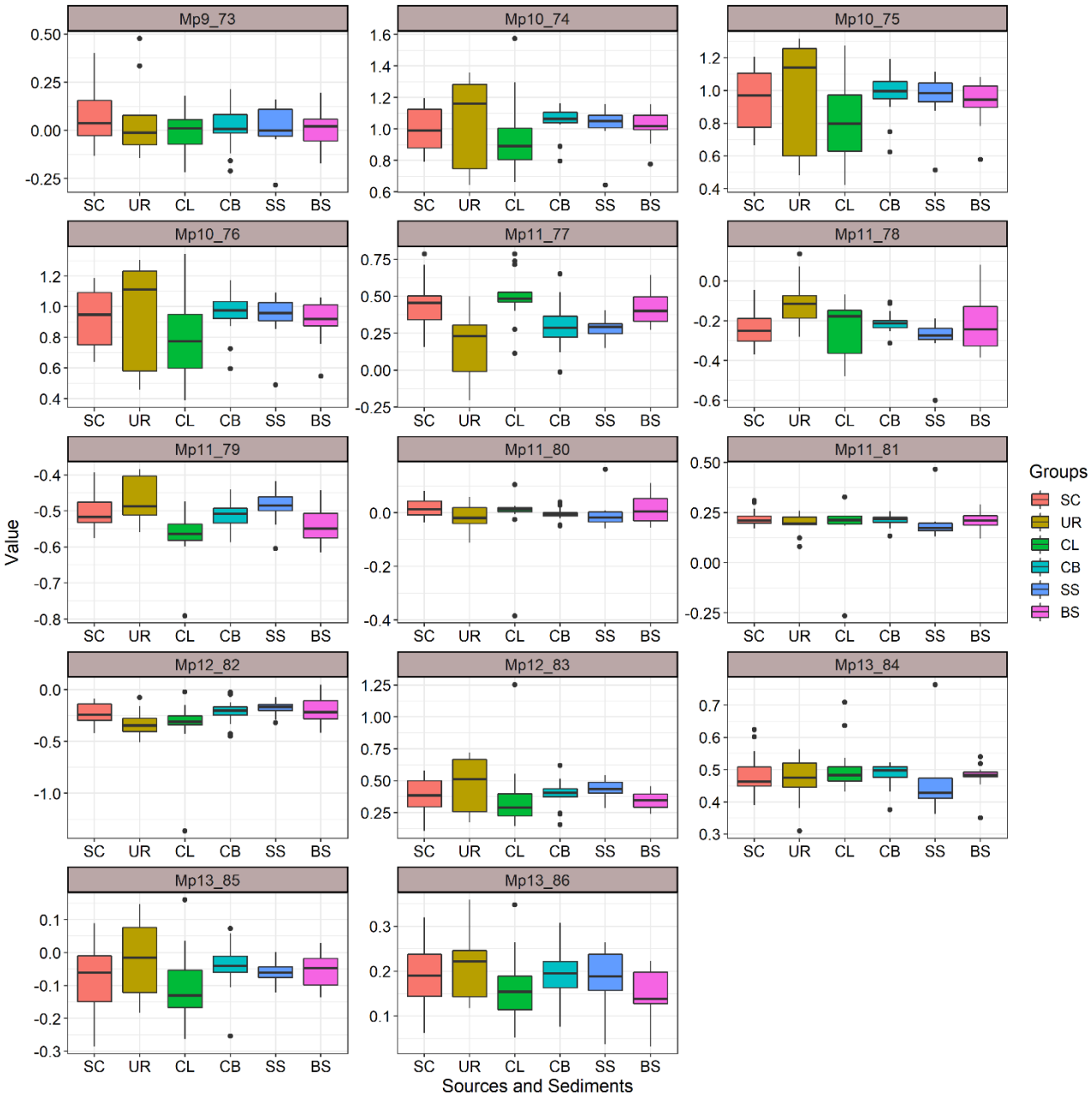

Figure S6. Distributions of MIR tracers for assessing conservative behaviour at sub-catchment scale. The median is shown by the central line, the interquartile range by the box, and outliers by the circles

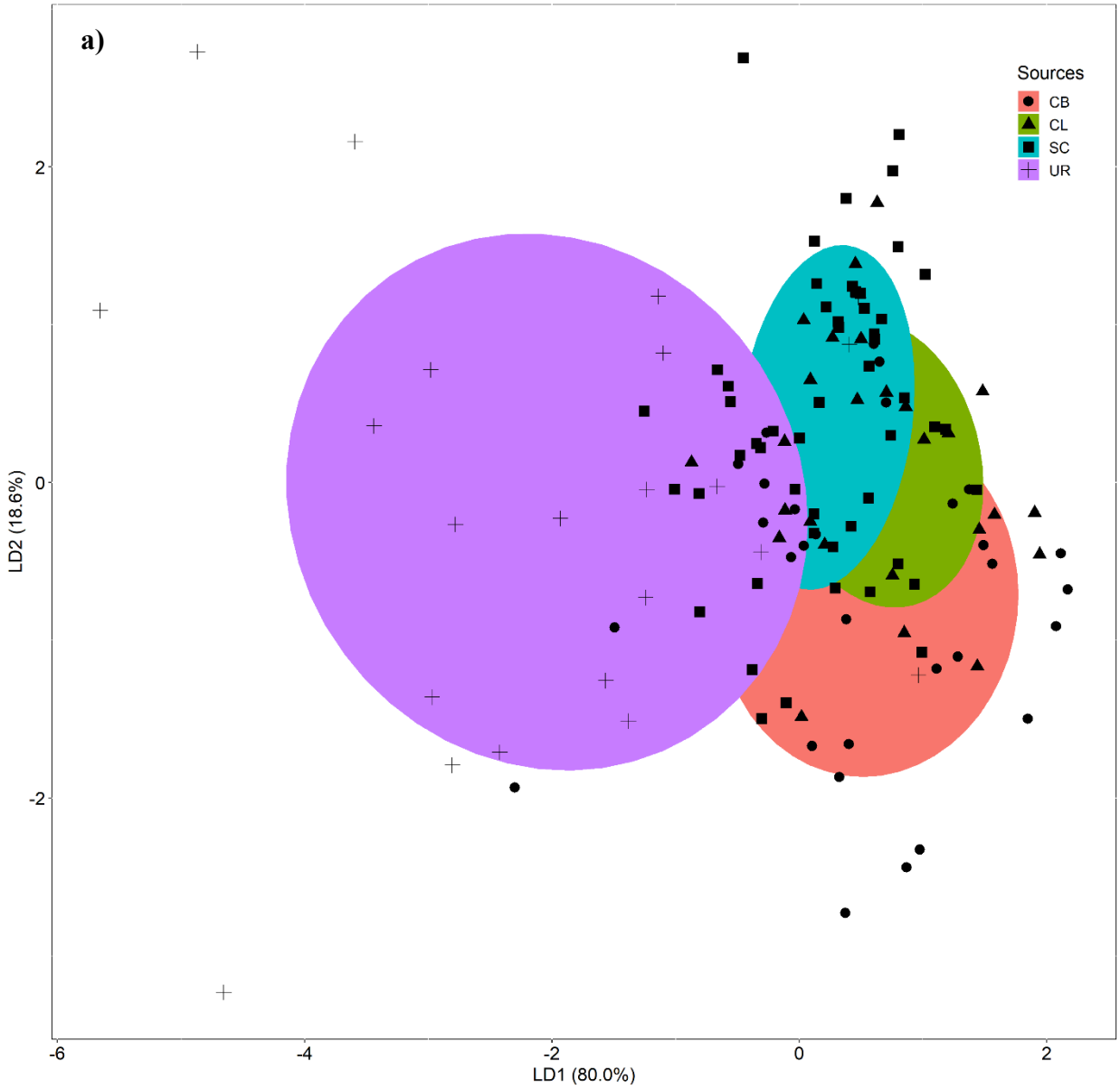
a)
Sources
CB
CL
SC
UR
LD2 (18.6%)
LD1 (80.0%)
2
0
-2
-6
-4
-2
0
2

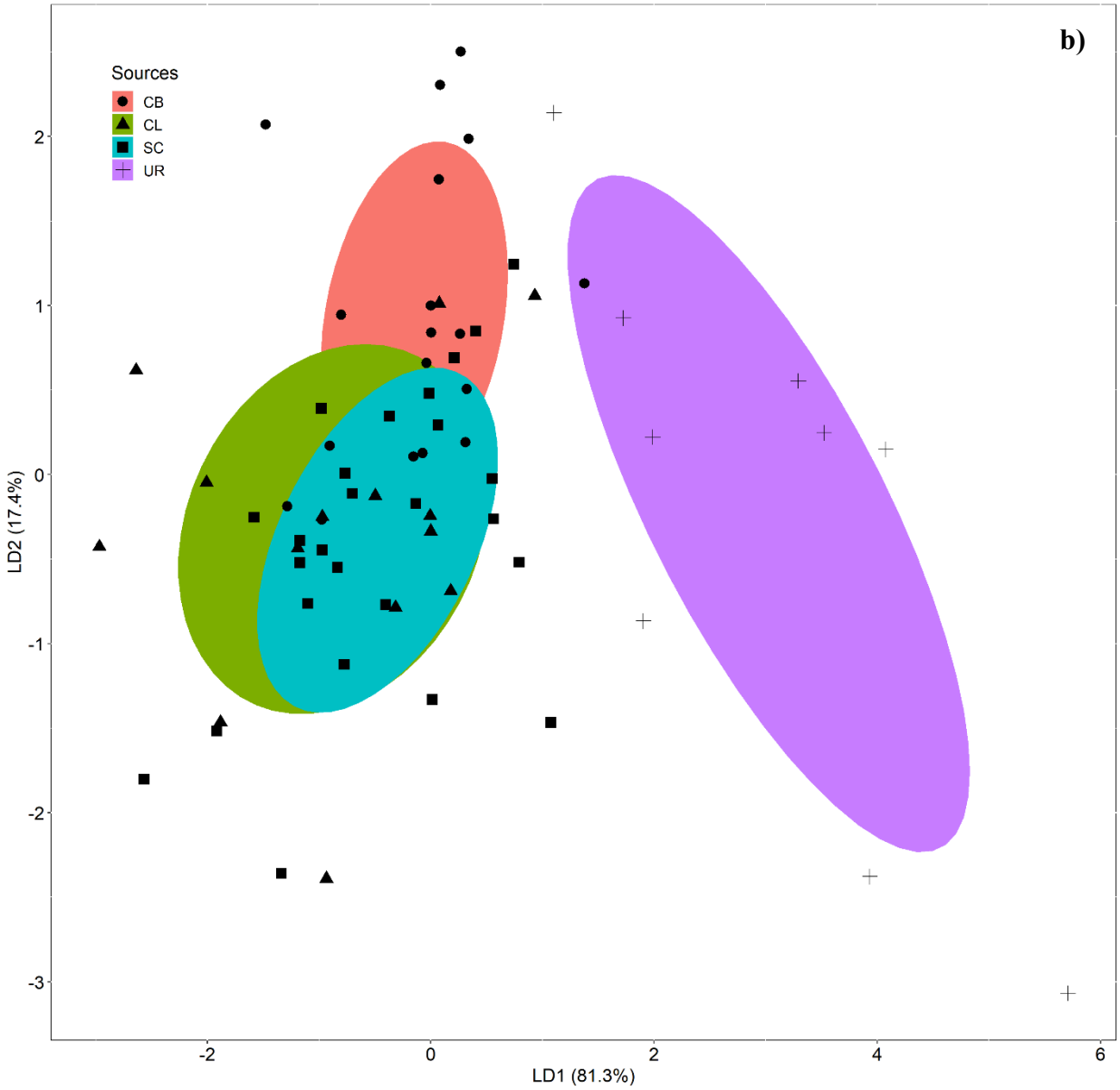

Figure S7. Results of forward stepwise Discriminant analysis using colour properties. Shaded ellipsoids comprise 50% of group variability. a) catchment-wide and b) sub-catchment scale

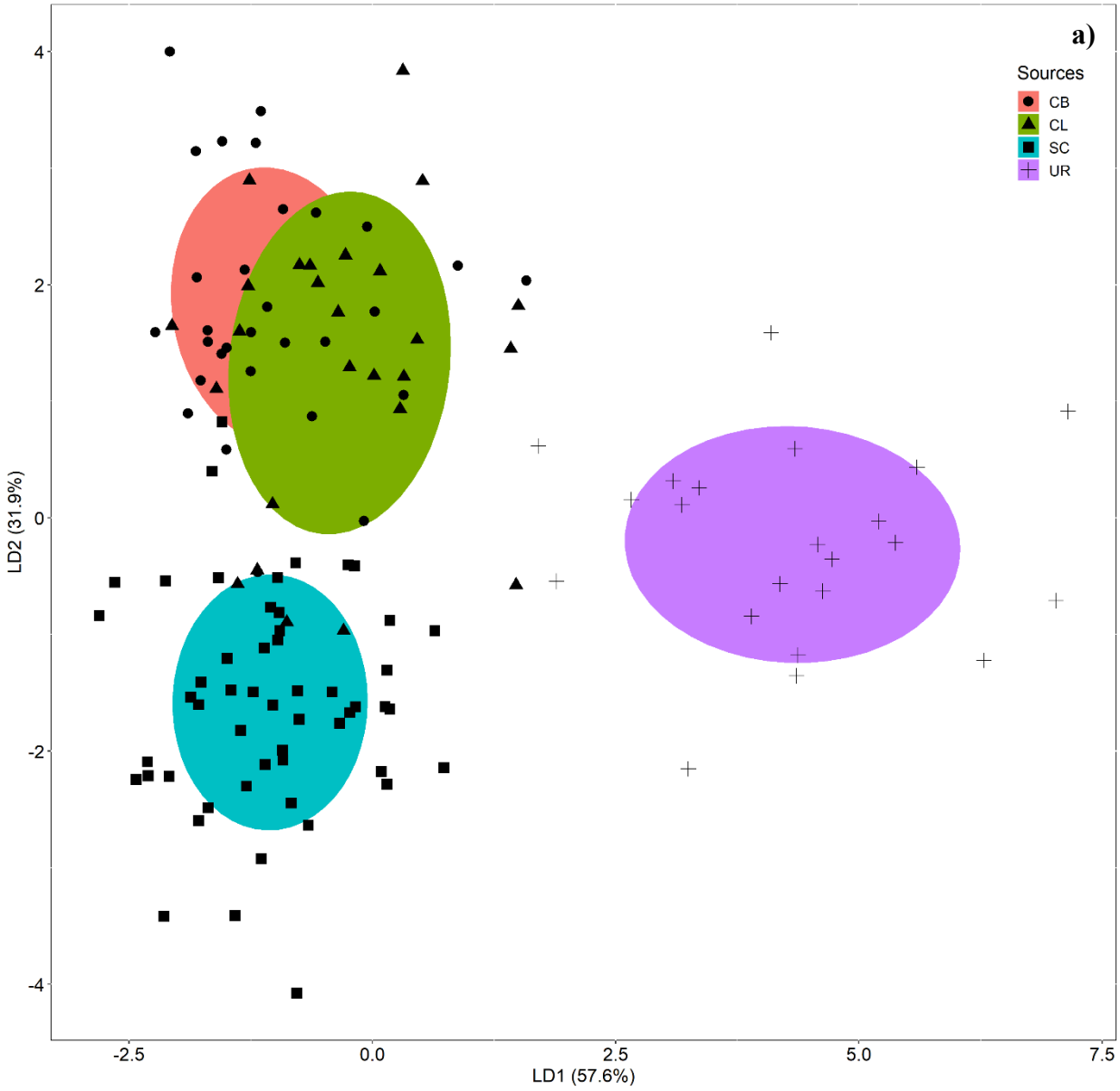
a)
Sources
CB
CL
SC
UR
LD2 (31.9%)
LD1 (57.6%)
4
2
0
-2
-4
-2.5
0.0
2.5
5.0
7.5

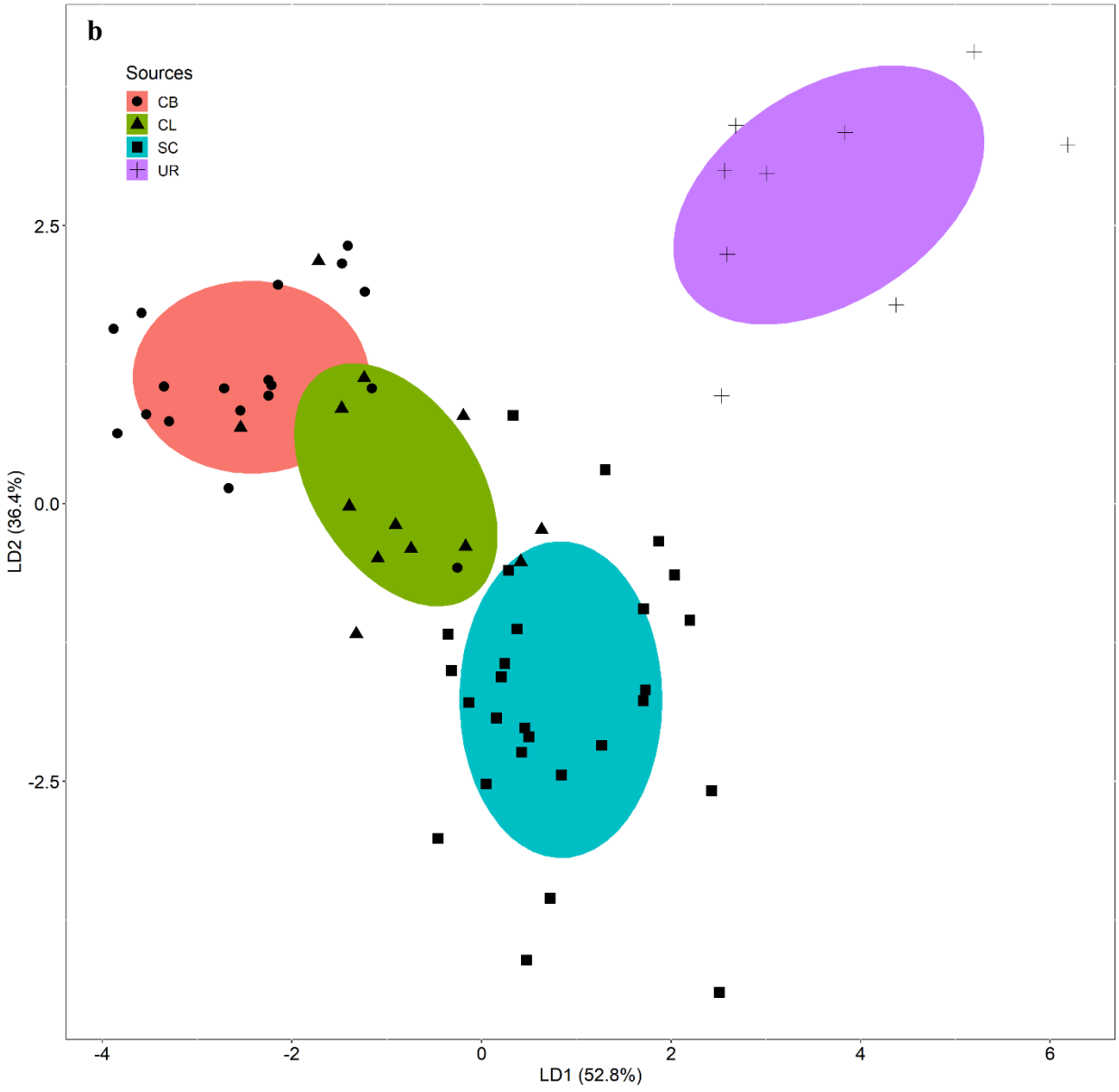

Figure S8. Results of forward Discriminant analysis using NIR properties. Shaded ellipsoids comprise 50% of group variability. a) catchment-wide and b) sub-catchment scales

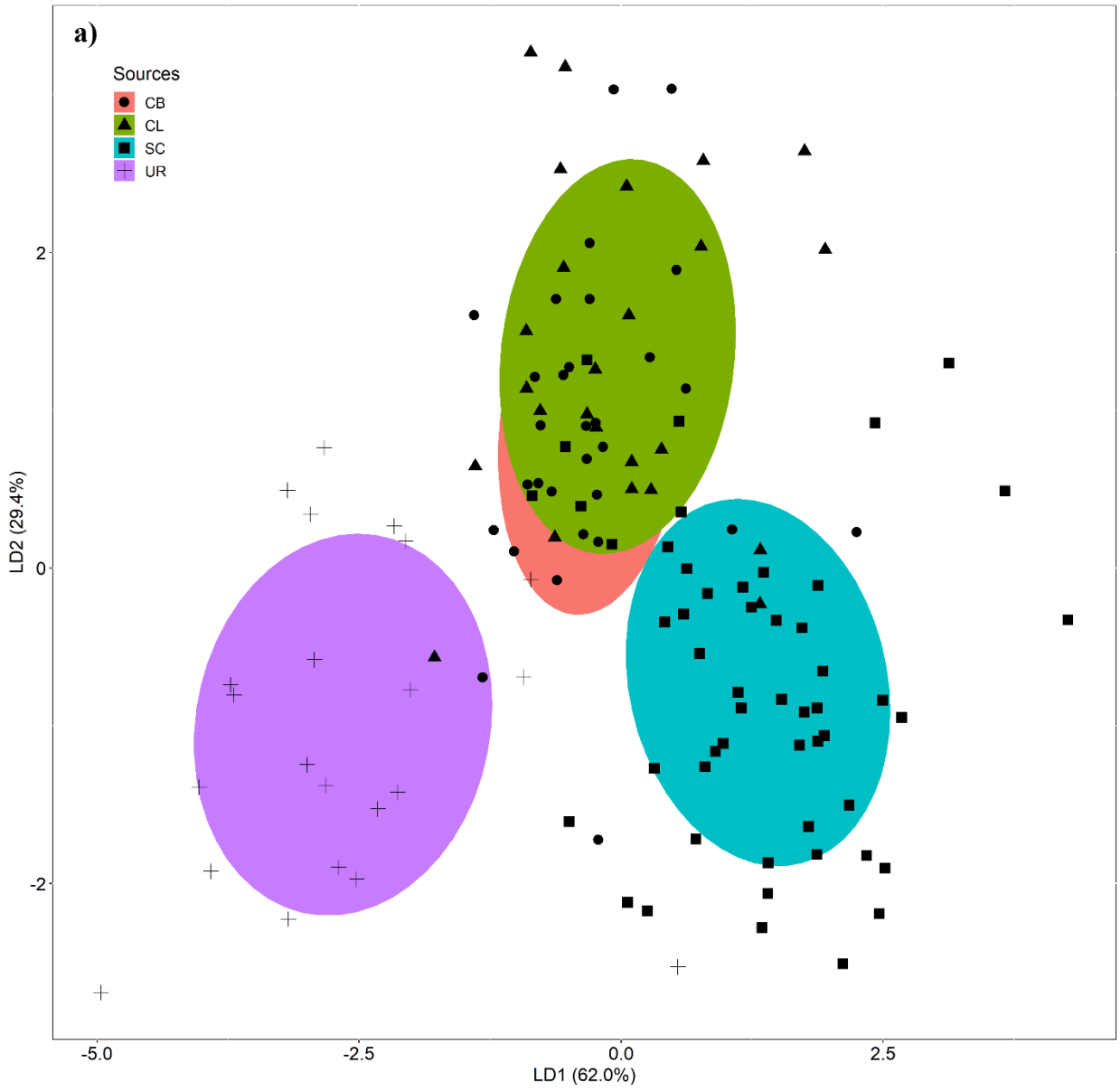
a)
Sources
CB
CL
SC
UR
2
0
-2
LD2 (29.4%)
-5.0
-2.5
0.0
2.5
LD1 (62.0%)

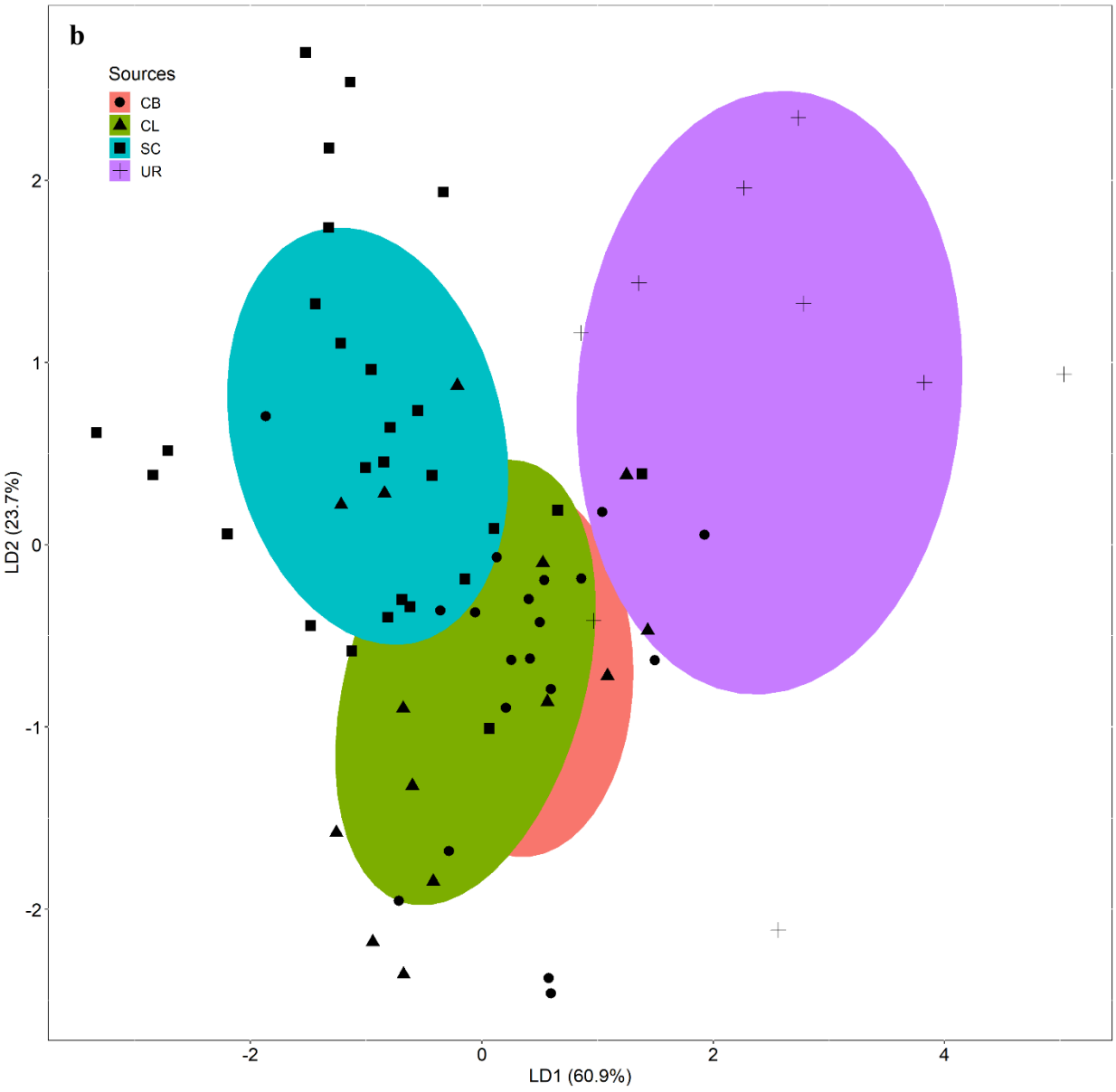

Figure S9. Results of forward Discriminant analysis using MIR properties. Shaded ellipsoids comprise 50% of group variability. a) catchment-wide and b) sub-catchment scales

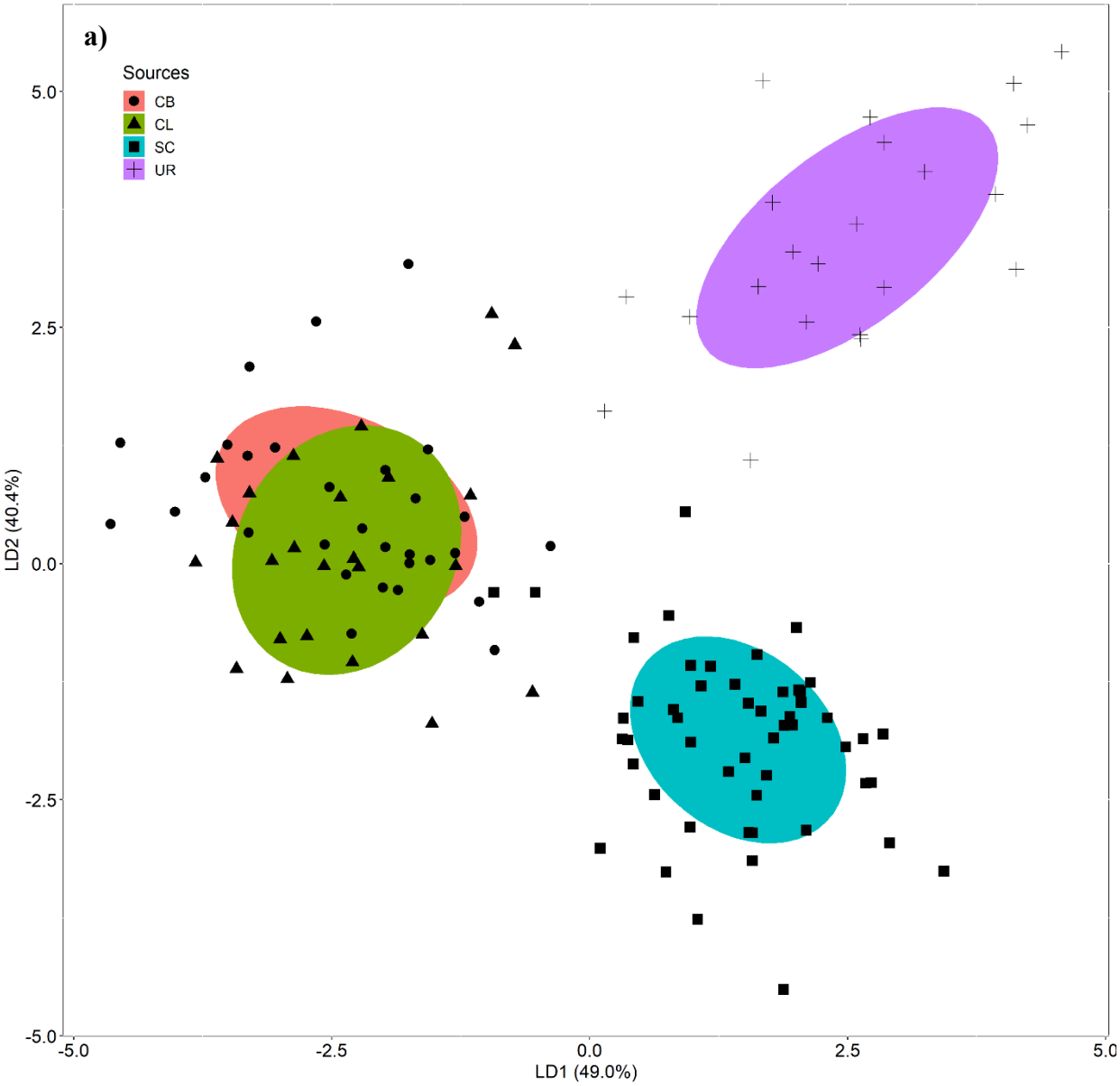
a)
Sources
CB
CL
SC
UR
5.0
2.5
0.0
-2.5
-5.0
LD2 (40.4%)
-5.0
-2.5
0.0
2.5
5.0
LD1 (49.0%)

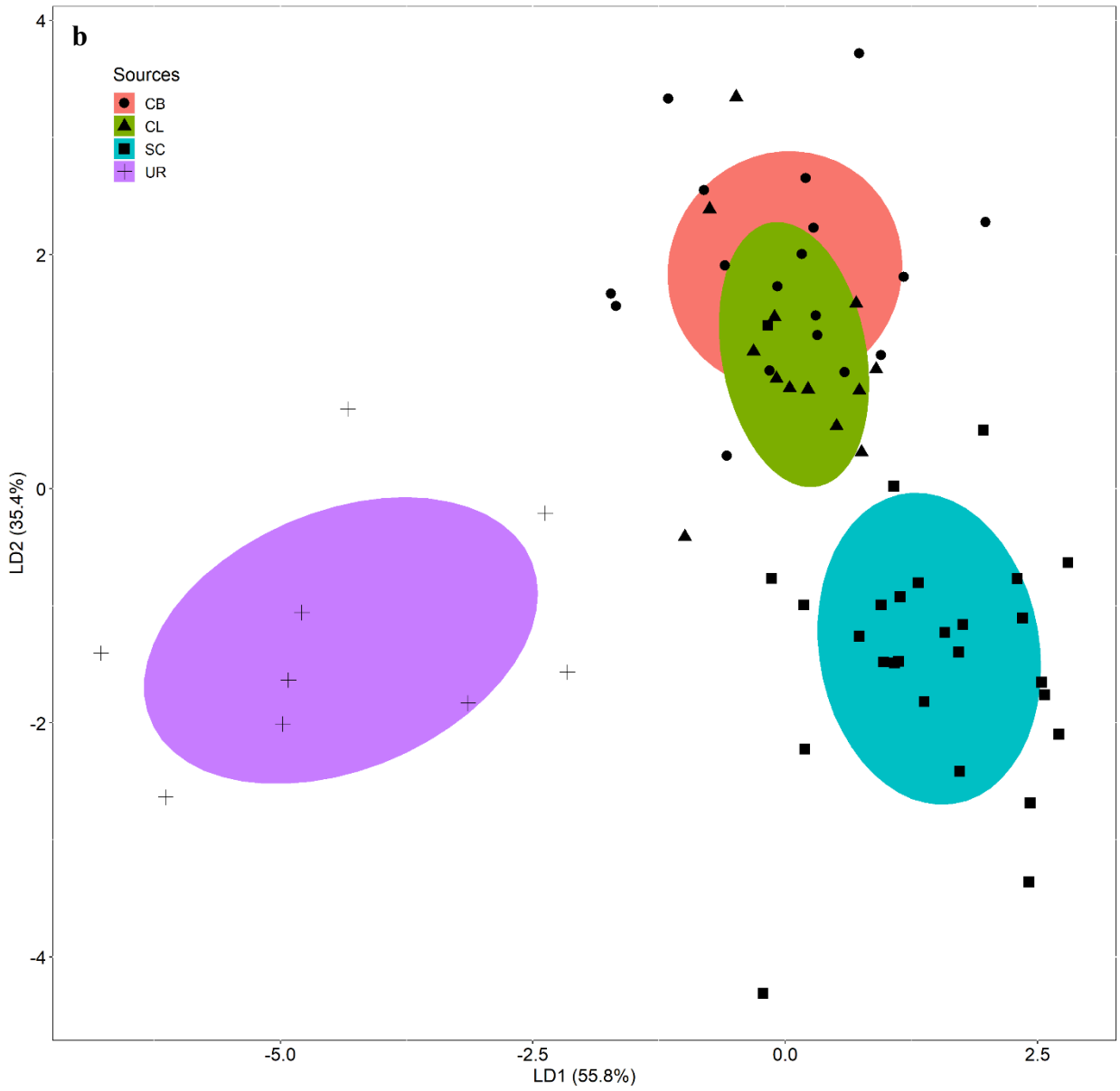

Figure S10. Results of forward Discriminant analysis using Colour + NIR + MIR properties. Shaded ellipsoids comprise 50% of group variability. a) catchment-wide and b) sub-catchment scales

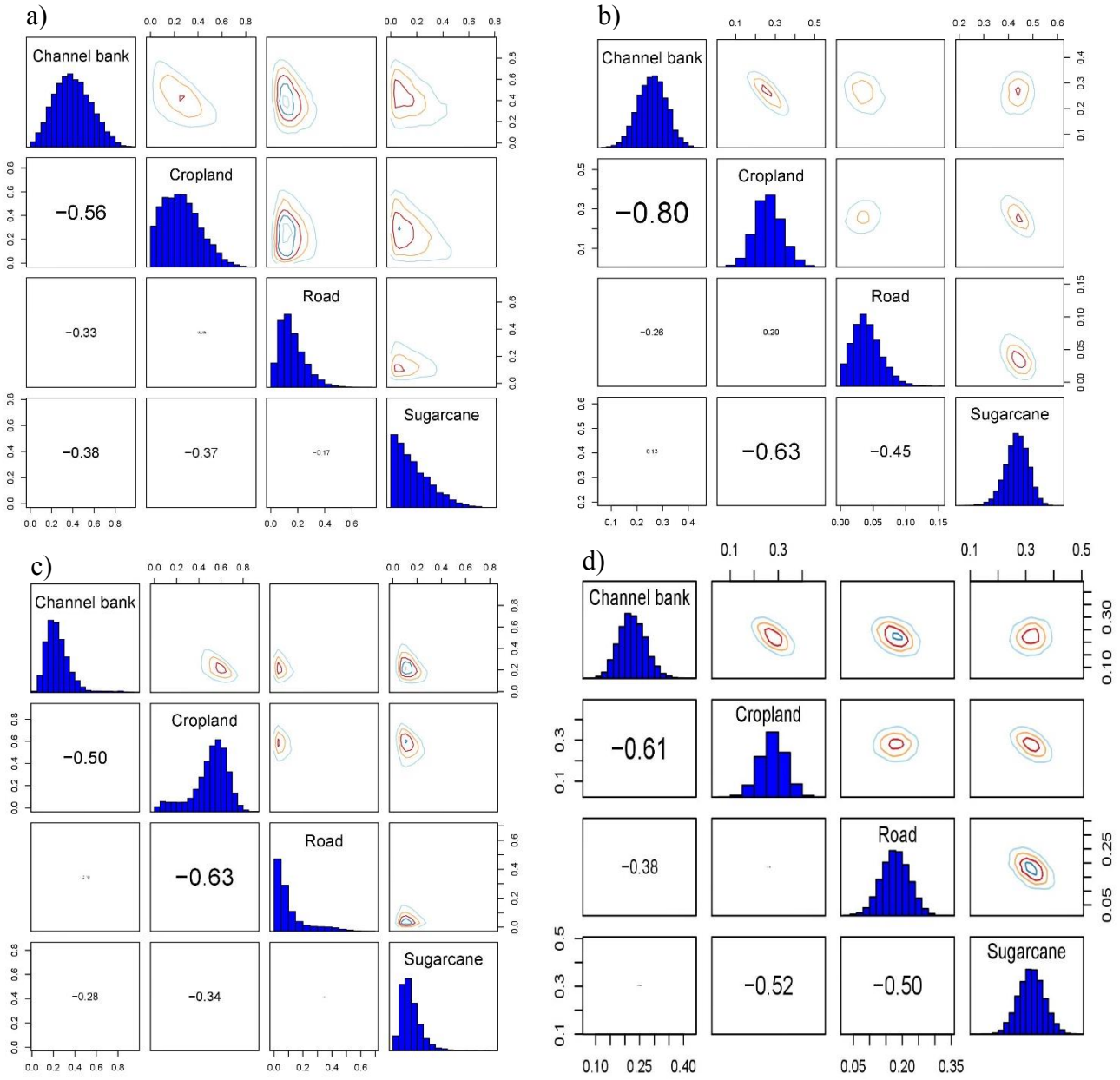

Figure S11. Correlations of posterior source contributions at catchment-wide scale using (a) Colour (b) NIR, (c) MIR and (d) CNM composite signatures. Diagonal histograms show the posterior distribution of source contributions

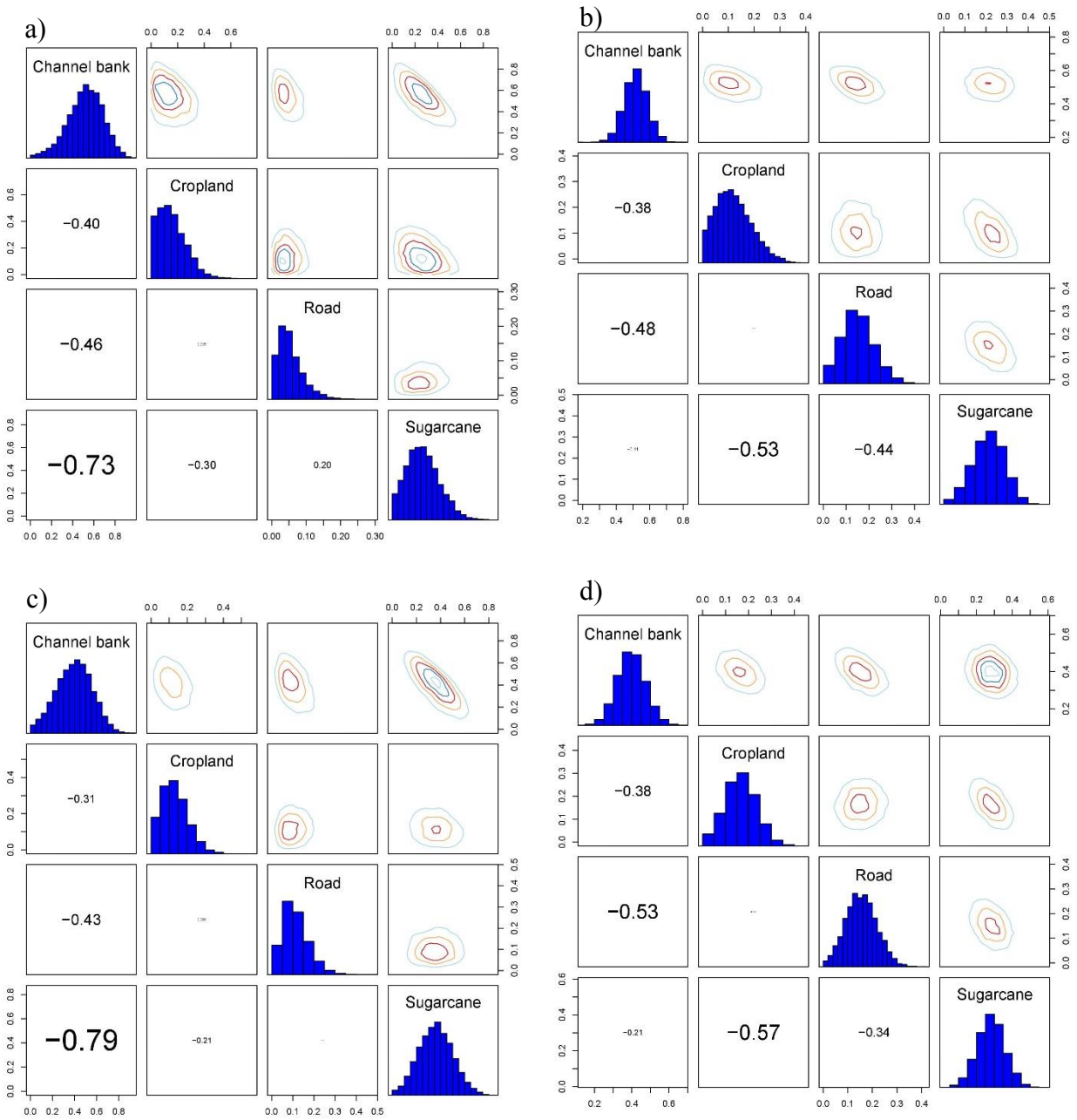

Figure S12. Correlations of posterior source contributions at sub-catchment scale using (a) Colour (b) NIR, (c) MIR and (d) CNM composite signatures. Diagonal histograms show the posterior distribution of source contributions